Appendix

Fish & Shellfish Immunology 31 (2011) 373–380

Contents lists available at ScienceDirect

Fish & Shellfish Immunology

journal homepage: www.elsevier.com/locate/fsi

A Tudor staphylococcal nuclease from *Penaeus monodon*: cDNA cloning and its involvement in RNA interference

Amnat Phetrungnapha [a], Sakol Panyim [a,b], Chalermporn Ongvarrasopone [a,*]

[a] Institute of Molecular Biosciences, Mahidol University (Salaya Campus), 25/25 Phutthamonthon 4 Road Salaya, Phutthamonthon District, Nakhon Pathom 73170, Thailand
[b] Department of Biochemistry, Faculty of Science, Mahidol University, Rama VI Road, Bangkok 10400, Thailand

ARTICLE INFO

Article history:
Received 22 March 2011
Accepted 25 May 2011
Available online 1 June 2011

Keywords:
RISC
RNAi
Double-stranded RNA
Black tiger shrimp

ABSTRACT

RNA interference (RNAi) plays an important role in an antiviral defense in shrimp. RNAi technology has been extensively used for inhibition of viral replication and studying gene function. However, the mechanism of shrimp RNAi pathway is still poorly understood. In this study, we identified and characterized an additional protein in the RNAi pathway, Tudor staphylococcal nuclease from *Penaeus monodon* (PmTSN). The full-length cDNA of PmTSN is 2897 bp, with an open reading frame encoding a putative protein of 889 amino acids. Phylogenetic analysis and domain structure comparison revealed that PmTSN is more closely related to vertebrate TSN by sharing the amino acid sequence identity of 57% with TSN of zebrafish. This represents a new type of TSN proteins by exhibiting the four tandem repeat of staphylococcal nuclease-like domain (SN), followed by a Tudor and a partially truncated C-terminal SN domain. Knockdown of *PmTSN* by dsRNA targeting SN3 domain resulted in the impairment of dsRNA targeting *PmRab7* gene to silence *PmRab7* expression. In addition, the efficiency of dsRNA targeting *YHV-protease* gene inhibiting yellow head virus replication was decreased in the *PmTSN*-knockdown shrimps. Our results imply that PmTSN is involved in dsRNA-mediated gene silencing in shrimp and thus we identified the additional protein involved in shrimp RNAi pathway.

1. Introduction

Eukaryotes possess a conserved post-transcriptional gene regulation mechanism known as RNA interference (RNAi) [1,2]. In this phenomenon, small RNA duplexes including short-interfering RNA (siRNA) and micro RNA (miRNA) trigger the silencing of the target mRNA in a sequence specific manner by mRNA degradation or translational repression. The ability of RNAi to silence the expression of a specific gene is a potential tool for analyzing gene function in eukaryotes [3]. In addition, RNAi acts as an antiviral immune defense which can be considered as a new promising therapeutic modality to combat viral diseases [4].

In penaeid shrimp, RNAi technology was employed as a powerful tool for studying gene function *in vivo* [5]. In addition, double-stranded RNA (dsRNA) is a potent trigger in the RNAi pathway and can induce both sequence-dependent and sequence-independent antiviral immunity in penaeid shrimp [6]. Therefore, RNAi technology was applied to prevent or cure viral infection in shrimp [7–9]. An understanding of the molecular mechanism of RNAi and identifying the proteins involved in the shrimp RNAi pathway will be essential before using RNAi as a tool for viral protective immunity or studying gene function in this economically important species.

Very little is known about the RNAi machineries in shrimp. Recently, the key proteins of the shrimp RNAi pathway have been identified including Dicer [10–12] and Argonaute [13–15]. In addition, the Dicer-interacting protein, the TAR-RNA binding protein (TRBP) has been identified in the Chinese shrimp, *Fenneropenaeus chinensis* [16]. However, other proteins that involved in the shrimp RNAi pathway are remained unknown. A number of the associated proteins in the RNA-induced silencing complex (RISC) such as dFXR, VIG and Tudor staphylococcal nuclease were indentified in *Caenorhabditis elegans*, *Drosophila* and human [17,18], whether these RNAi machineries play important roles in the shrimp RNAi pathway remains to be elucidated. Therefore, the purpose of this study is to clone and characterize one of the RNAi machineries, Tudor staphylococcal nuclease from black tiger shrimp, *Penaeus monodon*.

Tudor staphylococcal nuclease (TSN, also known as SND1 and P100) is a highly conserved protein ranging from yeasts to humans [19]. This protein contains five staphylococcal nuclease-like (SN) domains and a Tudor domain [20]. Biochemical purification of the RISC revealed that TSN is one of the components in the silencing complex [17,21]. Knockdown of *tsn-1* expression impairs RNAi in

* Corresponding author. Tel.: +66 2 800 3624x1280; fax: +66 2 4419906.
E-mail address: mbcov@mahidol.ac.th (C. Ongvarrasopone).

1050-4648/$ – see front matter © 2011 Elsevier Ltd. All rights reserved.
doi:10.1016/j.fsi.2011.05.026

C. elegans, indicating the requirement of TSN for the proper function of the RISC [17]. TSN was first identified in human as a transcriptional coactivator of Epstein-Barr virus nuclear antigen 2 (EBNA2) [22]. It interacts with several transcription factors and chromatin remodeler to enhance their activities, such as STAT5 [23], STAT6 and RNA polymerase II [24], and CREB-binding protein [25]. In addition, TSN interacts with small nuclear ribonucleoproteins (snRNP) and functions in spliceosome assembly and pre-mRNA splicing [26]. TSN was shown to bind and promote the cleavage of hyper-edited inosine-containing dsRNA [27]. Whether such diverse functions of TSN exist in shrimp remain to be elucidated.

In this study, we cloned and characterized the full-length cDNA encoding TSN from *P. monodon (PmTSN)*. We further demonstrated that RNAi knockdown of PmTSN expression diminished the efficiency of RNAi, suggesting the involvement of PmTSN in dsRNA-mediated gene silencing in shrimp.

2. Experimental procedures

2.1. Animals

Black tiger shrimps, *P. monodon* (4–5 g) were purchased from the commercial shrimp farms in Thailand. They were reared in the laboratory tanks with continuous aerated sea water (10 ppt) for 3 days before processing to allow acclimatization. Shrimps were fed *ab libitum* with commercial shrimp feed. Apparently healthy looking shrimp were picked and used in all experiments.

2.2. Virus stock and experimental infection

Yellow head virus (YHV) stock was kindly prepared by Dr. Witoon Tirasophon, Mahidol University. The YHV viral titer ($\sim 3 \times 10^9$ infectious virions ml^{-1}) was determined according to the method described by Assavalapsakul et al. [28]. The YHV stock was diluted to 10^7 fold and 50 μl of the diluted YHV stock was used to inject into shrimp [29].

2.3. RNA extraction and cDNA synthesis

The tissue samples were homogenized in TRI-REAGENT® or TRI-LS® (Molecular Research Center). Total RNA was extracted according to manufacturer's instruction. The RNA concentration was determined by NanoDrop ND-1000 spectrophotometer (Nanodrop Technologies). The absorbance ratio of A260 and A280 was 1.8–2.0, indicated that the RNA samples were relatively pure. Total RNA (1 μg) was used for cDNA synthesis. Reverse transcription was performed by using Improm-II™ reverse transcriptase (Promega), following the manufacturer's instruction with PRT-oligo-dT_{12} primer (Table 1).

2.4. Cloning of PmTSN cDNA

A partial *PmTSN* cDNA fragment was first amplified by RT-PCR with gene specific primers. Briefly, total RNA (5 μg) extracted from gills was primed with PRT-oligo-dT_{12} primer and reverse transcribed with SuperScript® III reverse transcriptase (Invitrogen). PCR was performed using TuF1 and TuR1 primers, following the condition: denaturation at 94 °C for 5 min, followed by 30 cycles of 94 °C for 30 s, 50 °C for 30 s, and 72 °C for 1 min. The final extension was carried out at 72 °C for 7 min. The amplified fragments were purified from the gel using QIAquick gel extraction kit (Qiagen). Purified PCR products were cloned into pGEM®-T Easy vector (Promega) and subsequently subjected for DNA sequencing by First Base Co., Ltd. (Malaysia).

Table 1
Sequences for primers used in this study.

Primers	Sequence (5′-3′)	Purposes
PRT-oligo-dT	CCGGAATTCAAGCTTCTAGAGGATCC TTTTTTTTTTTTTTT	Reverse transcription
TuF1	GAAGCTGTGGTGGAATTTGTT	RT-PCR
TuR1	GTATTCACTCACCACAGTCTG	RT-PCR
PM1	CCGGAATTCAAGCTTCTAGAGGATCC	5′ and 3′RACE
TuF2	CGGGAAGTTGAGATTGAGGTG	3′RACE
3RF1	CCAGCATTGGAACAGCTGAT	3′RACE
Tu5R	TGCTGAGGTTGAGTGCTTCCT	5′RACE
TuN5R	TCCAGATGCAACAAATTCCAC	5′RACE, Multiplex RT-PCR
P-5RACE	GACTCCTCGGATACTCTCC	Reverse transcription
S1	AGTAGAGAATTCTTGCGGAA	5′RACE
AS1	CATAAGGCTCATCCACTG	5′RACE
S2	ACTTCAACTGGTCGAGAATATG	5′RACE
AS2	GTGTTGGGTGAGACGCAG	5′RACE
CDS-F	ATGGCTGCGTCTCACCCAA	RT-PCR
CDS-R	GCTTCTCCATCAGCTGTTCC	RT-PCR
TSN-F1	GCTGCACAGTCAAGATTGGA	Multiplex RT-PCR
Actin-F	GACTCGTACGTCGGGCGACGA	Multiplex RT-PCR
Actin-R	AGCAGCGGTGGTCATCACCTG	Multiplex RT-PCR
SN3-FT7	TAATACGACTCACTATAGGCTGGC AAGGTCATAGAAGTCG	Preparation of dsRNA
SN3-R	CACGCTGGTCATCATCTTGT	Preparation of dsRNA
SN3-F	CTGGCAAGGTCATAGAAGTCG	Preparation of dsRNA
SN3-RT7	TAATACGACTCACTATAGGCACGC TGGTCATCATCTTGT	Preparation of dsRNA
qTSN-F3	TAAGCCCTCTGGTCCTAAGATTGC	Real-time PCR
qTSN-R3	CTCTGGTAGCCTGGGTGGTCTTAT	Real-time PCR
qRab7-F2	CTGGAGAATAGGGCGGTATCAACG	Real-time PCR
qRab7-R2	CGAGCAATGGTCTGGAAGGCTAAC	Real-time PCR
EF1a-F	GAACTGCTGACCAAGATCGACAGG	Real-time PCR
EF1a-R	GAGCATACTGTTGGAAGGTCTCCA	Real-time PCR
YHV-helF	CAAGGACCACCTGGTACCGGTAAGAC	Multiplex RT-PCR
YHV-helR	GCGGAAACGACTGACGGCTACATTCAC	Multiplex RT-PCR

2.4.1. Amplification of the 5′ and 3′ end sequences

Rapid amplification of cDNA ends (5′ and 3′ RACE) were used for identifying the 5′ and 3′ end sequences. Primers for RACE were designed from a partial sequence of *PmTSN* cDNA fragment. For 3′ RACE, PCR was performed using TuF2 primer and an adaptor primer, PM1. Subsequently, the nested PCR was performed with 3RF1 and PM1 primers. For 5′ RACE, a poly-A tail was added to the 3′-end of cDNA using terminal deoxynucleotidyl transferase (TdT) (Promega) and purified by QIAquick PCR purification kit (Qiagen). A-tailed cDNA was subsequently used for PCR with Tu5R and PRT- oligo-dT_{12} primers. The nested PCR was performed using TuN5R and PRT- oligo-dT_{12} primers. Identification of the remaining 5′end sequences was performed using 5′-Full Race Core Set (Takara) according to manufacturer's instruction. Briefly, cDNA was synthesized using 5′ end-phosphorylated primer, P-5RACE and was subsequently circularized by T4 RNA ligase (Takara). Then, PCR was performed by using S1 and AS1 primers. The nested PCR was subsequently performed with S2 and AS2 primers. All primers used for cloning were ordered from Pacific Science Co., Ltd. (Thailand) and were listed in Table 1. PCR products were purified, cloned and subjected for sequencing as described above.

2.4.2. Amplification of the full-length coding sequences of PmTSN

To amplify the coding region of *PmTSN* cDNA, RT-PCR was performed using VENT® DNA polymerase (New Englang Biolabs) with CDS-F and CDS-R primers, following the condition: denaturation at 95 °C for 3 min, followed by 30 cycles of 95 °C for 30 s, 55 °C for 30 s, and 72 °C for 3 min. The final extension was carried out at 72 °C for 7 min. PCR product was purified, cloned and subjected for sequencing as described above.

2.5. Sequence and phylogenetic analysis

The nucleotide and deduced amino acid sequences of *PmTSN* were compared with other known TSN sequences available in the GenBank database using BLAST search program [30]. The protein domain features of PmTSN were predicted by using ScanProsite [31] and Conserved Domain Architecture Retrieval Tool (CDART) [32]. Molecular weight and isoelectric point of the protein were predicted by tools in the Expasy website (www.expasy.org). For multiple sequence alignment and phylogenetic analysis, TSN sequences from several species were retrieved from the GenBank database. Multiple sequence alignment was performed by using ClustalW [33] and phylogenetic analysis was performed by using MEGA 4.1 program [34] based on the neighbor-joining methods [35]. Bootstrap values of 1000 replicates were calculated for each node of the consensus tree.

2.6. Tissue distribution study

Multiplex RT-PCR was employed to study the expression of *PmTSN* in various shrimp tissues. hemolymph, gill, lymphoid organ, hepatopancreas, stomach, testis, abdominal muscle, pleopods and thoracic ganglia were dissected out from male brood stock shrimps. Total RNA from different tissues were extracted and reverse transcribed to cDNA. To determine the expression of *PmTSN*, multiplex RT-PCR was performed. The *PmTSN* primers were TSN-F1 and TuN5R, and the *β-actin* primers were Actin-F and Actin-R (Table 1). The multiplex PCR was performed under the following condition: denaturation at 94 °C for 5 min, followed by 5 cycles of 94 °C for 30 s, 59 °C for 30 s (−1 °C/cycle) and 72 °C for 40 s, and 23 cycles of 94 °C for 30 s, 54 °C for 30 s, and 72 °C for 40 s. The final extension was carried out at 72 °C for 7 min. PCR products were analyzed on 1.2% agarose gel electrophoresis, stained with ethidium bromide and visualized under ultraviolet light.

2.7. Preparation of double-stranded RNA (dsRNA)

The dsRNA specific to SN3-like domain of *PmTSN* (dsSN3) was synthesized by *in vitro* transcription using RiboMAX® Large Scale RNA Production System (Promega) following the manufacturer's protocol. Briefly, sense and anti-sense DNA template strands were synthesized by PCR with the primers that contained T7 promoter sequences (Table 1) using VENT® DNA polymerase (New England Biolabs). Five micrograms of each purified PCR product was used for *in vitro* transcription. After the reaction, DNA template was removed by incubating with RQ1 DNase (Promega) (1 unit per μg of DNA template) at 37 °C for 15 min. The *in vitro* transcribed RNA product was annealed to produce dsRNA by incubating at 95 °C for 2 min. The temperature was decreased to 25 °C at the rate of 0.1 °C s^{-1} and hold at 25 °C for 30 min. The left-over single-stranded RNA (ssRNA) was degraded by adding 10 ng of Ribonuclease A (RNase A) (New Englang Biolabs) and incubated at 37 °C for 10 min. dsSN3 was further purified by TRI-LS® (Molecular Research Center) according to manufacturer's protocol.

The dsRNA specific to *PmRab7*, *gfp* and *YHV-protease* (dsRab7, dsGFP and dsYHV) were produced by *in vivo* bacterial expression [36]. The quality of dsRNAs was determined by ribonuclease digestion assay using RNase A and RNase III (New England Biolabs).

2.8. Knockdown of PmTSN expression

To knockdown *PmTSN* transcript, shrimps (size 4–5 g, 6 shrimps per group) were intramuscularly injected with 5 μg g^{-1} shrimp of dsSN3. Shrimps injected with dsGFP were used as a control group. To determine the earliest time point for complete *PmTSN* knockdown, hemolymph was individually collected at 0, 1, 3, 5 and 7 days post injection. To examine the expression of *PmTSN*, multiplex RT-PCR was performed as described above. The PCR products were analyzed on 1.5% agarose gel electrophoresis, stained with ethidium bromide and visualized under ultraviolet light. The intensity of each band was quantified by Scion image analysis program. The relative expression level of *PmTSN* was normalized against *β-actin* and expressed in arbitrary units.

2.9. Functional assay of PmTSN in dsRNA-mediated gene silencing

Shrimps (size 4–5 g, 6 shrimp per group) were intramuscularly injected with dsSN3 or dsGFP (5 μg g^{-1} shrimp) for 48 h prior to injecting with dsRab7 (0.63 μg g^{-1} shrimp). Hemolymph was individually collected at 48 h post dsRab7 injection. Shrimps injected with 150 mM NaCl or dsRab7 alone were used as control groups. Total RNA (1 μg) was used for cDNA synthesis. The expression of *PmTSN* and *PmRab7* was determined by quantitative real-time PCR (qRT-PCR) analysis.

qRT-PCR was performed in an ABI 7500 real-time detection system (Applied Biosystems) using KAPA™ SYBR® FAST master mix (2X) ABI Prism™ (KAPA Biosystems). The primers for *PmTSN* were qRTSN-F3and qRTSN-R3, and the primers for *PmRab7* were qRab7-F2 and qRab7-R2. The primers for an internal control gene, *EF1-α* were EF1a-F and EF1a-R. All primers used for qRT-PCR are listed in Table 1. qRT-PCR was carried out in triplicates for each sample in a 20-μl reaction containing 10 μl of 2X KAPA™ SYBR® FAST master mix, 5 μl of 1:50 diluted cDNA, 0.25 μl of 10 μM of each primer and 4.5 μl of sterile water. PCR amplification was performed under the following conditions: enzyme activation at 95 °C for 3 min, followed by 40 cycles of 95 °C for 3 s and 60 °C for 31 s. The specificity of primers was determined by melting curve analysis from the ABI Prism 7500 detection system. The cycle threshold (Ct) value for the *PmTSN* and *PmRab7* target genes and the internal control *EF1-α* gene were determined for each sample. The expression levels of *PmTSN* and *PmRab7* in each treatment group relative to NaCl-injected group were then determined by comparative Ct method ($2^{-\Delta\Delta Ct}$) [37].

2.10. Cumulative mortality assay

Shrimps (size 4–5 g, 9–15 shrimp per group) were injected with 5 μg g^{-1} shrimp of dsSN3, dsGFP or 150 mM NaCl for 48 h prior to injecting with a mixture of dsYHV (2.5 μg g^{-1} shrimp) and 50 μl of the 10^7 fold diluted YHV stock. Shrimps injected with 150 mM NaCl or YHV alone were used as control groups. Shrimp mortality was recorded twice a day for 10 days after the second injection. Expression of YHV was detected from gill tissues of death shrimps by using multiplex RT-PCR [38]. Only the death shrimp that can be detected YHV expression was used to calculate the cumulative percent mortality.

2.11. Statistical analysis

The data were expressed as mean ± standard error (SEM). The statistical analysis of the mean ± SEM was performed by using ANOVA in the Sigma Stat 3.5 program. A measurement of $P < 0.05$ was accepted as statistically significant.

3. Results

3.1. Cloning and sequence analysis of P. monodon Tudor staphylococcal nuclease

The full-length cDNA encoding TSN from *P. monodon* (*PmTSN*) was cloned by PCR approach. A 1043-bp fragment of *PmTSN*

corresponding to SN4 and Tudor domains was obtained by RT-PCR with TuF1 and TuR1 primers. A BLAST search of the nucleotide and deduced amino acid sequences revealed that the product shared high sequence similarity with TSN from other species. This partial sequence was used to design gene specific primers to clone the 3′ and 5′ ends of this gene by RACE. Amplification of the full-length *PmTSN* coding region was used to confirm the sequence. The full-length of *PmTSN* cDNA consisted of 2897 bp, containing 44 bp in the 5′ untranslated region (UTR), 2670 bp in an open reading frame (ORF), and 183 bp in the 3′ UTR with a poly A-tail (Fig. 1). The translation initiation sequence (nucleotides 42-47, CAA*CATG*G) was in an agreement with the Kozak's consensus sequence. In addition, atypical polyadenylation signal (AATTAAA) was found to reside 10 bp upstream of the poly (A) tail. The nucleotide sequence of *PmTSN* cDNA was submitted in the GenBank database under the accession number EF_429696.

The ORF of *PmTSN* encoded a polypeptide of 889 amino acids with an estimated molecular weight of 99.7 kDa and a predicted isoelectric point of 8. The deduced amino acid sequence of *PmTSN* was compared to TSN sequences from other known species.

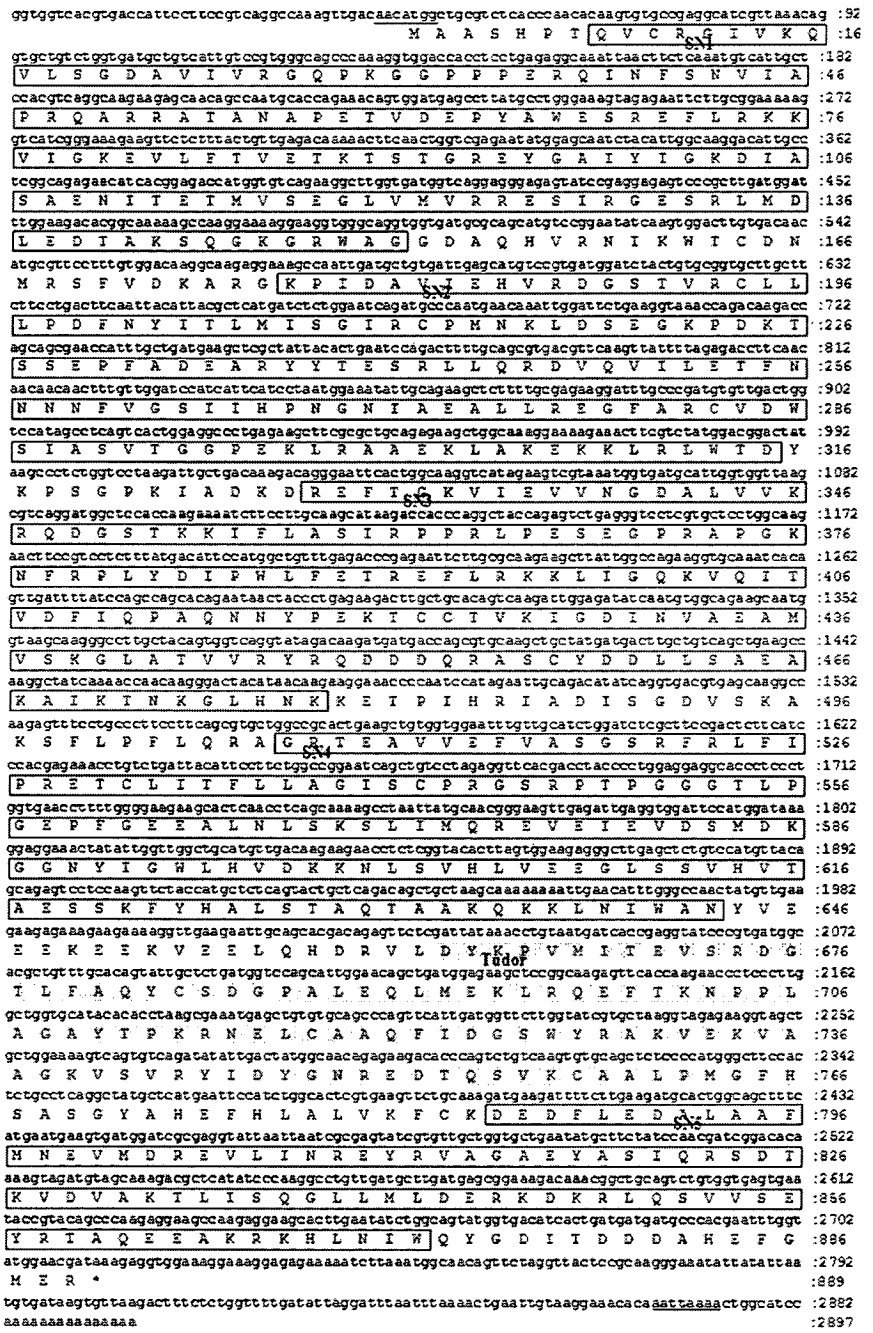

Fig. 1. The nucleotide and deduced amino acid sequences of *PmTSN* cDNA. Kozak's sequence and polyadenylation signal are underlined. The deduced amino acid sequence of *PmTSN* is shown in a single letter under the respective codon. Staphylococcal nuclease-like domains (SN) are boxed and a Tudor domain is shaded. The asterisk represents the stop codon. This nucleotide sequence is available in the GenBank database under the accession number EF_429696.

Sequence alignment showed that PmTSN had higher identities (54–57%) to vertebrate TSN. Among these, PmTSN showed the highest (57%) amino acid sequence identity to TSN of *Danio rerio* (GenBank ID: NP_878285). In addition, PmTSN showed 50%, 51% and 54% amino acid sequence identities with TSN of *C. elegans* (GenBank ID: NP_494839), *Anopheles gambiae* (GenBank ID: XP_315689) and *D. melanogaster* (GenBank ID: NP_612021), respectively, while it exhibited lower identities of 29–34% with plants, fungi and slime mold.

Phylogenetic analysis based on a bootstrapped NJ tree indicated that TSN proteins could be divided into four clusters, including vertebrates, other invertebrates, plants, and fungi (Fig. 2). Interestingly, PmTSN clustered on a separated branch from vertebrate and other invertebrate clusters. Similar tree was obtained from the analysis based on Maximum Parsimony method (data not shown). In addition, the domain structures of TSN proteins from shrimp and several organisms including *Homo sapiens* (GenBank ID: NP_055205), *C. elegans*, *D. melanogaster*, *Arabidopsis thaliana* (GenBank ID: NP_200986), *Aspergillus fumigatus* (GenBank ID: XP_753714), and *Schizosaccharomyces pombe* (GenBank ID: NP_588117) were compared (Fig. 3). PmTSN contained four SN domains at the N-terminus, followed by a Tudor and a partially truncated SN domain. A severely truncated SN5 domain was found in TSN of *H. sapiens*, whereas a SN5 domain of TSN of *C. elegans* and *D. melanogaster* overlapped with a Tudor domain. A SN5 domain was totally absent in TSN of *S. pombe*. In addition, a partially truncated SN5 domain was also found in TSN of *A. thaliana* and *A. fumigatus*, but distinct from PmTSN in term of amino acid sequence identities (26% identities, supplementary Table 1).

3.2. Tissue distribution study

The expression of *PmTSN* in various tissues of shrimp was determined by multiplex RT-PCR. The result in Fig. 4 revealed that

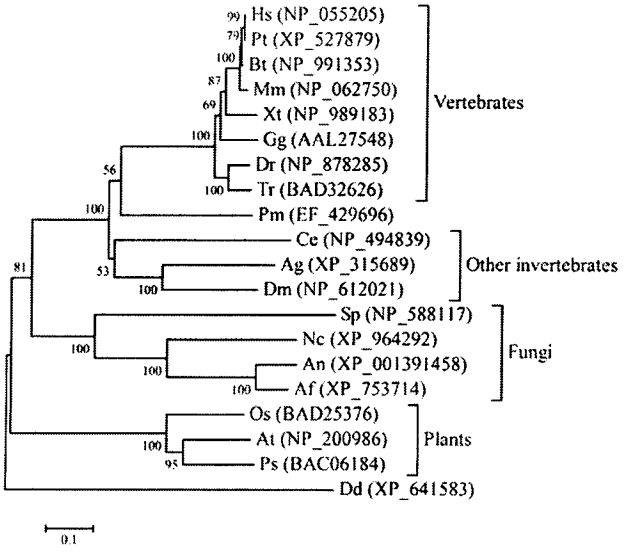

Fig. 2. Phylogenetic relationship of TSN on the basis of amino acid sequence using neighbor-joining distance analysis. *Hs, Homo sapiens*; *Pt, Pan troglodytes*; *Bt, Bos Taurus*; *Mm, Mus musulus*; *Gg, Gallus gallus*; *Xt, Xenopus tropicalis*; *Dr, Danio rerio*; *Tr, Takifugu rupripes*; *Pm, Penaeus monodon*; *Ce, Caenorhabditis elegans*; *Ag, Anopheles gambiae*; *Dm, Drosophila melanogaster*; *Sp, Schizosaccharomyces pombe*; *Nc, Neurospora crassa*; *An, Aspergillus niger*; *Af, Aspergillus fumigatus Os, Oryza sativa*; *At, Arabidopsis thaliana*; *Ps, Pisum sativum* and *Dd, Dictyostelium discoideum*. The GenBank accession number of TSN from each species was shown in the parenthesis. Bootstrap values from 1000 replicates are indicated at the nodes.

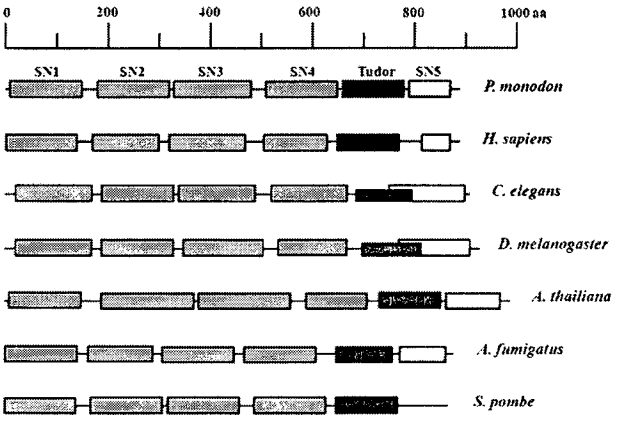

Fig. 3. Schematic diagram representation of the predicted domain structure of PmTSN (GenBank ID: EF_429696) and comparison with the predicted structure of TSN proteins of *H. sapiens* (GenBank ID: NP_0055205); *C. elegans* (GenBank ID: NP_494839); *D. melanogaster* (GenBank ID: NP_612021); *A. thaliana* (GenBank ID: NP_200986); *A. fumigatus* (GenBank ID: XP_753714) and *S. pombe* (GenBank ID: NP_588117). The locations of six functional domains are indicated: SN, staphylococcal nuclease-like domain; Tudor, Tudor domain.

PmTSN was ubiquitously expressed in all examined tissues including hemolymph, lymphoid, gill, thoracic ganglia, testis, stomach, hepatopancreas, abdominal muscle and pleopod.

3.3. Knockdown of PmTSN in vivo using dsRNA

The dsRNA targeting the SN3 domain of *PmTSN* (dsSN3) was used to knockdown the expression of *PmTSN in vivo* (Fig. 5A). Shrimps were intramuscularly injected with 5 $\mu g\, g^{-1}$ shrimp of dsSN3. Shrimps injected with dsGFP (5 $\mu g\, g^{-1}$ shrimp) were used as a control group. The knockdown effect of dsSN3 on *PmTSN* expression was shown in Fig. 5B and C. Injection of dsSN3 significantly decreased ($P < 0.05$) the *PmTSN* transcript approximately 86% at 1 day post dsSN3 injection. The knockdown effect of *PmTSN* persisted at least 7 days. However, injection of dsGFP, an unrelated dsRNA had no effect on the level of *PmTSN* transcript. This result suggested the sequence-specific inhibition of *PmTSN* by dsSN3.

3.4. The effect of PmTSN knockdown on dsRNA-mediated gene silencing in shrimp

To examine the involvement of *PmTSN* in the shrimp RNAi pathway, dsRNA-mediated gene silencing approach was used to knock down the expression of *PmTSN in vivo*. Subsequently, the ability of dsRab7 in inhibition of *PmRab7* expression was determined. The knockdown effect of *PmTSN* and *PmRab7* were determined by qRT-PCR. The representative amplification plots of *PmTSN*, *PmRab7* and *EF-1α* were shown in Supplementary Fig. 2. The result in Fig. 6 showed that similar reduction of *PmRab7* transcript at 85.5% and 85% was observed in shrimps injected with

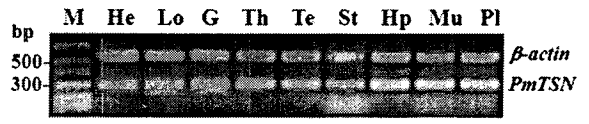

Fig. 4. Tissue distribution study of *PmTSN* expression in *P. monodon*. A representative gel represents RT-PCR products of *PmTSN* and *β-actin*. M, 1 kb + DNA ladder; He, hemolymph; Lo, lymphoid organ; G, gill; Th, thoracic ganglia; Te, testis; St, stomach; Hp, hepatopancreas; Mu, abdominal muscle; and Pl, pleopods.

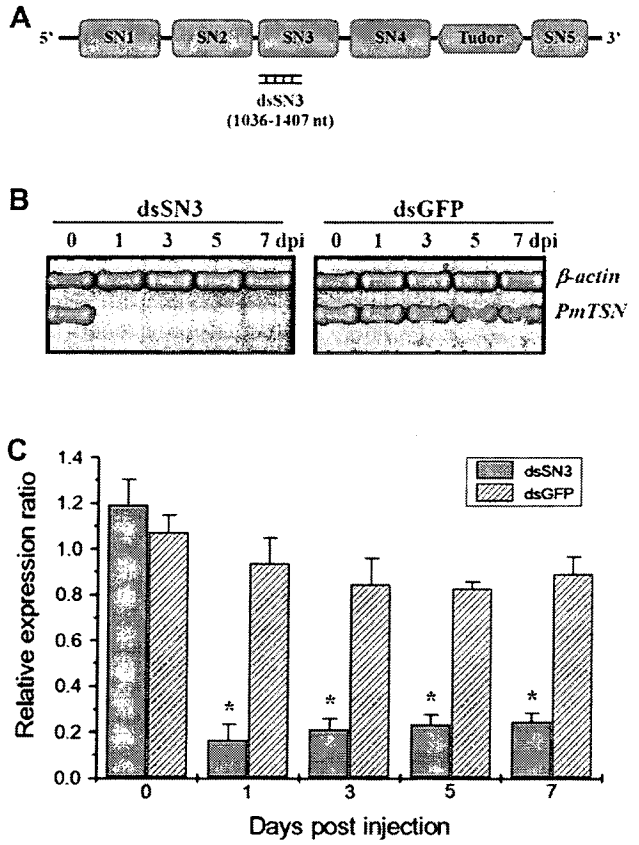

Fig. 5. RNAi knockdown of *PmTSN* transcript in *P. monodon* hemolymph. (A) Schematic diagram representation of *PmTSN* and the target region of dsSN3. (B) A representative gel of RT-PCR products showing *PmTSN* expression at 0, 1, 3, 5 and 7 days post dsSN3 or dsGFP injection. *β-actin* was used as an internal control. (C) Relative expression of *PmTSN* normalized with *β-actin*. Bars represent mean ± SEM ($n = 6$). The asterisks represent the significant difference ($P < 0.05$) between before and 1, 3, 5 or 7 days after dsRNA injection.

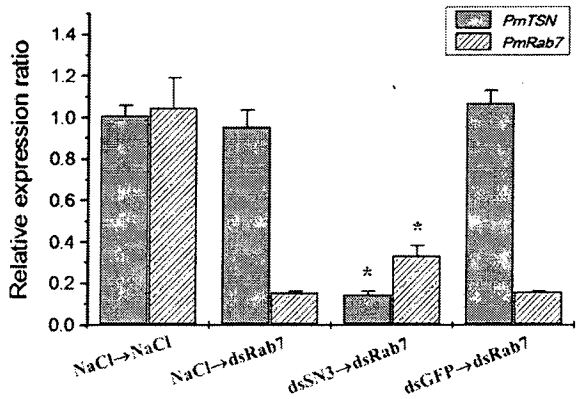

Fig. 6. Efficiency of RNAi in *PmTSN*-knockdown shrimp. Quantitative real-time PCR was performed with specific primers for *PmTSN* and *PmRab7*. *EF1-α* was used as an internal control for normalization. The relative expression of *PmTSN* and *PmRab7* was calculated by comparative Ct method ($2^{-\Delta\Delta Ct}$). Bars represent means ± SEM ($n = 6$). The asterisks (*) represent the significant difference ($P < 0.05$) of the relative *PmTSN* and *PmRab7* expression among dsSN3 → dsRab7 group and other groups.

dsRab7 alone (NaCl → dsRab7) and with dsGFP followed by dsRab7 (dsGFP → dsRab7), respectively. In contrast, only 68.3% reduction of *PmRab7* transcript was observed in *PmTSN*-knockdown shrimps (85.6% knockdown of *PmTSN*). The results showed a significant increase of the *PmRab7* transcript ($P < 0.05$) in *PmTSN*-knockdown shrimps when compared to the NaCl → dsRab7 and dsGFP → dsRab7 groups which had normal transcript levels of PmTSN. This result indicated that the ability of dsRab7 to knock down *PmRab7* was partially diminished in *PmTSN*-knockdown shrimp.

3.5. Cumulative mortality assay

To further examine the involvement of PmTSN in the shrimp RNAi pathway, the effect of *PmTSN* knockdown on the ability of dsYHV in inhibition of YHV replication was determined by cumulative mortality assay (Fig. 7). The *PmTSN*-knockdown shrimp (dsSN3 → dsYHV + YHV) had a cumulative mortality of 35% at 10 days post YHV challenge, whilst the mortalities of shrimps in the NaCl → dsYHV + YHV and dsGFP → dsYHV + YHV groups was 12% and 9%, respectively. The significant increase in shrimp mortality ($P < 0.05$) was observed in the *PmTSN*-knockdown shrimps. The multiplex RT-PCR analysis of *PmTSN* expression in survival shrimps showed that the knockdown effect was still observed in *PmTSN*-knockdown shrimps (Supplementary Fig. 3).

4. Discussion

In this study, we have cloned and characterized a Tudor staphylococcal nuclease (TSN) gene from black tiger shrimp, *P. monodon*. To our knowledge, this is the first report of TSN in crustacean. The full-length cDNA of *PmTSN* is 2897 bp, encoding a protein of 889 amino acids with a predicted molecular weight of 99.7 kDa. Analysis of the deduced amino acid sequence of *PmTSN* revealed that the PmTSN showed the domain organization similar to that seen in other organisms by exhibiting the four tandem repeats of SN domains followed by a Tudor and SN5 domain. Based on phylogenetic analysis and the characteristics of SN5 domain, TSN could be divided into five categories [39]. Our analysis showed that PmTSN contains a partially truncated SN5 domain, but distinct from higher plant and fungal types in term of amino acid sequence similarities. Interestingly, phylogenetic analysis revealed that PmTSN was more closely related to vertebrate TSN by sharing the highest sequence identity of 57% with TSN of *D. rerio*, and PmTSN clustered on a separated branch from vertebrate and other invertebrate clusters on the bootstrapped NJ tree. From these results, we proposed that

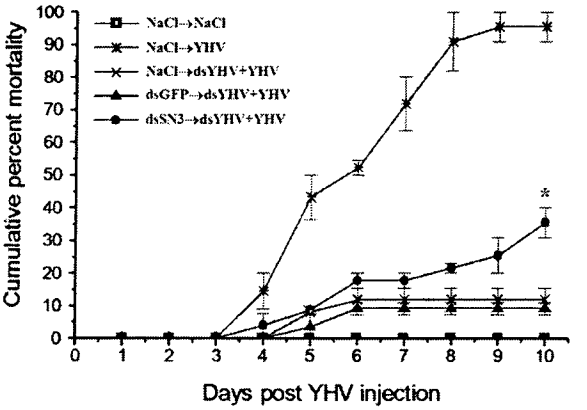

Fig. 7. Increase in cumulative mortality upon YHV challenge in *PmTSN*-knockdown shrimp. Cumulative percent mortality in each treatment group (9-15 shrimps per group) is presented as means ± SEM. Two independent experiments were performed. An asterisk (*) represents the significant difference ($P > 0.05$) among *PmTSN*-knockdown shrimp (dsSN3 → dsYHV + YHV) and other groups.

PmTSN represents a new type of TSN, a crustacean type. Further identification of the crustacean TSN will provide a better understanding of the evolutionary relatedness of this protein. Tissue distribution study revealed the expression of *PmTSN* in all examined tissues with the similar level of transcript. Given the fact that TSN involves in a variety of cellular processes, a ubiquitous distribution of *PmTSN* indicated that this protein may involve in one or more cellular processes common to all cell types in shrimp. In human, TSN exists in a wide range of organs and tissues, especially in epithelial cells [40].

In this study, knockdown of *PmTSN* diminished the efficiency of dsRNA-mediated gene silencing in shrimp. A partially impaired *PmRab7* silencing was observed in *PmTSN*-knockdown shrimps. However, it was not observed in shrimps injected with NaCl and dsGFP, suggesting the involvement of PmTSN in dsRNA-mediated gene silencing. In *C. elegans*, knockdown of *tsn-1* expression was also found to impair the efficiency of RNAi [17]. In shrimp, knockdown of the core RNAi machinery, *Pem-ago1* led to the impairment of RNAi to silence the endogenous gene in primary lymphoid cell culture [13]. In this study, we also found that knockdown of *PmTSN* resulted in a decrease of the ability of dsYHV in inhibition of YHV replication. An increase of the cumulative percent mortality was observed. The multiplex RT-PCR analysis of *PmTSN* expression in the survival shrimps showed that the knockdown effect is still observed in shrimps injected with dsSN3. Previous study reported that knockdown of PmDicer (*PmDcr-1*) enhanced the susceptibility of gill-associated virus infection [11]. In our study, knockdown of *PmTSN* did not increase the susceptibility of shrimp to YHV infection. The level of *PmTSN* transcript in hemolymph did not change significantly after YHV challenge (data not shown). This indicated that the decrease of the ability of dsYHV is the result of *PmTSN* knockdown. These results suggested that PmTSN involved in dsRNA-mediated gene silencing in shrimp.

Silencing of RNAi components resulted in a general loss of RNAi mechanism [41]. In *D. melanogaster*, *r2d2* and *loqs* mutants showed impaired silencing triggered by injection of exogenous dsRNA or by artificial and natural expression of endogenous dsRNA [42]. Knockdown of MOV10, a putative DExD-box helicase and TNRC6B, a marker of mRNA-degrading cytoplasmic processing bodies (P-bodies) resulted in failure of miRNA-guide mRNA cleavage in HeLa cells [43]. However, knockdown of some additional components which play a minor role in RNAi, such as dFXR and VIG were found to partially diminish RNAi activity in *Drosophila* [18]. It is noteworthy that knockdown of *PmTSN* expression did not substantially reduce the efficiency of dsRNA-mediated gene silencing in shrimp. We speculate that PmTSN may function as a minor component which affect the efficiency of RISC, but not absolutely required for RNAi in shrimp. However, we could not completely knockdown the expression of *PmTSN*. Therefore, the possibility that the residual PmTSN can function in the shrimp RNAi pathway cannot be ruled out. This effect may interfere us for observing the greater effect of *PmTSN* knockdown on dsRNA-mediated gene silencing in shrimp.

In conclusion, we provide the first description of the crustacean TSN from *P. monodon*. Our findings suggest that PmTSN involves in dsRNA-mediated gene silencing in shrimp. However, the mode of action of PmTSN in the shrimp RNAi pathway is still unknown. Therefore, identification of the PmTSN-interacting proteins will be essential for better understanding of the RNAi mechanism in the penaeid shrimp.

Acknowledgements

The authors thank Asst. Prof. Dr. Witoon Tirasophon for the viral stock, Ms. Chaweewan Chimwai and Ms. Pensri Hongthong for technical assistance. This work is supported by grants from the Thailand Research Fund (TRF), the Office of the Higher Education Commission (CHE) and Mahidol University under the National Research University Initiatives. A student fellowship granted to A.P. by the Royal Golden Jubilee Ph.D. Program.

Appendix. Supplementary data

Supplementary data associated with this article can be found in the online version, at doi:10.1016/j.fsi.2011.05.026.

References

[1] Carthew RW, Sontheimer EJ. Origins and mechanisms of miRNAs and siRNAs. Cell 2009;136:642–55.
[2] Fire A, Xu S, Montgomery MK, Kostas SA, Driver SE, Mello CC. Potent and specific genetic interference by double-stranded RNA in *Caenorhabditis elegans*. Nature 1998;391:806–11.
[3] Castanotto D, Rossi JJ. The promises and pitfalls of RNA-interference-based therapeutics. Nature 2009;457:426–33.
[4] Lopez-Fraga M, Wright N, Jimenez A. RNA interference-based therapeutics: new strategies to fight infectious disease. Infect Disord Drug Targets 2008;8: 262–73.
[5] Hirono I, Fagutao FF, Kondo H, Aoki T. Uncovering the mechanisms of shrimp innate immune response by RNA interference. Mar Biotechnol (NY); 2010. doi:10.1007/s10126-010-9292-0.
[6] Robalino J, Bartlett T, Shepard E, Prior S, Jaramillo G, Scura E, et al. Double-stranded RNA induces sequence-specific antiviral silencing in addition to nonspecific immunity in a marine shrimp: convergence of RNA interference and innate immunity in the invertebrate antiviral response? J Virol 2005;79: 13561–71.
[7] Attasart P, Kaewkhaw R, Chimwai C, Kongphom U, Namramoon O, Panyim S. Inhibition of *Penaeus monodon* densovirus replication in shrimp by double-stranded RNA. Arch Virol 2010;155:825–32.
[8] Ongvarrasopone C, Chomchay E, Panyim S. Antiviral effect of PmRab7 knockdown on inhibition of Laem-Singh virus replication in black tiger shrimp. Antiviral Res 2010;88:116–8.
[9] Xu J, Han F, Zhang X. Silencing shrimp white spot syndrome virus (WSSV) genes by siRNA. Antiviral Res 2007;73:126–31.
[10] Chen YH, Jia XT, Zhao L, Li CZ, Zhang S, Chen YG, et al. Identification and functional characterization of Dicer2 and five single VWC domain proteins of *Litopenaeus vannamei*. Dev Comp Immunol 2011;35:661–71.
[11] Su J, Oanh DT, Lyons RE, Leeton L, van Hulten MC, Tan SH, et al. A key gene of the RNA interference pathway in the black tiger shrimp, *Penaeus monodon*: identification and functional characterisation of Dicer-1. Fish Shellfish Immunol 2008;24:223–33.
[12] Yao X, Wang L, Song L, Zhang H, Dong C, Zhang Y, et al. A Dicer-1 gene from white shrimp *Litopenaeus vannamei*: expression pattern in the processes of immune response and larval development. Fish Shellfish Immunol 2010;29: 565–70.
[13] Dechklar M, Udomkit A, Panyim S. Characterization of Argonaute cDNA from *Penaeus monodon* and implication of its role in RNA interference. Biochem Biophys Res Commun 2008;367:768–74.
[14] Labreuche Y, Veloso A, de la Vega E, Gross PS, Chapman RW, Browdy CL, et al. Non-specific activation of antiviral immunity and induction of RNA interference may engage the same pathway in the Pacific white leg shrimp *Litopenaeus vannamei*. Dev Comp Immunol 2010;34:1209–18.
[15] Unajak S, Boonsaeng V, Jitrapakdee S. Isolation and characterization of cDNA encoding Argonaute, a component of RNA silencing in shrimp (*Penaeus monodon*). Comp Biochem Physiol B Biochem Mol Biol 2006;145:179–87.
[16] Wang S, Liu N, Chen AJ, Zhao XF, Wang JX. TRBP homolog interacts with eukaryotic initiation factor 6 (eIF6) in *Fenneropenaeus chinensis*. J Immunol 2009;182:5250–8.
[17] Caudy AA, Ketting RF, Hammond SM, Denli AM, Bathoorn AM, Tops BB, et al. A micrococcal nuclease homologue in RNAi effector complexes. Nature 2003; 425:411–4.
[18] Caudy AA, Myers M, Hannon GJ, Hammond SM. Fragile X-related protein and VIG associate with the RNA interference machinery. Genes Dev 2002;16: 2491–6.
[19] Tsuchiya N, Ochiai M, Nakashima K, Ubagai T, Sugimura T, Nakagama H. SND1, a component of RNA-induced silencing complex, is up-regulated in human colon cancers and implicated in early stage colon carcinogenesis. Cancer Res 2007;67:9568–76.
[20] Callebaut I, Mornon JP. The human EBNA-2 coactivator p100: multidomain organization and relationship to the staphylococcal nuclease fold and to the tudor protein involved in *Drosophila melanogaster* development. Biochem J 1997;321(Pt 1):125–32.
[21] Pham JW, Pellino JL, Lee YS, Carthew RW, Sontheimer EJ. A Dicer-2-dependent 80S complex cleaves targeted mRNAs during RNAi in *Drosophila*. Cell 2004; 117:83–94.

[22] Tong X, Drapkin R, Yalamanchili R, Mosialos G, Kieff E. The Epstein-Barr virus nuclear protein 2 acidic domain forms a complex with a novel cellular coactivator that can interact with TFIIE. Mol Cell Biol 1995;15:4735–44.
[23] Paukku K, Yang J, Silvennoinen O. Tudor and nuclease-like domains containing protein p100 function as coactivators for signal transducer and activator of transcription 5. Mol Endocrinol 2003;17:1805–14.
[24] Yang J, Aittomaki S, Pesu M, Carter K, Saarinen J, Kalkkinen N, et al. Identification of p100 as a coactivator for STAT6 that bridges STAT6 with RNA polymerase II. EMBO J 2002;21:4950–8.
[25] Valineva T, Yang J, Palovuori R, Silvennoinen O. The transcriptional coactivator protein p100 recruits histone acetyltransferase activity to STAT6 and mediates interaction between the CREB-binding protein and STAT6. J Biol Chem 2005;280:14989–96.
[26] Yang J, Valineva T, Hong J, Bu T, Yao Z, Jensen ON, et al. Transcriptional coactivator protein p100 interacts with snRNP proteins and facilitates the assembly of the spliceosome. Nucleic Acids Res 2007;35:4485–94.
[27] Scadden AD. The RISC subunit Tudor-SN binds to hyper-edited double-stranded RNA and promotes its cleavage. Nat Struct Mol Biol 2005;12:489–96.
[28] Assavalapsakul W, Smith DR, Panyim S. Propagation of infectious yellow head virus particles prior to cytopathic effect in primary lymphoid cell cultures of *Penaeus monodon*. Dis Aquat Organ 2003;55:253–8.
[29] Posiri P, Ongvarrasopone C, Panyim S. Improved preventive and curative effects of YHV infection in *Penaeus monodon* by a combination of two double stranded RNAs. Aquaculture 2011;314:34–8.
[30] Altschul SF, Gish W, Miller W, Myers EW, Lipman DJ. Basic local alignment search tool. J Mol Biol 1990;215:403–10.
[31] Gattiker A, Gasteiger E, Bairoch A. ScanProsite: a reference implementation of a PROSITE scanning tool. Appl Bioinformatics 2002;1:107–8.
[32] Geer LY, Domrachev M, Lipman DJ, Bryant SH. CDART: protein homology by domain architecture. Genome Res 2002;12:1619–23.
[33] Chenna R, Sugawara H, Koike T, Lopez R, Gibson TJ, Higgins DG, et al. Multiple sequence alignment with the Clustal series of programs. Nucleic Acids Res 2003;31:3497–500.
[34] Kumar S, Nei M, Dudley J, Tamura K. MEGA: a biologist-centric software for evolutionary analysis of DNA and protein sequences. Brief Bioinform 2008;9:299–306.
[35] Saitou N, Nei M. The neighbor-joining method: a new method for reconstructing phylogenetic trees. Mol Biol Evol 1987;4:406–25.
[36] Ongvarrasopone C, Chanasakulniyom M, Sritunyalucksana K, Panyim S. Suppression of PmRab7 by dsRNA inhibits WSSV or YHV infection in shrimp. Mar Biotechnol (NY) 2008;10:374–81.
[37] Pfaffl MW. A new mathematical model for relative quantification in real-time RT-PCR. Nucleic Acids Res 2001;29. e45.
[38] Tirasophon W, Yodmuang S, Chinnirunvong W, Plongthongkum N, Panyim S. Therapeutic inhibition of yellow head virus multiplication in infected shrimps by YHV-protease dsRNA. Antiviral Res 2007;74:150–5.
[39] Abe S, Sakai M, Yagi K, Hagino T, Ochi K, Shibata K, et al. A Tudor protein with multiple SNc domains from pea seedlings: cellular localization, partial characterization, sequence analysis, and phylogenetic relationships. J Exp Bot 2003;54:971–83.
[40] Saarikettu J, Ovod V, Vuoksio M, Grönholm J, Yang J, Silvennoinen O. Monoclonal antibodies against human Tudor-SN. Hybridoma 2010;29:231–6.
[41] Kuehbacher A, Urbich C, Zeiher AM, Dimmeler S. Role of Dicer and Drosha for endothelial microRNA expression and angiogenesis. Circ Res 2007;101:59–68.
[42] Marques JT, Kim K, Wu PH, Alleyne TM, Jafari N, Carthew RW. Loqs and R2D2 act sequentially in the siRNA pathway in *Drosophila*. Nat Struct Mol Biol 2009;17:24–30.
[43] Meister G, Landthaler M, Peters L, Chen PY, Urlaub H, Luhrmann R, et al. Identification of novel argonaute-associated proteins. Curr Biol 2005;15:2149–55.

Fish & Shellfish Immunology 34 (2013) 875–884

Contents lists available at SciVerse ScienceDirect

Fish & Shellfish Immunology

journal homepage: www.elsevier.com/locate/fsi

Penaeus monodon Tudor staphylococcal nuclease preferentially interacts with N-terminal domain of Argonaute-1

Amnat Phetrungnapha [a], Sakol Panyim [a,b], Chalermporn Ongvarrasopone [a,*]

[a] *Institute of Molecular Biosciences, Mahidol University (Salaya Campus), 25/25 Phutthamonthon 4 Road, Salaya, Phutthamonthon District, Nakhon Pathom 73170, Thailand*
[b] *Department of Biochemistry, Faculty of Science, Mahidol University, Rama VI Road, Phayathai, Bangkok 10400, Thailand*

ARTICLE INFO

Article history:
Received 16 November 2012
Received in revised form
17 December 2012
Accepted 23 December 2012
Available online 18 January 2013

Keywords:
RISC
RNAi
In vitro pull-down
Yeast two-hybrid system
Black tiger shrimp

ABSTRACT

RNA interference (RNAi) plays a crucial role as an antiviral defense in several organisms including plants and invertebrates. An understanding of RNAi machineries especially protein components of the RNA-induced silencing complex (RISC) is essential for prior to applying RNAi as a tool for viral protective immunity in shrimp. Tudor staphylococcal nuclease (TSN) is an evolutionarily conserved protein and is one of the RISC components. In previous study, suppression of *Penaeus monodon* TSN (*PmTSN*) by double-stranded RNA (dsRNA) resulted in decreasing dsRNA-mediated gene silencing activity. To elucidate the functional significance of PmTSN in shrimp RNAi pathway, interactions between PmTSN and three Argonaute proteins (PmAgo) were characterized by yeast two-hybrid and *in vitro* pull-down assays. The results demonstrated that PmTSN interacted with PmAgo1, but not with PmAgo2 or PmAgo3. The interaction between PmAgo and PmTSN was mediated through the N-terminal domain of PmAgo1 and the SN1-2 domains of PmTSN. Analysis of the nuclease activity of the recombinant PmTSN indicated that PmTSN possessed calcium-dependent nuclease activity specific to single-stranded RNA (ssRNA), but not dsRNA and DNA. Knockdown of *PmAgo1* and *PmTSN* diminished the ability of dsRNA-Rab7 to knockdown *PmRab7* expression, indicating the involvement of PmAgo1 and PmTSN in shrimp RNAi pathway. Taken together, the results imply that PmTSN is one of the components of PmAgo1-RISC, thus providing new insights in the RNAi-based mechanism in shrimp.

1. Introduction

Invertebrates employ RNAi as a major host-defense mechanism against viruses [1]. In *Drosophila melanogaster*, the dsRNA-replicative intermediate of viruses is recognized and cleaved by Dicer, generating viral-derived small RNA which is subsequently incorporated into RISC, and mediated the degradation of viral RNA [1–3]. In addition, mutation of the core RNAi machineries such as Dicer-2, Ago2, and R2D2 substantially increases susceptibility of the mutant flies to viruses, indicating the crucial role of RNAi as an antiviral immunity in invertebrates [4–7]. A number of evidences emphasized that dsRNA triggered an antiviral response in shrimp in both sequence-independent [8] and sequence-specific manners [9–12]. Even though, there are several evidences revealing the existence of RNAi, the mechanism by which the RNAi operates in shrimp cells is not yet completely understood. An understanding of the RNAi machineries especially the components of RISC will provide insights into an innate antiviral immunity and the host–viral interaction in this economically important species.

Tudor staphylococcal nuclease (TSN, also known as SND1 or p100) is an evolutionarily conserved protein which is composed of four tandem repeats of staphylococcal nuclease-like domains (SN), followed by Tudor and C-terminal SN domains. It is a multifunctional protein involved in a variety of cellular processes. For example, TSN can interact with several transcription factors to modulate their activities such as a transcriptional co-activator of Epstein–Barr virus nuclear antigen 2 (EBNA2), STAT5, STAT6, c-Myb, and Pim-1 [13–16]. In RNA splicing, TSN regulates small nuclear ribonucleoprotein (snRNP) assembly by interacting with SmB/B′ and SmD1/D3, the core proteins of snRNP complex [17]. In addition, cleavage of TSN by caspase-3 is important for the execution of apoptosis in plant and human [18]. Despite its roles in several biological processes as described above, Caudy et al., 2003 revealed that TSN also involved in RNAi pathway in *Caenorhabditis elegans*, *D. melanogaster*, and mammals. Biochemical fractionation of RISC from these organisms revealed that TSN was co-purified with other proteins of RISC including Ago, VIG, and FMRP, and also resided in miRNA-ribonucleoprotein complex (miRNP) [19]. In addition,

* Corresponding author. Tel.: +66 2 8003624x1280; fax: +66 2 4419906.
E-mail address: chalermporn.ong@mahidol.ac.th (C. Ongvarrasopone).

1050-4648/$ – see front matter © 2013 Elsevier Ltd. All rights reserved.
http://dx.doi.org/10.1016/j.fsi.2012.12.012

suppression of *TSN* expression impaired the RNAi activity indicating the importance of this protein in the RNAi mechanism [19–21].

In previous study, we identified and characterized a TSN gene from the black tiger shrimp, *Penaeus monodon*. The *P. monodon* TSN gene (*PmTSN*) encoded a polypeptide of 889 amino acids with an estimated molecular weight of 99.7 kDa. It contained the four tandem repeats of SN domains followed by a Tudor and a partially truncated C-terminal SN domain. Silencing of *PmTSN* expression by dsRNA resulted in diminishing of the dsRNA-mediated gene silencing in shrimp [22]. In this study, to elucidate the functional insights of PmTSN as one of the components of RISC, we characterized the interaction between PmTSN and the catalytic engine of RNAi, PmAgo by using yeast two-hybrid (Y2H) and *in vitro* pull-down assays. In addition, the nuclease activity of the recombinant PmTSN was also investigated.

2. Materials and methods

2.1. Shrimp

The black tiger shrimps, *P. monodon* (~10 g body weight) were purchased from the commercial shrimp farms in Thailand. They were reared in the laboratory tanks with continuous aerated artificial sea water (10 ppt) for 2–3 days before processing to allow acclimatization, and were fed *ad libitum* with commercial shrimp feed. Apparently healthy shrimp free of yellow head virus (YHV) and white spot syndrome virus (WSSV) were selected and used in all experiments.

2.2. Plasmid construction

The plasmids pGEM-T containing coding regions of PmTSN (GenBank acc. no. JF429696), PmAgo1 (GenBank acc. no. DQ663629), PmAgo2 (kindly provided by Dr. Apinunt Udomkit, Mahidol University, Thailand), and PmAgo3 (GenBank acc. no. JX845575) were used as templates for PCR. VENT® DNA polymerase (New England Biolabs) was used for all PCR amplifications. For Y2H assay, the DNA fragment of PmTSN (amino acid residues 1–889) was amplified and cloned into *NdeI/SalI* sites of pGBKT7 to create plasmid expressing GAL4-DNA-binding domain fusion protein (BD-TSN). To generate plasmids expressing GAL4-activation domain fusion protein of PmAgo (AD-Ago), the DNA fragments of PmAgo1 (amino acids residues 1–939) and PmAgo2 (amino acid residues 1–810) were amplified and cloned into *NdeI/XhoI* sites, and PmAgo3 (amino acid residues 1–825) was amplified and cloned into *EcoRI/XhoI* sites of pGADT7, respectively.

For *in vitro* pull-down assay, the DNA fragments of TSN (amino acid residues 1–889), SND (amino acid residues 1–660) and SN34 (amino acid residues 320–889) were amplified and cloned into *XmaI/XhoI* sites of pGEX-5X-1 to generate N-terminal GST-fusion constructs of PmTSN and its deletion mutants. For N-terminal His_6-tagged constructs, the DNA fragments of PmAgo1 (amino acid residues 1–939), NTD-Ago1 (amino acid residues 1–291), NPAZ-Ago1 (amino acid residues 1–409), PAZ-Ago1 (amino acid residues 274–409), PIWI-Ago1 (amino acid residues 402–939), PmAgo2 (amino acid residues 1–810), and PmAgo3 (amino acid residues 1–825) were amplified and cloned into *EcoRI/XhoI* sites of pET-28a(+). All primers used for cloning are listed in Table 1. All constructs were subsequently sequenced to confirm gene sequences and correct reading frames.

2.3. Yeast two-hybrid assay

Matchmaker GAL4 Two-hybrid System 3 (Clontech) was used for yeast two-hybrid studies, according to the manufacturer's protocol. *Saccharomyces cerevisiae* strains Y187 and AH109 were kindly provided by Dr. Saengchan Senapin (Biotec, Thailand). The yeast strain Y187 harboring pGBKT7-TSN was used for mating with the yeast strain AH109 harboring pGADT7-Ago1, -Ago2, or -Ago3. The mated cultures were selected on synthetic double dropout medium (SD/-L/-W). Protein interaction was further indicated on synthetic quadruple dropout medium (SD/-L/-W/-H/-A) containing X-α-Gal (40 μg/ml). Yeast harboring pGBKT7-TSN and pGADT7-Laminin receptor (AD-Lamr) served as a positive control whereas yeast harboring pGBKT7-TSN and empty pGADT7 served as a negative control. Preparation of yeast protein extracts was performed according to Yeast Protocol Handbook (Clontech). Expression of BD-TSN and AD-Ago in yeasts were confirmed before performing two-hybrid experiments using anti-c-Myc antibody and anti-HA antibody (US Biological), respectively.

2.4. Protein expression and purification

All GST-fusion and His_6-tagged constructs were expressed in *Escherichia coli* Rossetta (DE3) (Novagen). The recombinant GST-TSN, GST-SND, and GST-SN34 were expressed by using auto-induction approach [23]. Briefly, overnight cultures in non-inducing media ZYP-505 (1% N-Z-amine, 0.5% yeast extract, 50 mM Na_2HPO_4, 50 mM KH_2PO_4, 25 mM $(NH_4)_2SO_4$, 2 mM $MgSO_4$, 0.5% glycerol, and 0.05% glucose) were inoculated in auto-inducing media ZYZ-5052 (1% N-Z-amine, 0.5% yeast extract, 50 mM Na_2HPO_4, 50 mM KH_2PO_4, 25 mM $(NH_4)_2SO_4$, 2 mM $MgSO_4$, 0.5% glycerol, 0.05% glucose, and 0.2% lactose) containing ampicillin (100 μg/ml) and chloramphenicol (34 μg/ml) and incubated at 37 °C with shaking until A_{600} reached ~1.0. The cultures were then incubated at 18 °C for 20 h with shaking. For GST-fusion protein purification, cells were collected by centrifugation, resuspended in lysis buffer (PBS, pH 7.4, 0.2% Triton X-100, 1 mM DTT, 1 mM PMSF, and 100 μg/ml lysozyme) and lysed by sonication. Following centrifugation, the clear cell lysates containing GST-fusion proteins were filtrated and applied to the GSTrap FF column (GE Healthcare) for affinity purification. GST-TSN and GST-SN34 were further purified by anion-exchange chromatography using HiTrap Q column (GE Healthcare). On the other hand, GST-SND was further purified by cation-exchange chromatography using HiTrap SP column (GE Healthcare). The purified proteins were dialyzed against binding buffer (25 mM HEPES, pH 7.5, 150 mM NaCl, 1 mM DTT, 0.2% Triton X-100, 10% glycerol, 1 mM PMSF), concentrated by Vivaspin 6 (GE Healthcare), and determined the concentration by Bradford's assay.

Expression of His_6-tagged fusion proteins were induced by the addition of Isopropyl-β-D-thiogalactopyranoside (IPTG) to a final concentration of 0.2 mM at A_{600} ~ 0.6 and proceeded for 6 h for His-Ago1 and its deletion mutants, or 20 h for His-Ago2 and His-Ago3 at 18 °C with shaking. Following centrifugation, the cells were resuspended in binding buffer at the ratio of 100 OD per ml, lysed by sonication, and centrifuged at 48,000× *g* for 30 min at 4 °C to separate inclusion bodies and cell debris. The clear cell lysates containing His_6-tagged proteins were then divided into small aliquots, flash frozen with liquid nitrogen, and stored at −80 °C until used.

2.5. In vitro pull-down assay

In vitro pull-down assay was performed according to Adachi et al. with some modifications [24]. Ten micrograms of the purified GST-fusion proteins or GST alone were immobilized on 30 μl of 50% (v/v) glutathione-agarose resin (Sigma) for 2 h at 4 °C with rotating. The resins were then washed three times with washing buffer (25 mM HEPES, pH 7.5, 150 mM NaCl, 1 mM DTT, 1% Triton X-100, 10% glycerol, 0.2 mM PMSF). Subsequently, the resins were incubated with the lysates of *E. coli* expressing His_6-tagged proteins for 4 h at 4 °C

Table 1
Primers used in this study. Nucleotides that are underlined indicate restriction sites or T7 promoter sequences.

Primers	Sequence (5′ → 3′)	Purposes
His-Ago1-F	CCGGAATTCATGTACCCTGTCGGGCAGC	Protein expression of His-Ago1
His-Ago1-R	GCCGCTCGAGTTAAGCAAAGTACATGACTCTGT	
His-Ago2-F	CCGGAATTCATGGACGCAGCAAAGGGAAG	Protein expression of His-Ago2
His-Ago2-R	GCCGCTCGAGTTAACTCTCTTGTATATTTA	
His-Ago3-F	CCGGAATTCATGCCTTGGATATCAGAAGTC	Protein expression of His-Ago3
His-Ago3-R	CGGTGCTCGAGTTTACCCTTCTTCCCTTTGCTCGTAT	
NTD-F	GCATTGGAATTCATGTACCCTGTCGGGCAGCC	Protein expression of NTD-Ago1
NTD-R	CAATGCCTCGAGTTATAACACTTCACACAT AAACTC	
NTD-F	GCATTGGAATTCATGTACCCTGTCGGGCAGCC	Protein expression of NPAZ-Ago1
PAZ-R	CAATGCCTCGAGTTATAGTTTCTTGATGCATCGTTG	
PAZ-F	GCATTGGAATTCGCTACAGCATTCTACAAGGC	Protein expression of PAZ-Ago1
PAZ-R	CAATGCCTCGAGTTATAGTTTCTTGATGCATCGTTG	
PIWI-F	GCATTGGAATTCGGACAACGATGCATCAAGAAAC	Protein expression of PIWI-Ago1
PIWI-R	CAATGCCTCGAGTTAAGCAAAGTACATGACTCT GTTTG	
YAgo1-F	GCCAGTCATATGTACCCTGTCGGGCAGC	Y2H: AD-Ago1
YAgo1-R	CTGCAGCTCGAGCAAAGTACATGACTCTGT	
YAgo2-F	GCCAGTCATATGGACGCAGCAAAGGGAAG	Y2H: AD-Ago2
YAgo2-R	CTGCAGCTCGAGCACTCTCTTGTATATTTA	
YAgo3-F	GCCAGTGAATTCATGCCTTGGATATCAGAAGTC	Y2H: AD-Ago3
YAgo3-R	CTGCAGCTCGAGCCCCTTCTTCCCTTTGCTCGTAT	
YTSN-F	GGGAATTCCATATGGCTGCGTCTCACCCAAC	Y2H: BD-TSN
YTSN-R	GGACGCGTCGACGTCGTTCCATACCAAATTCG	
GST-TSN-F	TCCCCCGGGTATGGCTGCGTCTCACCCAAC	Protein expression of GST-TSN
GST-TSN-R	GCCGCTCGAGTTATCGTTCCATACCAAATTCG	
GST-TSN-F	TCCCCCGGGTATGGCTGCGTCTCACCCAAC	Protein expression of GST-SND
GST-SND-R	GCCGCTCGAGTTATCTGTCGTGCTGCAATTCTT	
GST34-F	TCCCCCGGGTGGTCCTAAGATTGCTGACAAAG	Protein expression of GST-SN34
GST-TSN-R	GCCGCTCGAGTTATCGTTCCATACCAAATTCG	
TSN-F1	GCTGCACAGTCAAGATTGGA	Multiplex RT-PCR
TuN5R	TCCAGATGCAACAAATTCCAC	
Actin-F	GACTCGTACGTCGGGCGACGA	Multiplex RT-PCR
Actin-R	AGCAGCGGTGGTCATCACCTG	
Ago1-F	CAAGAATTTGGTCTGACGAT	RT-PCR
Ago1-R	AGTGTCACCCACACGCTTCAC	
qRab7-F2	CTGGAGAATAGGGCGGTATCAACG	qRT-PCR
qRab7-R2	CGAGCAATGGTCTGGAAGGCTAAC	
EF1a-F	GAACTGCTGACCAAGATCGACAGG	qRT-PCR
EF1a-R	GAGCATACTGTTGGAAGGTCTCCA	
Luci-F	GGTGTCGCTCTGCCTCATAG	*In vitro* transcription
Luci-R	GCAGATGGAACCTCTTGGC	
Luci-FT7	TAATACGACTCACTATAGGGGTGTCGCTCTGCCTCATAG	
Luci-RT7	TAATACGACTCACTATAGGGCAGATGGAACCTCTTGGC	
PRT oligo	CCGGAATTCAAGCTTCTAGAGGATCCTTTTTTTTTTTTTTT	cDNA synthesis

with rotating. After incubation, the resins were washed four times with washing buffer. The protein complex was eluted from the beads by boiling in SDS-loading buffer. The complex was separated on SDS-PAGE and subsequently transferred to nitrocellulose membrane. The presence of His_6-tagged proteins was detected by western blot with anti-His antibody (GE Healthcare). For detection GST-fusion proteins, bound proteins were diluted 10 fold, separated on SDS-PAGE, and blotted with anti-GST antibody (Sigma).

2.6. Nuclease activity assay

The recombinant GST-TSN was evaluated for its ability to cleave both RNA and DNA. The luciferase (luc) oligonucleotide substrates with ~400 nucleotides in length (nucleotides 619–1000) were synthesized by using plasmid pGL3-Basic (Promega) as a template. The luc-ssRNA and luc-dsRNA substrates were synthesized by *in vitro* transcription using RiboMAX® Large Scale RNA Production System (Promega), according to the manufacturer's protocol. The luc-DNA was synthesized by PCR and purified from the gel using QIAquick gel extraction kit (Qiagen). To assay the nuclease activity of the recombinant GST-TSN, 2 pmol of luc-ssRNA, luc-dsRNA, or luc-DNA were incubated with 10 pmol of the purified GST-TSN or GST in 20-μl reaction containing 20 mM Tris, pH 7.0, 1 mM DTT, 100 mM NaCl, 2 mM $MgCl_2$, 2 mM $CaCl_2$ and 2 mM $MnCl_2$ at 37 °C for 4 h. The reactions were analyzed on 6% non-denaturing polyacrylamide gel for reactions containing luc-dsRNA and luc-DNA, or 6% denaturing polyacrylamide for reactions containing luc-ssRNA. The presence of oligonucleotide substrate was visualized by ethidium bromide staining. In the assays, RQ1 DNase (Promega), RNase A (US Biological), and RNase III (New England Biolabs) were included as controls.

2.7. Preparation of double-stranded RNA

The double-stranded RNA (dsRNA) targeting PAZ domain of *PmAgo1* (kindly provided by Dr. Apinunt Udomkit, Mahidol University, Thailand), *PmRab7* [25], and *gfp* (kindly provided by Dr. Witoon Tirasophon, Mahidol University, Thailand) were produced in bacterial expression system [26]. Briefly, the plasmid pET-17b-stAgo1, pET-17b-stRab7 and pET-3a-stGFP were transformed into *E. coli* HT115 (DE3). The induction of dsRNA expression was carried out by the addition of IPTG to the final concentration of 0.1 mM (for dsRNA-Ago1 and dsRNA-Rab7) or 0.4 mM (for dsRNA-GFP) at A_{600} ~ 0.6 and proceeded for 4 h at 37 °C with shaking. Extraction and purification of dsRNA was performed as previously described [27]. For preparation of dsRNA targeting *PmTSN*, *in vitro* transcription was performed as previously described [22]. The concentration of the dsRNA was measured by Nanodrop ND-1000 spectrophotometer (Nanodrop technologies) and gel electrophoresis. The quality of dsRNA was determined by RNase A and RNase III digestion assay.

2.8. In vivo gene knockdown and RNAi against RNAi assay

To knockdown *PmAgo* and *PmTSN* expression, 50 μg of dsRNA-Ago1 or dsRNA-TSN was injected into shrimps (~10 g body weight) via intramuscular injection. Shrimps injected with dsRNA-GFP were used as negative control. Hemolymph was individually collected before and after dsRNA injection (1, 2 and 4 days). Total RNA was extracted from hemolymph using TRI Reagent® LS (Molecular Research Center, Inc.). Transcription levels of *PmAgo1* and *PmTSN* were determined by RT-PCR.

The effects of *PmAgo1* and *PmTSN*-knockdown on RNAi in shrimp were determined by using RNAi against RNAi assay, as previously described [22,28]. Briefly, shrimps ($n = 6$) were injected with dsRNA-Ago1, dsRNA-TSN or dsRNA-GFP as described above. Two days later, shrimps were injected with 6.3 μg of dsRNA-Rab7. Hemolymph was individually collected 2 days after the second injection. Transcription level of *PmRab7* was observed by quantitative real-time PCR (qRT-PCR) [22]. The data obtained from qRT-PCR were analyzed by comparative Ct method ($2^{-\Delta\Delta Ct}$) [29]. The data were expressed as mean ± standard error of mean (SEM) and analyzed by using one-way ANOVA in the Sigma Stat 3.5 program. A measurement of $P < 0.05$ was accepted as statistically significant. All primers used for RT-PCR and qRT-PCR are listed in Table 1.

3. Results

3.1. Interaction between PmTSN and three PmAgo proteins

TSN was identified as one of the components of RISC in *C. elegans*, *Drosophila*, and mammals [19,30]. In previous study, identification and characterization of a TSN gene from *P. monodon* (*PmTSN*) demonstrated the involvement of PmTSN in the shrimp RNAi pathway [22]. To investigate whether PmTSN was one of the components of RISC in shrimp, the yeast two-hybrid assay (Y2H) was performed to study the interaction between PmTSN and the core component of RISC, PmAgo. PmTSN was fused with GAL4-DNA-binding domain (BD-TSN), and the three PmAgo proteins including PmAgo1, PmAgo2, and PmAgo3 were fused with GAL4-activation domain (AD-Ago). The expression of BD-TSN and AD-Ago proteins in yeasts were confirmed before Y2H was performed with anti-c-Myc and anti-HA antibodies, respectively. The results showed that western blotting with anti-c-Myc antibody could detect the expression of BD-TSN at the expected band of 120 kDa. Expression of AD-Ago1, AD-Ago2, and AD-Ago3 could be detected by anti-HA antibody and showed the expected bands of 118 kDa, 105 kDa, and 107 kDa, respectively (Fig. 1A). By using Y2H, the diploids harboring BD-TSN and AD-Ago1 showed the positive interaction observed by the growth and blue color on the quadruple dropout medium (SD/-W/-L/-H/-A/X-α-gal), similar to the results observed in the diploids harboring BD-TSN and AD-Laminin receptor (AD-Lamr) which were used as a positive control. The positive interaction was not observed in the diploids harboring BD-TSN and AD-Ago2 or AD-Ago3. In addition, no sign of the interaction was observed in the negative control diploids harboring BD-TSN and Empty pGADT7. Therefore, this data confirmed that the interaction of BD-TSN and AD-Ago1 was not the result of an auto-activation of the reporter genes.

The interaction between PmTSN and PmAgo1 was further confirmed by using *in vitro* pull-down assay. PmTSN was expressed as a GST-fusion protein (GST-TSN) by an auto-induction approach and showed an expected band of 126 kDa in both soluble and insoluble fractions when compared to the non-induced condition. After purification by chromatographic techniques, the purified protein was confirmed by western blotting with anti-GST antibody

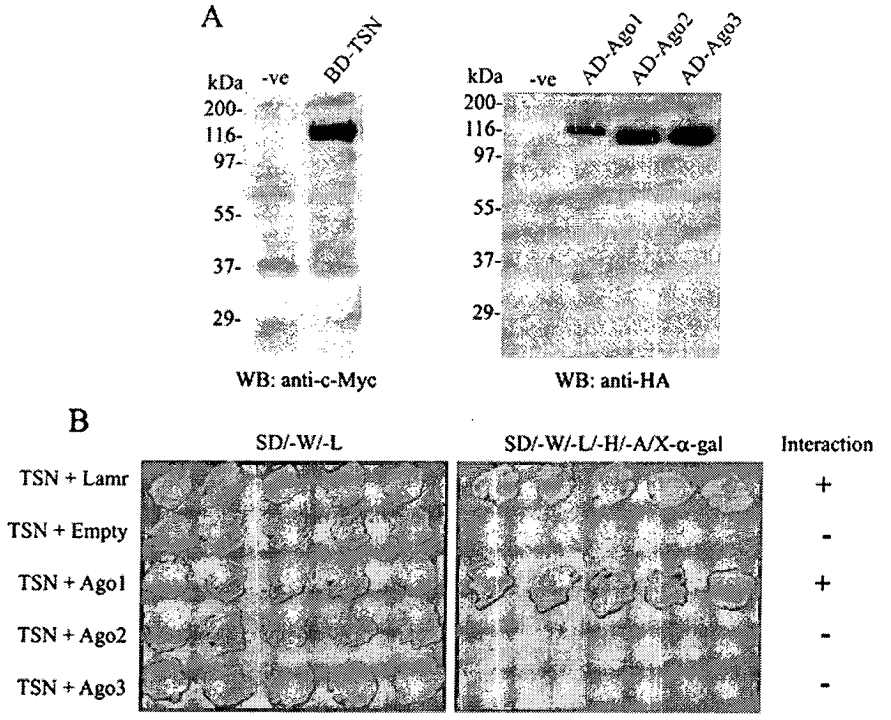

Fig. 1. PmTSN interacts with PmAgo1 in Y2H assay. (A) Western blot analysis of BD-TSN and AD-Ago expression in yeasts confirmed by using anti-c-Myc and anti-HA antibodies, respectively. Lane -ve represents untransformed yeasts. (B) Y2H assay showing the interaction between PmTSN and PmAgo1. *S. cerevisiae* Y187 expressing BD-TSN was mated with *S. cerevisiae* AH109 expressing AD-Ago1, AD-Ago2, or AD-Ago3, respectively. The mated cultures were selected on SD/-W/-L medium and subsequently confirmed on SD/-W/-L/-H/-A/X-α-gal medium. Yeast expressing BD-TSN and AD-Lamr served as a positive control whereas yeast harboring pGBKT7-TSN and empty pGADT7 served as a negative control. (+) and (−) represent the presence and absence of the interaction.

(Fig. 2A). The expression of His-Ago proteins were observed in both soluble and insoluble fractions by using western blotting with anti-His antibody. The expected bands of His-Ago1, His-Ago2, and His-Ago3 were shown at 105, 92, and 94 kDa, respectively. In addition, no band was observed in the *E. coli* harboring the empty pET-28a(+) (Fig. 2B). *In vitro* pull-down assay was performed by incubating immobilized GST-TSN with cell lysate from *E. coli* expressing His-Ago1, His-Ago2 or His-Ago3. The presence of GST- and His_6-tagged proteins was detected by western blotting with anti-GST and anti-His antibody, respectively. The results demonstrated that GST-TSN could interact with His-Ago1, but not interact with His-Ago2 or His-Ago3, confirming the results of Y2H (Fig. 2C). In addition, GST alone could not interact with all three His-Ago proteins, indicating the specific interaction between GST-TSN and His-Ago1. Taken together, by using both Y2H and *in vitro* pull-down assay, the results demonstrated that PmTSN specifically interacts with PmAgo1, suggesting that PmTSN is one of the components of PmAgo1-RISC.

3.2. Mapping of PmAgo1-PmTSN interaction

To identify the PmTSN-binding site of PmAgo1, a variety of His-Ago1 deletion mutants, including N-terminal domain (NTD), NTD and PAZ domains (NPAZ), PAZ domain, and MID-PIWI domains (PIWI) was generated and used for *in vitro* pull-down assay with GST-TSN. Western blotting with anti-His antibody revealed the expected bands of His-NTD, His-NPAZ, His-PAZ, and His-PIWI at 29, 48, 19, and 61 kDa in both soluble and insoluble fractions, respectively. In addition, no band was observed in the *E. coli* harboring the empty pET-28a(+) (Fig. 3A and B). The full-length His-Ago1 (FL) was also included in pull-down experiments as a positive control. The results of an *in vitro* pull-down assay demonstrated that FL,

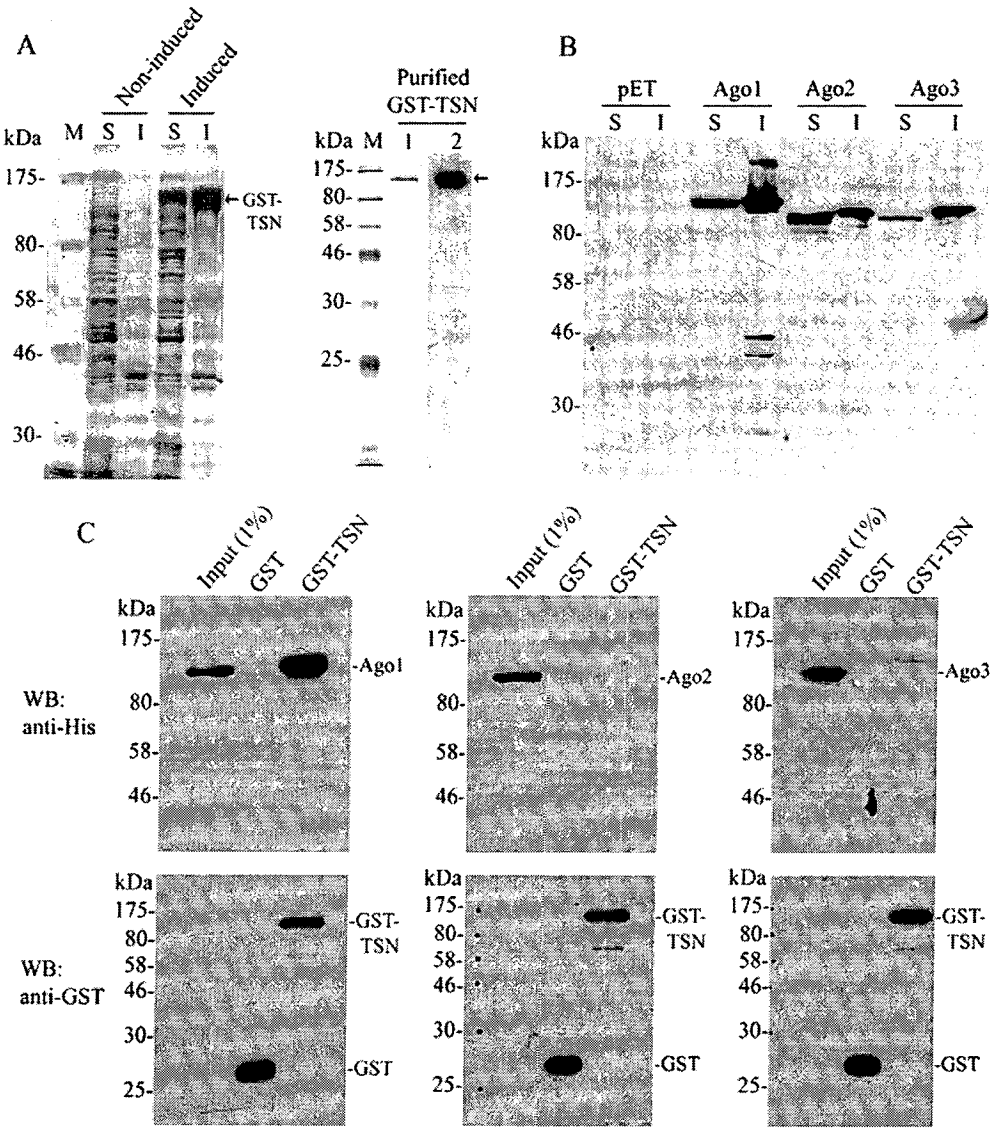

Fig. 2. *In vitro* pull-down assay confirming PmAgo1-PmTSN interaction. (A) Expression and purification of the recombinant GST-TSN using auto-induction approach and further purified by chromatographic techniques. Lane M, pre-stained protein marker; lane S, soluble fraction; lane I, insoluble fraction; lane 1, coomassie blue staining; lane 2, western blot analysis detected with anti-GST antibody. The arrows indicate GST-TSN. (B) Western blot analysis using anti-His antibody to detect the expression of His-Ago1 (105 kDa), His-Ago2 (92 kDa), and His-Ago3 (94 kDa) in *E. coli* Rosetta (DE3). Lane pET shows soluble and insoluble fractions from *E. coli* harboring empty pET-28a(+). (C) *In vitro* pull-down assay showing PmTSN-PmAgo1 interaction analyzed by western blotting with anti-His and anti-GST antibodies.

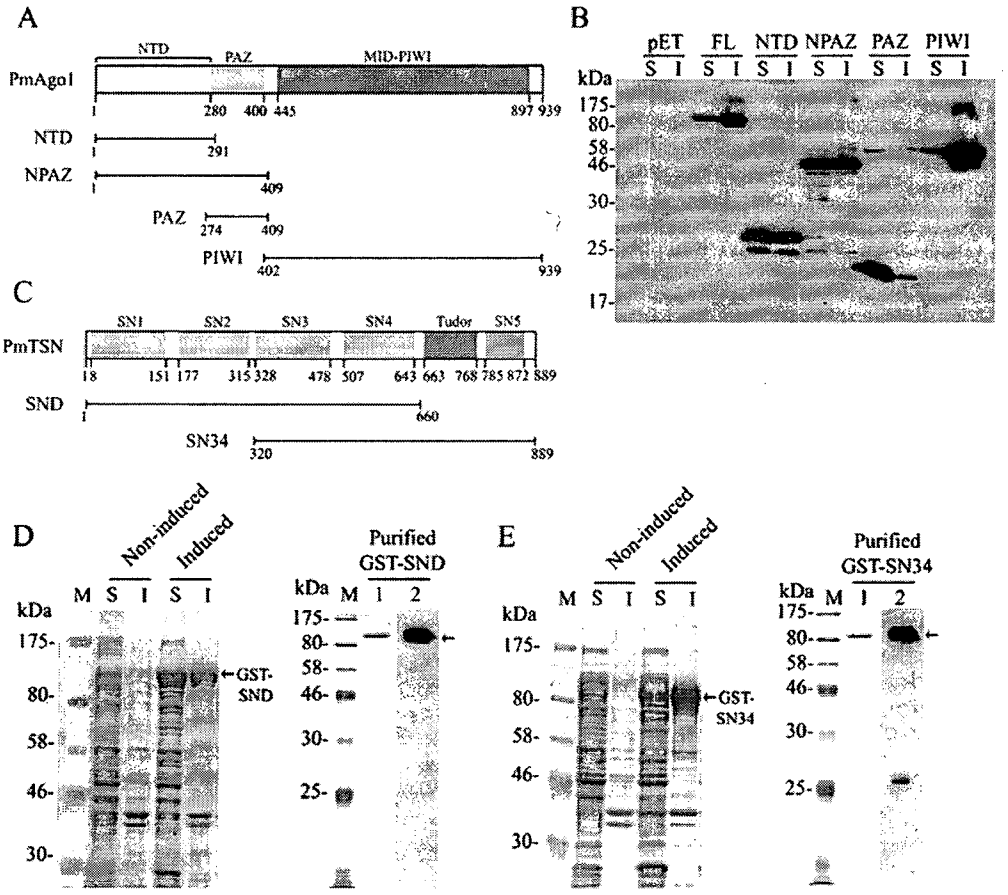

Fig. 3. Expression of the deletion mutant proteins used for mapping of PmTSN-PmAgo1 interaction. (A) Schematic diagram showing PmAgo1-deletion mutants used to map the PmTSN-interacting domain. The positions of amino acid residues at various domain junctions are indicated. (B) Western blot analysis using anti-His antibody to detect the expression of His-Ago1 (FL, 105 kDa) and its deletion mutants, including His-NTD (29 kDa), His-NPAZ (48 kDa), His-PAZ (19 kDa), and His-PIWI (61 kDa) in *E. coli* Rosetta (DE3). Lane pET shows soluble and insoluble fractions from *E. coli* harboring empty pET-28a(+); lane S and I represent soluble and insoluble fractions. (C) Schematic diagram showing PmTSN-deletion mutants used to map the PmAgo1-interacting domain. The positions of amino acid residues at various domain junctions are indicated. Expression and purification of the recombinant GST-SND (D) and -SN34 (E) in *E. coli* Rosetta (DE3). The recombinant GST-SND (100 kDa) and GST-SN34 (90 kDa) were expressed by auto-induction approach and further purified by chromatographic techniques. The arrows indicate GST-SND and GST-SN34. Lane M, pre-stained protein marker; lane 1, coomassie blue staining; lane 2, western blot analysis with anti-GST antibody.

NTD and NPAZ were able to interact with GST-TSN, but PAZ and PIWI were not (Fig. 4A). In addition, no interaction was observed in the pull-down reactions containing GST. These results suggest that NTD of PmAgo1 serves as an interacting domain for PmAgo1 to interact with PmTSN, and PAZ and PIWI are not involved in the interaction between these two proteins.

The PmAgo1-binding site of PmTSN was further characterized. The GST-fusion proteins of PmTSN-deletion mutants including GST-SND (contains SN1-SN4 domains) and GST-SN34 (contains SN3, SN4, Tudor, and C-terminal SN5 domains) (Fig. 3C) were expressed by an auto-induction approach and showed the expected bands of 100 and 90 kDa in both soluble and insoluble fraction, respectively, compared to a non-induced condition. Both GST-fusion proteins were purified by chromatographic techniques and were subsequently confirmed by western blotting with anti-GST antibody (Fig. 3D and E). The PmTSN-deletion mutant containing Tudor and SN5 domains (GST-Tud) was also generated. Unfortunately GST-Tud was expressed as inclusion bodies. Attempts to refold the recombinant protein were unsuccessful. Therefore GST-Tud was not included in this experiment (data not shown). To identify the PmAgo1-binding site of PmTSN, His-NTD was used to perform *in vitro* pull-down assay with GST-TSN and its deletion mutants. The results showed that His-NTD could be pulled-down with GST-TSN and GST-SND. A faint band of His-NTD was also observed in the GST-SN34 reaction. However, this minor interaction of His-NTD with GST-SN34 was possibly at the background level when compared to the control reaction containing GST only (Fig. 4B). Similar results were observed with His-FL instead of His-NTD for *in vitro* pull-down assay. His-FL could be pulled-down by GST-TSN and GST-SND, but not GST-SN34 (Fig. 4C). These results suggest that SN1 and SN2 domains are required for PmTSN to interact with the N-terminal domain of PmAgo1, and SN3, SN4, Tudor and SN5 domains are not involved in PmTSN-PmAgo1 interaction.

3.3. Nuclease activity assay of the recombinant GST-TSN

The nuclease activity of TSN has been reported in *Drosophila* [19], parasites [31], human, and plant [18]. To investigate whether PmTSN possessed the nuclease activity, purified GST-TSN was incubated with luc-DNA, luc-ssRNA and luc-dsRNA. The results showed that only GST-TSN could cleave luc-ssRNA, while the cleavages of luc-DNA and luc-dsRNA were not observed (Fig. 5A), indicating that PmTSN was a single-stranded RNase. The effect of metal ion on PmTSN RNase activity was further determined. The GST-TSN was incubated with luc-ssRNA in the presence or absence of Ca^{2+}, Mg^{2+}, or Mn^{2+}. The RNase activity of the recombinant protein was strongly

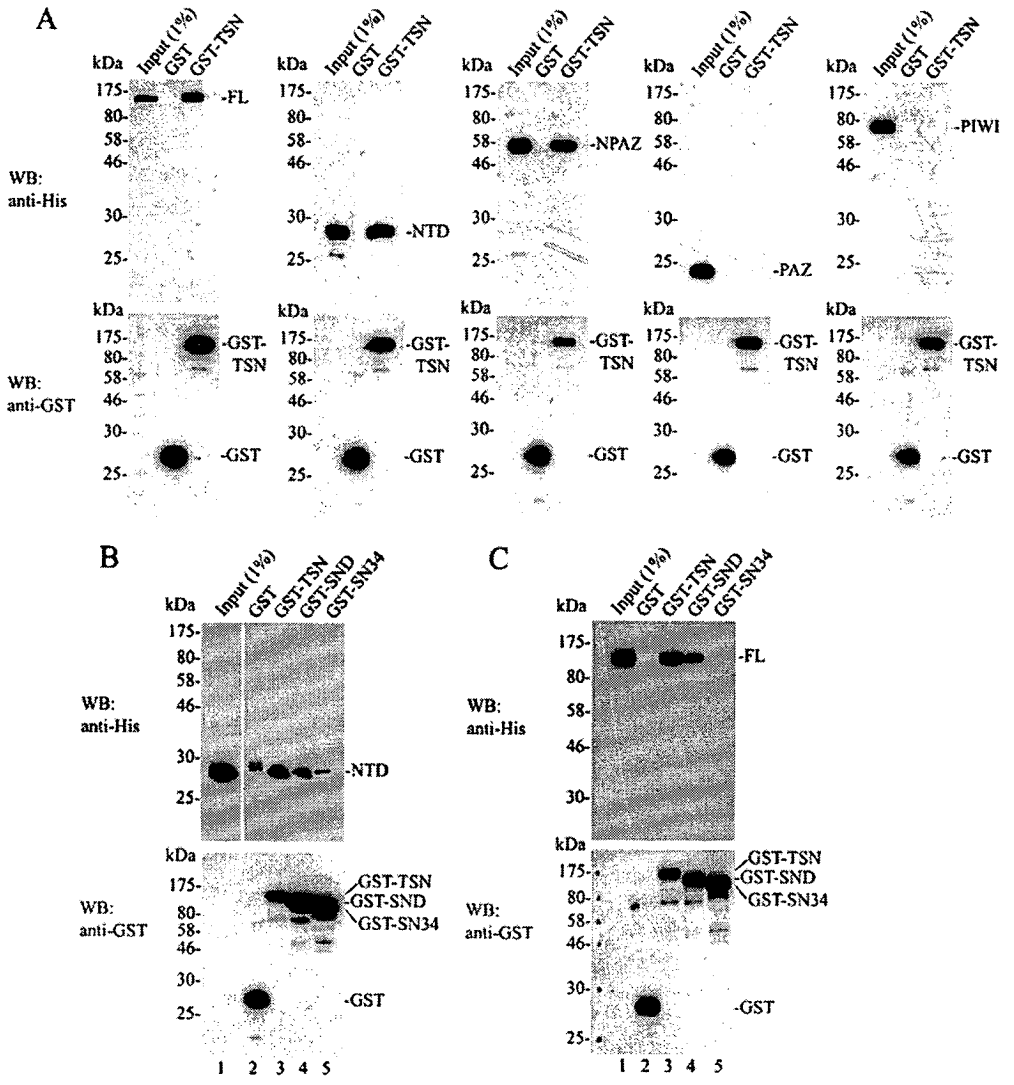

Fig. 4. Mapping of PmTSN-PmAgo1 interaction. (A) Mapping of PmTSN-binding site of PmAgo1. Full-length (FL) and deletion mutants of His-Ago1 were analyzed their abilities to interact with the immobilized GST-TSN using *in vitro* pull-down assay. (B and C) Mapping of PmAgo1-binding site of PmTSN. The immobilized GST-TSN, GST-SND, and GST-SN34 were used for *in vitro* pull-down assay with His-NTD or His-FL. The immobilized GST was used as a negative control in all experiments. The presence of GST- and His-tagged proteins was analyzed by western blotting with anti-GST and anti-His antibody, respectively.

inhibited in the absence of Ca^{2+} (Fig. 5B, lane 3, 4, 7, and 8), indicating the calcium-dependent RNase activity of PmTSN.

3.4. *PmAgo1 and PmTSN are involved in dsRNA-mediated gene silencing*

According to the results from Y2H and *in vitro* pull-down assay, the interaction between PmAgo1 and PmTSN indicates that PmTSN is one of the components of PmAgo1-RISC. Therefore, the roles of PmAgo1 and PmTSN in shrimp RNAi pathway were further investigated. The dsRNA corresponding to *PmAgo1* and *PmTSN* were synthesized and used for gene knockdown *in vivo*. Injection of dsRNA-Ago1 or dsRNA-TSN could significantly knockdown the transcripts of *PmAgo1* or *PmTSN* in shrimp, respectively. The transcription levels of *PmAgo1* and *PmTSN* were substantially reduced approximately 80% and 83% after 2 days dsRNA injection, respectively. In addition, injection of dsRNA-GFP had no effect on the transcripts of *PmAgo1* and *PmTSN* (Fig. S1). Two-fold increase of the dosage of dsRNA did not completely knockdown *PmAgo1* and *PmTSN* (data not shown). We speculated that PmAgo1 and PmTSN are indispensable for RNAi in shrimp.

The effects of suppression *PmAgo1* and *PmTSN* on the abilities of dsRNA-Rab7 to knockdown *PmRab7* expression were determined by qRT-PCR (Fig. 6, Fig. S2 and Fig. S3). Shrimps injected with dsRNA-Rab7 alone (NaCl → dsRab7) and dsRNA-GFP followed by dsRNA-Rab7 (dsGFP → dsRab7) showed similar reduction in *PmRab7* transcripts approximately 91% and 96%, respectively. *PmRab7* transcripts were significantly increased ($P < 0.05$) in *PmAgo1*-knockdown (dsAgo1 → dsRab7) and *PmTSN*-knockdown groups (dsTSN → dsRab7) when compared to the NaCl → dsRab7 and dsGFP → dsRab7 groups, as they showed 58% and 76% knockdown of *PmRab7*, respectively. These results indicated that PmAgo1 and PmTSN are involved in dsRNA-mediated gene silencing in shrimp.

4. Discussion

In this study, the interaction between PmTSN and the core component of RISC, PmAgo was demonstrated. Three Ago proteins

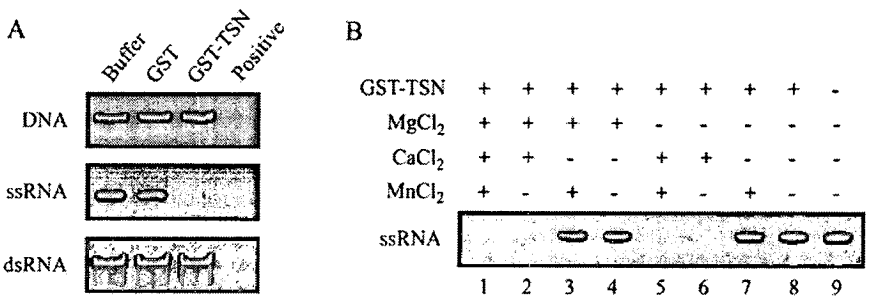

Fig. 5. Nuclease activity of the recombinant GST-TSN. (A) Purified GST-TSN (10 pmol) was incubated with various nucleic acids (2 pmol). The reactions were incubated at 37 °C for 4 h. Purified GST was used as a negative control. The commercial DNase, RNase A, and RNase III were included as positive controls. (B) GST-TSN exhibits calcium-dependent nuclease activity. Purified GST-TSN was incubated with Luc-ssRNA in the presence of Ca^{2+}, Mg^{2+}, or Mn^{2+}. (+) and (−) indicate the presence and absence of the divalent cations.

are identified in *P. monodon*. PmAgo1 or Pem-Ago1 is involved in dsRNA-mediated gene silencing [28], and is responded to yellow head virus infection [32]. Recent study in *Marsupenaeus japonicus* reveals that there are three Ago1 isoforms encoded by shrimp Ago1 gene. Two of the isoforms, including MjAgo1A and MjAgo1B contain an insert sequence in the PIWI domain and play key roles in host RNAi antiviral responses [33]. PmAgo2 is a germ cell-specific Ago protein which its function is not yet to be identified (Udomkit et al., unpublished data). PmAgo3 shares amino acid sequence similarity to *Litopenaeus vannamei* Ago2 [34] and is expressed ubiquitously in various shrimp tissues (Phetrungnapha et al., unpublished data). Recently, Huang and Zhang, 2012 demonstrated that MjAgo2 (which showed 77% amino acid sequence identity with PmAgo3) is required for the function of viral-derived siRNA, suggesting its important role in shrimp RNAi pathway against an invasion of DNA virus [35]. By using Y2H and *in vitro* pull-down assay, it was found that PmTSN specifically interacts with PmAgo1, but not PmAgo2 or PmAgo3, suggesting that PmTSN is one of the components of PmAgo1-RISC. In *C. elegans* and *Drosophila*, the organisms that contain multiple Ago proteins, TSN resides in both RISC and miRNP complex, suggesting that it is a common factor in RISC [19]. Nevertheless, the specific interaction of PmTSN and PmAgo1 indicates that PmTSN is predominantly involved in some sub-class of the RNAi pathways in shrimp.

The mapping of the interaction between PmTSN and PmAgo1 showed unique domains that were required for their binding. PmTSN directly interacted with the N-terminal domain of PmAgo1 via SN1-2 domains, while SN3, SN4, Tudor and SN5 domains were not involved in this interaction. Previous evidences demonstrated that TSN used different domains to interact with different proteins. The four tandem repeats of SN domains interacted with several basal transcription machineries and activator proteins such as EBNA2, TFIIE [16], STAT5 [13], STAT6, RNA polymerase II [14], Pim-1 [15], CBP/p300 [36], and RNA helicase A [37], whereas Tudor-SN5 domains formed a hook to interact with symmetrical dimethylated arginine-containing proteins, SmB/B′ and SmD1/D3, and involved in snRNP assembly [17,38,39]. Intriguingly, recent study in mouse has revealed that Tudor-SN5 domains recognized Piwi, a germ-line-specific clade of Argonaute family proteins, in an arginine methylation-dependent manner, suggesting the role of TSN in Piwi-interacting RNA (piRNA) pathway [40]. In our case, analysis of amino acid sequences of three PmAgo proteins did not show the RG/RA-rich motif, the signature motif of arginine methylation [41]. We speculate that PmTSN uses different domains to interact with distinct PmAgo proteins in different manners. Identification and characterization of the Piwi protein in shrimp will clarify this point better.

TSN is the first RISC-associated protein to be identified. It contains recognizable nuclease domains [19]. Nuclease activity assay revealed that PmTSN possessed a calcium-dependent nuclease activity which was specific to ssRNA, but not dsRNA and DNA. The nuclease activity of TSN has been reported in *Drosophila*, parasites, human, and plants [18,19,31]. The presence of RNase activity of TSN may involve in the degradation of the remaining mRNA after the site-specific cleavage by Ago [42,43]. Recently, Musiyenko et al., 2012 have demonstrated that, in parasite, *Toxoplasma gondii*, TSN interacted with a single Ago protein in an arginine methylation-dependent manner, and functioned as a potent second slicer of the parasitic RISC [44]. Whether PmTSN functions as a second slicer in PmAgo1-RISC remains to be clarified.

Our previous study demonstrated that knockdown of *PmTSN* significantly affected the dsRNA-mediated gene silencing in shrimp [22]. According to the results of Y2H and *in vitro* pull-down showing that PmTSN was one of the components of PmAgo1-RISC, we hypothesized that PmAgo1-RISC involved in dsRNA-mediated gene silencing in shrimp. To address this question, the knockdown effects of *PmAgo1* and *PmTSN* on the ability of dsRNA-Rab7 in *PmRab7* silencing were analyzed. Knockdown of *PmAgo1* significantly diminished the ability of dsRNA-Rab7 to inhibit *PmRab7* expression in shrimp. Similarly, the ability of dsRNA-5HT receptor to inhibit *5HT receptor gene* expression in Oka cells was also diminished in *PmAgo1*-knockdown [28]. These results suggest the crucial role of PmAgo1 in shrimp RNAi pathway. Diminishing of the RNAi activity in *PmTSN*-knockdown shrimps can be demonstrated by targeting either an endogenous PmRab7 or an exogenous protease gene of YHV [22]. A reduction in the efficiency of dsRNA-YHV to inhibit YHV replication was shown in *PmTSN*-knockdown shrimps [22]. Even though TSN was reported to function in various aspects of gene expression such as transcription and RNA splicing, expression of β-actin was not changed in *PmTSN*-knockdown shrimp (Fig. S1A). The results implied that an indirect effect of the *PmTSN*-knockdown on other endogenous shrimp gene expression could be excluded. The silencing effect of *PmTSN*-knockdown was less than that observed in *PmAgo1*-knockdown, suggesting that PmTSN is a minor component in PmAgo1-RISC. Recent study has revealed that TSN acted as a scaffold protein which recruited Astrocyte-elevated gene-1 (AEG-1), another RISC-associated factor, to Ago2-RISC, and was essential for the RISC activity in hepatocyte cells [20]. We hypothesized that PmTSN may also function as a bridging or scaffold protein in PmAgo1-RISC. Therefore, knockdown of PmTSN may disrupt the recruitment of other RISC-associated factors to PmAgo1-RISC, resulted in diminishing the RNAi activity in shrimp.

In conclusion, our study demonstrated that PmTSN was a component of PmAgo1-RISC, but not PmAgo2 and PmAgo3. The PmAgo1-PmTSN interaction was mediated through the N-terminal domain of PmAgo1 and SN1-2 domains of PmTSN. To our knowledge, this study is the first study that maps TSN and Ago interacting

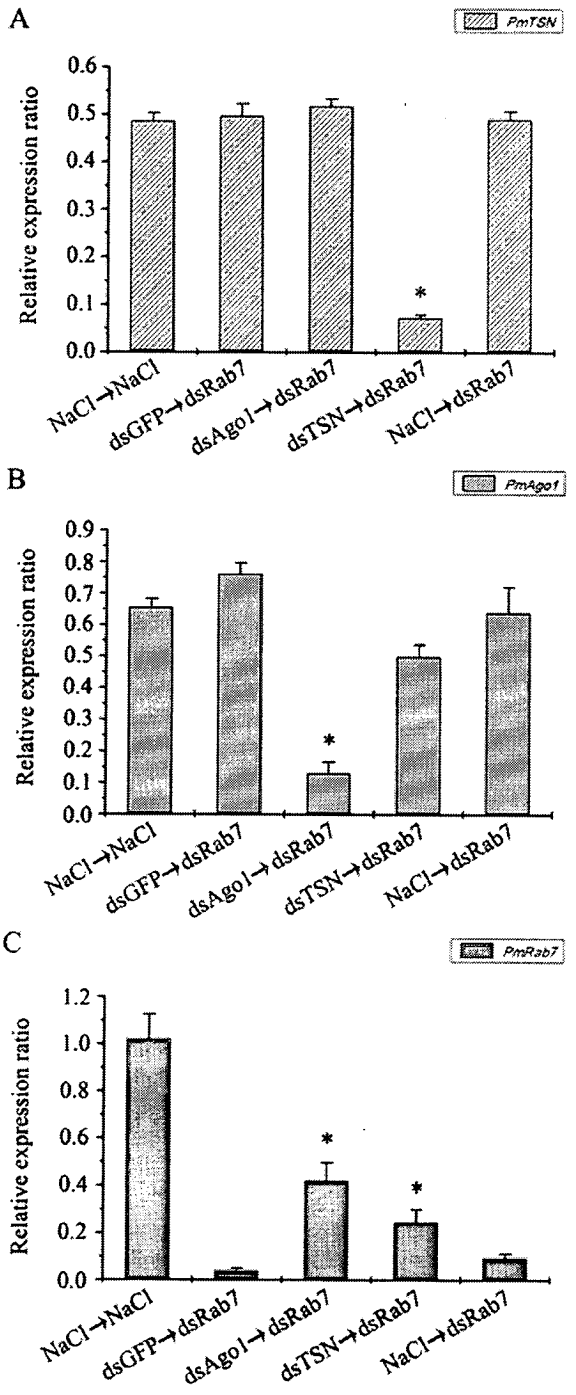

Fig. 6. Knockdown of *PmTSN* and *PmAgo1* diminished RNAi activity in shrimp. dsRNA-Rab7 was injected into control (NaCl → dsRab7 and dsGFP → dsRab7), *PmAgo1*-knockdown (dsAgo1 → dsRab7), and *PmTSN*-knockdown shrimps (dsTSN → dsRab7), and qRT-PCR was used to determine the transcription levels of *PmRab7*. (A, B) Semi-quantitative analysis of *PmTSN* and *PmAgo1* expression. *β-actin* was used as an internal control for normalization. The asterisks (*) represent a significant difference ($P < 0.05$) in the relative transcription levels of *PmTSN* and *PmAgo1*, compared to control groups. (C) qRT-PCR analysis of *PmRab7* transcripts. *EF1-α* was used as an internal control for normalization. The relative transcription levels of *PmRab7* were calculated by comparative Ct method ($2^{-\Delta\Delta Ct}$). Bars represents means ± SEM ($n = 6$). Statistical analysis was performed by using one-way ANOVA. The asterisks (*) represent a significant difference ($P < 0.05$) in the relative transcription levels of *PmRab7* in dsAgo1 → dsRab7 or dsTSN → dsRab7 groups, compared to control groups.

domains. We also demonstrated that PmTSN possessed a calcium-dependent single-stranded RNase activity, and PmTSN and PmAgo1 were important for dsRNA-mediated gene silencing in shrimp. Our study provided new insights in RISC in shrimp RNAi pathway, expanding the understanding of RNAi-based mechanisms in this economically important species.

Acknowledgments

The authors would like to thank Dr. Apinunt Udomkit for plasmids pGEM-T-Pem-Ago1, pGEM-T-PemAgo2, pET-17b-stAgo1, and primers for *PmAgo1* amplification, Dr. Witoon Tirasophon for plasmid pET-3a-stGFP, Dr. Saengchan Senapin for plasmid pGBKT7, pGADT7, and yeasts strains AH109 and Y187, and Ms. Chaweewan Chimwai for technical assistance. This work is supported by grants from the Thailand Research Fund (RSA5480002 to C.O.), the Office of the Higher Education Commission and Mahidol University under the National Research University Initiatives. A student fellowship granted to A.P. by the Royal Golden Jubilee Ph.D. Program.

Appendix A. Supplementary data

Supplementary data related to this article can be found at http://dx.doi.org/10.1016/j.fsi.2012.12.012.

References

[1] Sabin LR, Hanna SL, Cherry S. Innate antiviral immunity in *Drosophila*. Curr Opin Immunol 2010;22:4–9.
[2] Kemp C, Imler JL. Antiviral immunity in *Drosophila*. Curr Opin Immunol 2009; 21:3–9.
[3] Aliyari R, Wu Q, Li HW, Wang XH, Li F, Green LD, et al. Mechanism of induction and suppression of antiviral immunity directed by virus-derived small RNAs in *Drosophila*. Cell Host Microbe 2008;4:387–97.
[4] Galiana-Arnoux D, Dostert C, Schneemann A, Hoffmann JA, Imler J- L. Essential function *in vivo* for Dicer-2 in host defense against RNA viruses in *Drosophila*. Nat Immunol 2006;7:590–7.
[5] van Rij RP, Saleh M-C, Berry B, Foo C, Houk A, Antoniewski C, et al. The RNA silencing endonuclease Argonaute 2 mediates specific antiviral immunity in *Drosophila melanogaster*. Genes Dev 2006;20:2985–95.
[6] Wang X-H, Aliyari R, Li W-X, Li H-W, Kim K, Carthew R, et al. RNA interference directs innate immunity against viruses in adult *Drosophila*. Science 2006;312: 452–4.
[7] Zambon RA, Vakharia VN, Wu LP. RNAi is an antiviral immune response against a dsRNA virus in *Drosophila melanogaster*. Cell Microbiol 2006;8:880–9.
[8] Robalino J, Browdy CL, Prior S, Metz A, Parnell P, Gross P, et al. Induction of antiviral immunity by double-stranded RNA in a marine invertebrate. J Virol 2004;78:10442–8.
[9] Assavalapsakul W, Chinnirunvong W, Panyim S. Application of YHV-protease dsRNA for protection and therapeutic treatment against yellow head virus infection in *Litopenaeus vannamei*. Dis Aquat Org 2009;84:167–71.
[10] Tirasophon W, Yodmuang S, Chinnirunvong W, Plongthongkum N, Panyim S. Therapeutic inhibition of yellow head virus multiplication in infected shrimps by YHV-protease dsRNA. Antivir Res 2007;74:150–5.
[11] Tirasophon W, Roshorm Y, Panyim S. Silencing of yellow head virus replication in penaeid shrimp cells by dsRNA. Biochem Biophys Res Commun 2005;334:102–7.
[12] Robalino J, Bartlett T, Shepard E, Prior S, Jaramillo G, Scura E, et al. Double-stranded RNA induces sequence-specific antiviral silencing in addition to nonspecific immunity in a marine shrimp: convergence of RNA interference and innate immunity in the invertebrate antiviral response? J Virol 2005;79: 13561–71.
[13] Paukku K, Yang J, Silvennoinen O. Tudor and nuclease-like domains containing protein p100 function as coactivators for signal transducer and activator of transcription 5. Mol Endocrinol 2003;17:1805–14.
[14] Yang J, Aittomaki S, Pesu M, Carter K, Saarinen J, Kalkkinen N, et al. Identification of p100 as a coactivator for STAT6 that bridges STAT6 with RNA polymerase II. EMBO J 2002;21:4950–8.
[15] Leverson JD, Koskinen PJ, Orrico FC, Rainio EM, Jalkanen KJ, Dash AB, et al. Pim-1 kinase and p100 cooperate to enhance c-Myb activity. Mol Cell 1998;2: 417–25.
[16] Tong X, Drapkin R, Yalamanchili R, Mosialos G, Kieff E. The Epstein-Barr virus nuclear protein 2 acidic domain forms a complex with a novel cellular coactivator that can interact with TFIIE. Mol Cell Biol 1995;15:4735–44.
[17] Gao X, Zhao X, Zhu Y, He J, Shao J, Su C, et al. Tudor staphylococcal nuclease (Tudor-SN) participates in small ribonucleoprotein (snRNP) assembly via

interacting with symmetrically dimethylated Sm proteins. J Biol Chem 2012; 287:18130–41.
[18] Sundstrom JF, Vaculova A, Smertenko AP, Savenkov EI, Golovko A, Minina E, et al. Tudor staphylococcal nuclease is an evolutionarily conserved component of the programmed cell death degradome. Nat Cell Biol 2009;11:1347–54.
[19] Caudy AA, Ketting RF, Hammond SM, Denli AM, Bathoorn AM, Tops BB, et al. A micrococcal nuclease homologue in RNAi effector complexes. Nature 2003; 425:411–4.
[20] Yoo BK, Santhekadur PK, Gredler R, Chen D, Emdad L, Bhutia S, et al. Increased RNA-induced silencing complex (RISC) activity contributes to hepatocellular carcinoma. Hepatology 2011;53:1538–48.
[21] Grishok A, Sinskey JL, Sharp PA. Transcriptional silencing of a transgene by RNAi in the soma of *C. elegans*. Genes Dev 2005;19:683–96.
[22] Phetrungnapha A, Panyim S, Ongvarrasopone CA. Tudor staphylococcal nuclease from *Penaeus monodon*: cDNA cloning and its involvement in RNA interference. Fish Shellfish Immunol 2011;31:373–80.
[23] Studier FW. Protein production by auto-induction in high density shaking cultures. Protein Expr Purif 2005;41:207–34.
[24] Adachi M, Hamazaki Y, Kobayashi Y, Itoh M, Tsukita S, Furuse M. Similar and distinct properties of MUPP1 and Patj, two homologous PDZ domain-containing tight-junction proteins. Mol Cell Biol 2009;29:2372–89.
[25] Ongvarrasopone C, Saejia P, Chanasakulniyom M, Panyim S. Inhibition of Taura syndrome virus replication in *Litopenaeus vannamei* through silencing the LvRab7 gene using double-stranded RNA. Arch Virol 2011;156:1117–23.
[26] Ongvarrasopone C, Roshorm Y, Panyim S. A simple and cost effective method to generate dsRNA for RNAi studies in invertebrates. ScienceAsia 2007;33:35–9.
[27] Ongvarrasopone C, Chanasakulniyom M, Sritunyalucksana K, Panyim S. Suppression of PmRab7 by dsRNA inhibits WSSV or YHV infection in shrimp. Mar Biotechnol (NY) 2008;10:374–81.
[28] Dechklar M, Udomkit A, Panyim S. Characterization of Argonaute cDNA from *Penaeus monodon* and implication of its role in RNA interference. Biochem Biophys Res Commun 2008;367:768–74.
[29] Pfaffl MW. A new mathematical model for relative quantification in real-time RT-PCR. Nucleic Acids Res 2001;29:e45.
[30] Pham JW, Pellino JL, Lee YS, Carthew RW, Sontheimer EJ. A Dicer-2-dependent 80S complex cleaves targeted mRNAs during RNAi in *Drosophila*. Cell 2004; 117:83–94.
[31] Hossain MJ, Korde R, Singh S, Mohmmed A, Dasaradhi PV, Chauhan VS, et al. Tudor domain proteins in protozoan parasites and characterization of *Plasmodium falciparum* tudor staphylococcal nuclease. Int J Parasitol 2008;38: 513–26.
[32] Unajak S, Boonsaeng V, Jitrapakdee S. Isolation and characterization of cDNA encoding Argonaute, a component of RNA silencing in shrimp (*Penaeus monodon*). Comp Biochem Physiol B Biochem Mol Biol 2006;145:179–87.
[33] Huang T, Zhang X. Contribution of the argonaute-1 isoforms to invertebrate antiviral defense. PLoS One 2012;7:e50581.
[34] Labreuche Y, Veloso A, de la Vega E, Gross PS, Chapman RW, Browdy CL, et al. Non- specific activation of antiviral immunity and induction of RNA interference may engage the same pathway in the Pacific white leg shrimp *Litopenaeus vannamei*. Dev Comp Immunol 2010;34:1209–18.
[35] Huang T, Zhang X. Host defense against DNA virus infection in shrimp is mediated by the siRNA pathway. Eur J Immunol 2012;43:1–10.
[36] Valineva T, Yang J, Palovuori R, Silvennoinen O. The transcriptional co-activator protein p100 recruits histone acetyltransferase activity to STAT6 and mediates interaction between the CREB-binding protein and STAT6. J Biol Chem 2005;280:14989–96.
[37] Valineva T, Yang J, Silvennoinen O. Characterization of RNA helicase A as component of STAT6-dependent enhanceosome. Nucleic Acids Res 2006;34: 3938–46.
[38] Yang J, Valineva T, Hong J, Bu T, Yao Z, Jensen ON, et al. Transcriptional co-activator protein p100 interacts with snRNP proteins and facilitates the assembly of the spliceosome. Nucleic Acids Res 2007;35:4485–94.
[39] Shaw N, Zhao M, Cheng C, Xu H, Saarikettu J, Li Y, et al. The multifunctional human p100 protein 'hooks' methylated ligands. Nat Struct Mol Biol 2007;14: 779–84.
[40] Liu K, Chen C, Guo Y, Lam R, Bian C, Xu C, et al. Structural basis for recognition of arginine methylated Piwi proteins by the extended Tudor domain. Proc Natl Acad Sci U S A 2010;107:18398–403.
[41] Chen C, Jin J, James DA, Adams-Cioaba MA, Park JG, Guo Y, et al. Mouse Piwi interactome identifies binding mechanism of Tdrkh Tudor domain to arginine methylated Miwi. Proc Natl Acad Sci U S A 2009;106:20336–41.
[42] Sontheimer EJ. Assembly and function of RNA silencing complexes. Nat Rev Mol Cell Biol 2005;6:127–38.
[43] Schwarz DS, Tomari Y, Zamore PD. The RNA-induced silencing complex is a Mg2+-dependent endonuclease. Curr Biol 2004;14:787–91.
[44] Musiyenko A, Majumdar T, Andrews J, Adams B, Barik S. PRMT1 methylates the single Argonaute of *Toxoplasma gondii* and is important for the recruitment of Tudor nuclease for target RNA cleavage by antisense guide RNA. Cell Microbiol 2012;14:882–901.

Fish & Shellfish Immunology 35 (2013) 874–882

Contents lists available at SciVerse ScienceDirect

Fish & Shellfish Immunology

journal homepage: www.elsevier.com/locate/fsi

Molecular cloning and functional characterization of Argonaute-3 gene from *Penaeus monodon*

Amnat Phetrungnapha [a,1], Teerapong Ho [a,1], Apinunt Udomkit [a], Sakol Panyim [a,b], Chalermporn Ongvarrasopone [a,*]

[a] Institute of Molecular Biosciences, Mahidol University, Phutthamonthon 4 Road, Salaya, Nakhon Pathom 73170, Thailand
[b] Department of Biochemistry, Faculty of Science, Mahidol University, Rama VI Road, Phayathai, Bangkok 10400, Thailand

ARTICLE INFO

Article history:
Received 15 November 2012
Received in revised form
8 June 2013
Accepted 21 June 2013
Available online 30 June 2013

Keywords:
Argonaute
RNAi
Double-stranded RNA
Black tiger shrimp
YHV

ABSTRACT

Argonaute (Ago) proteins play a crucial role in the shrimp RNA interference pathway. In this study, we identified and characterized a novel Ago gene from black tiger shrimp, *Penaeus monodon*. The complete open reading frame of *P. monodon* Ago3 (*PmAgo3*) consisted of 2559 nucleotides encoding a polypeptide of 852 amino acids with a predicted molecular weight of 97 kDa and an isoelectric point of 9.42. Analysis of the deduced amino acid sequence of *PmAgo3* revealed the presence of two signature domains of the proteins in Argonaute family including PAZ and PIWI. Phylogenetic analysis indicated that *PmAgo3* is classified into Ago subfamily and shared the highest amino acid sequence identity (83%) with *Litopenaeus vannamei* Ago2. Monitoring of the *PmAgo3* expression by quantitative real-time PCR revealed that this gene was significantly up-regulated following dsRNA administration, while no significant difference in its expression was observed following yellow head virus (YHV) challenge. In contrast, inhibition of YHV mRNA expression was observed in *PmAgo3*-knockdown shrimp. These data imply that PmAgo3 is involved in the dsRNA-mediated gene silencing mechanism and plays an important role in YHV replication in the black tiger shrimp.

1. Introduction

RNA interference (RNAi) is a post-transcriptional gene silencing process mediated by a unique family of RNA-binding proteins named Argonaute (Ago). Ago proteins bind small regulatory RNAs such as siRNA (short-interfering RNA), miRNA (microRNA), and piRNA (Piwi-interacting RNA) to form the RNA-induced silencing complex (RISC), and then direct either target RNA degradation or translational inhibition. All Ago proteins share two main structural features including PAZ (PIWI/Argonaute/Zwile) and PIWI domains [1]. Crystallographic studies of Ago protein structures from both prokaryotes and eukaryotes revealed the presence of a bilobed structure composing of four distinct domains including N, PAZ, MID and PIWI connected through two linkers [2,3]. The N domain is involved in small RNA duplex unwinding during RISC assembly [4]. The PAZ domain exhibits oligonucleotide-binding fold which can recognize the 2-nt overhang at the 3′-end of the small RNA duplex [5,6]. The MID domain forms a binding pocket for anchoring 5′-phosphate of the small RNA [7,8]. The PIWI domain is structurally similar to ribonuclease H (RNase H) enzyme, and consists of the conserved catalytic residues Asp-Asp-His (DDH) motif which is crucial for the endonucleolytic "slicer" activity of the RISC [3,9].

Argonaute proteins are evolutionarily conserved in a wide range of eukaryotes. Based on phylogenetic analysis, Ago proteins can be classified into three categories including Ago subfamily, Piwi subfamily, and worm-specific Argonautes (WAGO) [10]. The Ago subfamily is ubiquitously expressed and is involved in siRNA and miRNA pathways, whereas the Piwi subfamily is a germ-cell specific Ago family involving in piRNA pathway. WAGO is a worm-specific Ago family which was identified in *Caenorhabditis elegans*, and was found to be involved in a variety of cellular processes in worm, such as chromosome segregation, fertility, and endogenous RNAi pathway [11]. The number of Ago genes presented in different species is varied. Some species such as *Schizosaccharomyces cerevisiae* encodes a single Ago protein whereas most species contain multiple Ago proteins. For example, 5, 8, 10, and 27 Ago genes were identified in *Drosophila*, human, *Arabidopsis thaliana*, and *C. elegans*, respectively [1]. In penaeid shrimp, two Ago genes, including *PmAgo1* (*Pem-Ago1*) and *PmAgo2* were identified and

* Corresponding author. Institute of Molecular Biosciences, Mahidol University (Salaya Campus), 25/25 Phutthamonthon 4 Rd., Salaya, Phutthamonthon District, Nakhon Pathom 73170, Thailand. Tel.: +66 2 8003624x1280; fax: +66 2 4419906.
E-mail address: chalermporn.ong@mahidol.ac.th (C. Ongvarrasopone).
[1] Both authors have equal contribution.

1050-4648/$ – see front matter © 2013 Elsevier Ltd. All rights reserved.
http://dx.doi.org/10.1016/j.fsi.2013.06.025

characterized in the black tiger shrimp. PmAgo1 was involved in dsRNA-mediated gene silencing, and responded to yellow head virus (YHV) infection [12,13]. PmAgo2 is a germ cell-specific Ago protein with an unknown function (Udomkit et al., unpublished data). In pacific white shrimp, *Litopenaues vannamei*, two Ago genes, including *LvAgo1* and *LvAgo2* were identified and characterized. Chen et al. demonstrated that LvAgo2 interacted with LvDicer2 and LvTRBP1 [14]. Robalino et al. demonstrated that *LvAgo2*, but not *LvAgo1*, responded to double-stranded RNA (dsRNA) [15]. In addition, two Ago genes were also identified and characterized in *Marsupenaeus japonicas* [16,17].

Accumulating evidence demonstrates that RNAi plays an important role in antiviral immunity in penaeid shrimp [18–20]. Nevertheless, the information of the RNAi-based mechanism in penaeid shrimp is still largely elusive. Identification of the RNAi-related proteins is not only important for elucidating their functions but also provides more insights into RNAi-based mechanism and antiviral defense in these economically important species. Here, we identified and characterized a novel Ago gene from *P. monodon*, *PmAgo3*. The expression of *PmAgo3* in response to dsRNA administration and YHV challenge was also investigated. The functional significance of *PmAgo3* on YHV replication was also investigated.

Table 1
Primers used in this study.

Primers	Sequences (5′ → 3′)	Purposes
PRT-oligo-dT	CCGGAATTCAAGCTTCTAGAGGATCC TTTTTTTTTTTTTTT	Reverse transcription
NPAZ-F3	ATGCCTTGGATATCAGAAGTC	RT-PCR
NPAZ-R3	GTTCAAAGATTTTGTGACCCT	RT-PCR
Ago3-F2	CCAAAGGACAGAGGGTCACA	3′ RACE
PIWI-R3	CAGGGATTGACACTGATCTTG	3′ RACE
Ago3-F3	CGTTGACCAGATCATCACTC	3′ RACE
LvAgo2-R	CTACAAGAAGTACATTTTAT	3′ RACE
PmAgo3-F1	GGTGGAAGGATTTCCCACTT	RT-PCR and qRT-PCR
PmAgo3-R1	CACTGGGGAGTGAGTTGCTT	RT-PCR and qRT-PCR
PmAgo1-F	CAAGAATTTGGTCTGACGAT	RT-PCR
PmAgo1-R	AGTGTCACCCACACGCTTCAC	RT-PCR
PmActin-F	GACTCGTACGTCGGGCGACGA	RT-PCR
PmActin-R	AGCAGCGGTGGTCATCACCTG	RT-PCR
EF1a-F	GAACTGCTGACCAAGATCGACAGG	qRT-PCR
EF1a-R	GAGCATACTGTTGGAAGGTCTCCA	qRT-PCR
dsAgo3 *XbaI*_F1	GCTCTAGATCAGCTCAGGGAAT CAGACT	dsRNA expression plasmid
dsAgo3 *XhoI*_F2	CCGCTCGAGTCAGCTCAGGGAAT CAGACT	dsRNA expression plasmid
dsAgo3 *BamHI*_R1	CGGGATCCGGGAGGCAAAATTC GACCAT	dsRNA expression plasmid
dsAgo3 *BamHI*_R2	CGGGATCCCTCAAATGGATATCT GGCAGC	dsRNA expression plasmid

2. Materials and methods

2.1. Shrimp and virus stock

Black tiger shrimp, *P. monodon* (approximately 10 g body weight) were obtained from local shrimp farms in Thailand. They were reared in the laboratory tanks containing artificial sea water (10 ppt) and fed *ad libitum* for a week to gradually acclimatize to the laboratory condition. Apparently healthy shrimps free of yellow head virus (YHV) and white spot syndrome virus (WSSV) were chosen for the experiments. Preparation of YHV stock and determination of the viral titer ($\sim 3 \times 10^9$ virions ml^{-1}) were performed as described by Assavalapsakul et al. [21]. YHV stock was diluted 10^5 fold prior to use.

2.2. Total RNA extraction and reverse transcription

Total RNA was extracted from tissues using TRI-REAGENT® or TRI-LS® (Molecular Research Center), according to the manufacturer's protocol. The concentration of RNA was determined by Nanodrop® ND-1000 spectrophotometer (Nanodrop Technologies). The A_{260}/A_{280} ratio of 1.8–2.0 indicated that the RNA samples were relatively pure. One microgram of total RNA was reverse transcribed into cDNA by Impromp-II™ reverse transcriptase (Promega) following the manufacturer's protocol. The PRT-oligo-dT_{12} primer used for reverse transcription is shown in Table 1.

2.3. Cloning of the full-length open reading frame (ORF) of PmAgo3

Hemolymph was used as a source of total RNA for *PmAgo3* cloning. Total RNA extraction and reverse transcription were performed as described above. VENT® DNA polymerase (New England Biolabs) was used for all PCR amplifications. The partial fragment of *PmAgo3* was amplified using the primers designed based on *LvAgo2* sequence, NPAZ-F3 and NPAZ-R3 primers, following the condition: denaturation at 95 °C for 3 min, followed by 30 cycles of 95 °C for 30 s, 49 °C for 30 s, and 72 °C for 90 s. The final extension was carried out at 72 °C for 7 min. The PCR product was purified from the gel using QIAquick gel extraction kit (Qiagen) and subsequently added A-tail. The tailed PCR product was cloned into pGEM®-T Easy vector (Promega) and subsequently subjected for sequencing by First Base Co., Ltd. (Malaysia).

To identify the sequences at the 3′-end of *PmAgo3*, 3′ RACE-PCR was performed with Ago3-F2 and PIWI-R3 primers. The second 3′ RACE-PCR was performed with Ago3-F3 and LvAgo2-R primers. Gel purification of the PCR product, A-tailing, cloning, and sequencing were performed as described above. All primers used for cloning are listed in Table 1.

2.4. Sequence and phylogenetic analysis

The deduced amino acid sequence of *PmAgo3* was compared with other known Ago sequences available in the GenBank database using Blast program. To perform multiple sequence alignment and phylogenetic analysis, Ago protein sequences from several organisms were retrieved from the GenBank database. Multiple sequence alignment was performed by using ClustalW program. Phylogenetic tree was constructed by using MEGA 5.05 program, based on the Neighbor-joining method [22]. Bootstrap values of 1000 replicates were used for the consensus tree. The Ago protein sequences from various species used for multiple sequence alignment and phylogenetic analysis are listed in Table 2. Molecular weight and isoelectric point were predicted by tools in Expasy website (www.expasy.org). Motifs of proteins were identified by using ScanProsite.

2.5. Tissue distribution study

Several tissues including hemolymph, gill, lymphoid organ, hepatopancreas, heart, thoracic ganglia, nerve cord, brain, eyestalks were collected from wild broodstock shrimps. Total RNA extraction and reverse transcription were performed as described above. Expression of *PmAgo3* was determined by RT-PCR with PmAgo3-F1 and PmAgo3-R1 primers, following the condition: denaturation at 94 °C for 5 min, followed by 30 cycles of 94 °C for 30 s, 60 °C for 30 s, and 72 °C for 30 s. The final extension was carried out at 72 °C for 7 min. The internal control gene, *β-actin* was amplified following the condition: denaturation at 94 °C for 5 min, followed by 21 cycles of 94 °C for 30 s, 55 °C for 30 s, and 72 °C for 45 s. The final

Table 2
Argonaute proteins used for multiple sequence alignment and phylogenetic analysis.

Species	Proteins	Abbreviations	Acc. numbers
Apis mellifera	Aubergine	ApAub	NP_001159378
Bombyx mori	Argonaute-1	BmAgo1	NP_001095931
	Argonaute-2	BmAgo2	BAD91160
	Argonaute-3	BmAgo3	BAF73717
Bos taurus	Argonaute-2	BtAgo2	NP991363.1
Caenorhabditis elegans	ALG1	CeALG1	CAR97837
	ALG2	CeALG2	CCD73271
	PRG-1	CePRG1	CAA98113
	PRG-2	CePRG2	CCD62443
	RDE-1	CeRDE1	CAB05546
Drosophila melanogaster	Argonaute-1	DmAgo1	AAF58313
	Argonaute-2	DmAgo2	NP_730054
	Argonaute-3	DmAgo3	EAA45981
	Aubergine	DmAub	CAA64320
	Piwi	DmPiwi	AAP08705
Homo sapiens	Argonaute-1	HsAgo1	NP_036331
	Argonaute-2	HsAgo2	NP_036286
	Argonaute-3	HsAgo3	NP_079128
	Argonaute-4	HsAgo4	NP_060099
	Hiwi	HsHiwi	AAC97371
	Hili	HsHili	NP060538.2
Litopenaeus vannamei	Argonaute-1	LvAgo1	ADK25180
	Argonaute-2	LvAgo2	ADK25181
Marsupenaeus japonicus	Argonaute-1	MjAgo1	ADB44074
	Argonaute-2	MjAgo2	BAM37459
Mus musculus	Argonaute-2	MmAgo2	NP_694818
	Miwi	MmMiwi	BAA93705
	Mili	MmMili	BAA93706
Neurospora crassa	QDE-2	NcQDE2	AAF43641
Penaeus monodon	Argonaute-1	PmAgo1	ABG66640
	Argonaute-3	PmAgo3	JX845575

extension was carried out at 72 °C for 7 min. PCR products were analyzed on 2% agarose gel electrophoresis, stained by ethidium bromide, and visualized under ultraviolet light.

2.6. Construction of a hair-pin dsRNA expression plasmid (pET17b-St-PmAgo3)

Recombinant plasmids expressing stem loop *PmAgo3* dsRNA were constructed in pET17b vector (Novagen, USA). A sense-loop PCR fragment (517 bp, located at nucleotide position 747–1263) covering the PAZ domain of *PmAgo3* gene was amplified using specific primers; dsAgo3-*Xba*I_F1 and dsAgo3-*BamH*I_R1, The antisense PCR fragment (394 bp, located at nucleotide position 747–1140) was amplified using primers; dsAgo3-*Xho*I_F2 and *BamH*I_R2. The sense-loop PCR fragment and pET17b vector were digested with *Xba*I and *BamH*I whereas the antisense PCR fragment was digested with *Xho*I and *BamH*I. The PCR products and the linearized vectors were purified using QIAquick gel extraction kit (QIAGEN). Finally, the recombinant plasmid containing an inverted repeat of the stem loop *PmAgo3*, pET17b-st-*PmAgo3* was obtained and used for *in vivo* bacterial expression of dsRNA. The insert fragment of stem loop *PmAgo3* was subjected for automated DNA sequencing (First Base Co., Ltd. (Malaysia)).

2.7. Preparation of double-stranded RNAs (dsRNA)

The dsRNA-*PmAgo3* and dsRNA-GFP were produced by using bacterial expression system [23]. Briefly, the plasmids, pET17b-st-*PmAgo3* and pET-3a containing stem-loop GFP insert (pET3a-st-GFP) were transformed into *Escherichia coli* HT115 (DE3). Expression of dsRNA-*PmAgo3* and dsRNA-GFP was induced by an addition of IPTG to the final concentration of 0.4 mM at $A_{600} \sim 0.6$ and proceeded for 4 h at 37 °C with shaking. Extraction and purification of both dsRNAs were performed as previously described by Ongvarrasopone et al. [24]. The concentration of both dsRNAs was determined by agarose gel electrophoresis and Nanodrop® ND-1000 spectrophotometer (Nanodrop Technologies). The quality of dsRNAs was determined by ribonuclease A (RNase A) and ribonuclease III (RNase III) digestion assay.

2.8. Expression analysis of PmAgo3

To determine the expression of *PmAgo3* in response to dsRNA or YHV injection, shrimps ($n = 6–8$) were injected with 25 μg of dsRNA-GFP, or challenged with 50 μl of the diluted YHV stock. Injection of dsRNA or YHV was done intramuscularly via the fourth abdominal segment. Hemolymph was collected from individual shrimps at 0, 3, 6, 9, 12, 24, 48 and 72 h-post injection (hpi). Total RNA extraction from hemolymph and reverse transcription were performed as described above. Expression of *PmAgo3* in response to YHV or dsRNA-GFP injection was further determined by quantitative real-time PCR (qRT-PCR). qRT-PCR was performed in a Mastercycler® ep realplex (Eppendorf) using KAPA™ SYBR® FAST qPCR kit (KAPA Biosystems). *PmAgo3* was amplified by PmAgo3-F1 and PmAgo3-R1 primers. The internal control gene, EF1-α was amplified by EF1a-F and EF1a-R primers. The primers used for qRT-PCR are listed in Table 1, qRT-PCR was carried out in triplicates for each sample. A 20-μl qRT-PCR reaction contains 10 μl of 2× SYBR® FAST qPCR master mix, 2 μl of 1:20 diluted cDNA, 1 μl of 10 mM of PmAgo3 primers or 1 mM of EF1-α primers, and 7 μl of DEPC-treated water. qRT-PCR was performed under the following condition: denaturation at 95 °C for 3 min, followed by 40 cycles of 95 °C for 5 s and 60 °C for 30 s. The melting curved analysis was performed after PCR amplification in order to determine the specificity of primers. The cycle threshold (Ct) of *PmAgo3* and EF1-α was determined by the Mastercycler® ep realplex software. Relative expression of *PmAgo3* normalized by EF1-α was calculated by comparative Ct method [25] and expressed as mean ± standard error of mean (SEM). The statistical analysis was performed by using Levene's test of independent sample *t*-test in SPSS program. A *p*-value below 0.05 ($p < 0.05$) was accepted as statistically significance.

2.9. Functional assay of PmAgo3

Shrimps (size 10 g, 5–10 shrimp per group) were intramuscularly injected with dsAgo3 or dsGFP (2.5 μg g^{-1} shrimp) for 48 h prior to injection with 50 μl of the 100 fold diluted YHV. Hemolymph was individually collected at 0 and 48 h-post dsAgo3 injection. After YHV challenge, hemolymph was individually collected at 0, 24, 30, 36, and 48 h-post YHV injection. Shrimps injected with 150 mM NaCl alone or dsGFP were used as control groups. Total RNAs of hemolymph were extracted and used for cDNA synthesis. To determine sequence specific knockdown by dsAgo3, expression of *PmAgo3* (using PmAgo3-F1 and PmAgo3-R1 primers) and *PmAgo1* (using PmAgo1-F and PmAgo1-R primers) (Table 1) was used to perform multiplex RT-PCR analysis. PmActin was used as an internal control. In addition, a multiplex RT-PCR analysis of helicase gene of *YHV* and PmActin was also performed [24].

3. Results

3.1. Cloning and sequence analysis of PmAgo3

Two types of Ago proteins were identified in *P. monodon*, including *PmAgo1* (*Pem-Ago1*) [12,13] and *PmAgo2* (Udomkit et al., unpublished data). Therefore, in this study, our newly identified Ago gene was designated as *PmAgo3*. A 1089-bp fragment of

PmAgo3 was first amplified by the primers designed based on *LvAgo2* sequence, NPAZ3-F and NPAZ3-R. Blastp against GenBank database revealed that the deduced amino acid sequence of this fragment shared a significant homology with LvAgo2 and *M. japonicus* Ago2 (MjAgo2) (*E*-value = 0.0). Based on the sequence of the amplified fragment, gene specific primers were designed, and 3′ RACE-PCR was performed in order to identify the remaining sequence at the 3′ end of *PmAgo3*. After two rounds of 3′ RACE-PCR, the nucleotide sequences of each fragment were combined to obtain the complete ORF of *PmAgo3*. The *PmAgo3* mRNA sequence was submitted to GenBank under the accession number JX845575.

The ORF of *PmAgo3* was 2559 bp, encoding a polypeptide of 852 amino acids with a molecular weight of 97.02 kDa and isoelectric point of 9.42. Motifs scan by using ScanProsite revealed the presence of two distinctive domains, PAZ and PIWI which are the signature domains of Ago proteins (Fig. 1). The result obtained from Blastp analysis showed that PmAgo3 shared the highest amino acid sequence identity of 83% and 77% with LvAgo2 and MjAgo2, respectively. PmAgo3 shared 40%, 27%, and 26% amino acid sequence identities with human, *Drosophila melanogaster* and *Bombyx mori* Ago2, respectively. In addition, only 41% amino acid sequence identity was observed between PmAgo1 and PmAgo3. To compare the sequence features, the deduced amino acid sequence of *PmAgo3* and some representative Ago proteins were analyzed by using multiple sequence alignment based on the conserved PIWI domain. The alignment revealed several conserved motifs within the PIWI domain. These motifs were predicted to be involved in an anchoring of the 5′-end of the small

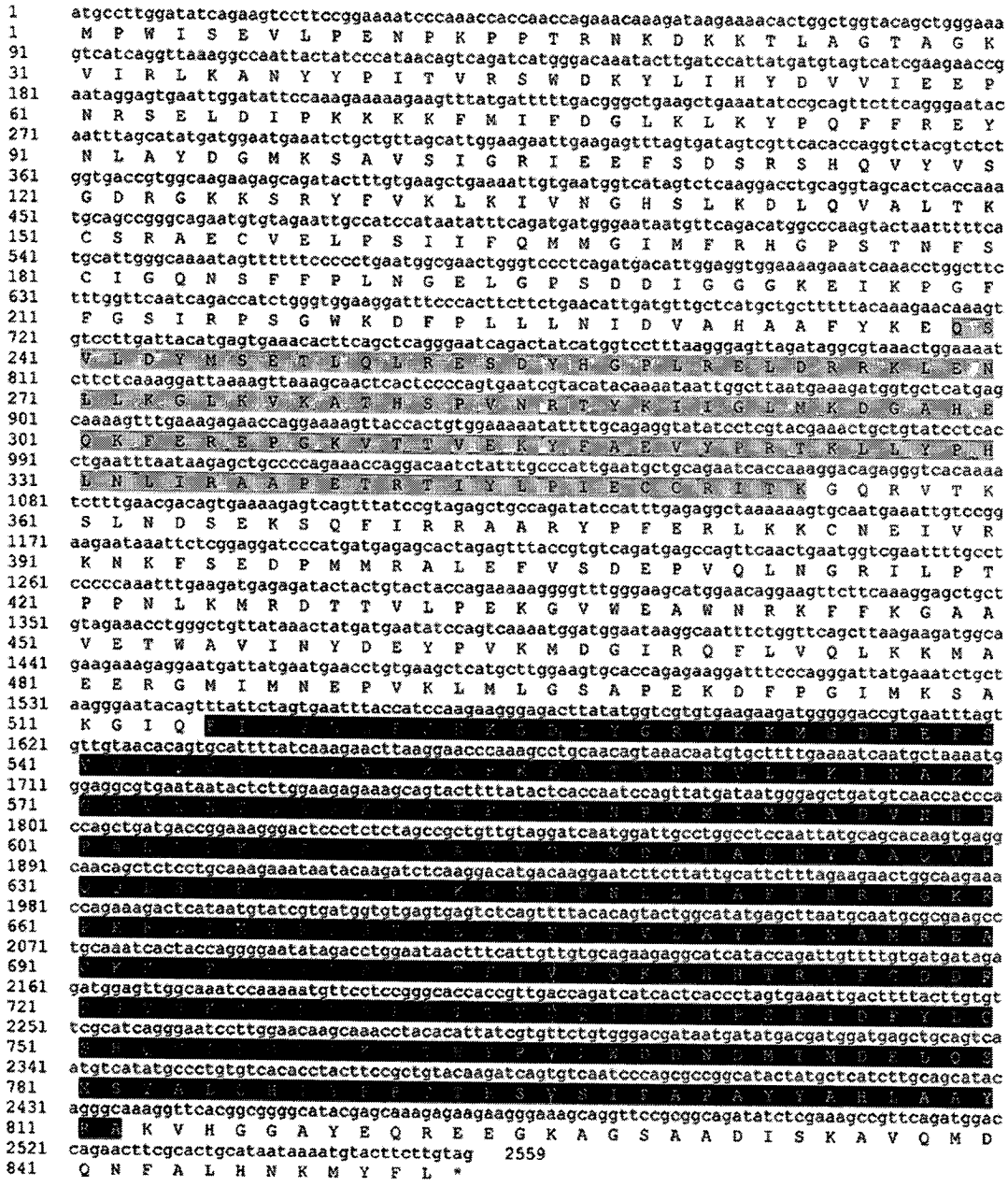

Fig. 1. Nucleotide and the deduced amino acid sequences of the complete ORF of *PmAgo3*. The deduced amino acid sequence of *PmAgo3* is shown in a single letter under the respective codon. The PAZ and PIWI domains are highlighted in light gray and black, respectively. The nucleotide sequence is available in the GenBank database under the accession number JX845575.

RNA to target RNA degradation. The conserved catalytic triad composing of DDH motif was also identified (Fig. 2). To study the molecular evolution of PmAgo3, several Ago proteins sequences from vertebrate and invertebrate organisms were retrieved. The Neighbor-joining tree was constructed based on the multiple sequence alignment of the PIWI domain. However, WAGO family was not included into this analysis. The bootstrapped NJ tree separated Ago proteins into two subfamily, including Ago and Piwi subfamilies. PmAgo3 was classified into the Ago subfamily and clustered in the same group with LvAgo2 and MjAgo2. This cluster was on a separated branch that located between invertebrate Ago1 and Ago2 clusters (Fig. 3).

3.2. Expression of PmAgo3 in shrimp tissues

RT-PCR was employed to determine *PmAgo3* expression in various tissues of shrimp. The result showed that *PmAgo3* was ubiquitously expressed in all examined tissues, such as hemolymph, ovary, hepatopancreas, lymphoid, gill, heart, nerve, thoracic ganglia, brain, and eyestalk (Fig. 4).

3.3. Expression of PmAgo3 in response to dsRNA and YHV injection

To examine the expression of *PmAgo3* in response to dsRNA or YHV injection, shrimps were injected with dsRNA-GFP or challenged with YHV. Expression of *PmAgo3* in response to dsRNA or YHV injection at various time points was determined by qRT-PCR. The results showed that the expression of *PmAgo3* significantly increased following injection of dsRNA-GFP ($p < 0.05$) (Fig. 5(A)). The expression of *PmAgo3* reached the peak at 9 h-post injection and then decreased gradually. On the other hand, in the shrimps challenged with YHV, no significant difference in *PmAgo3* expression was observed at any time point (Fig. 5(B)). To confirm the expression of YHV mRNA in these samples, multiplex RT-PCR

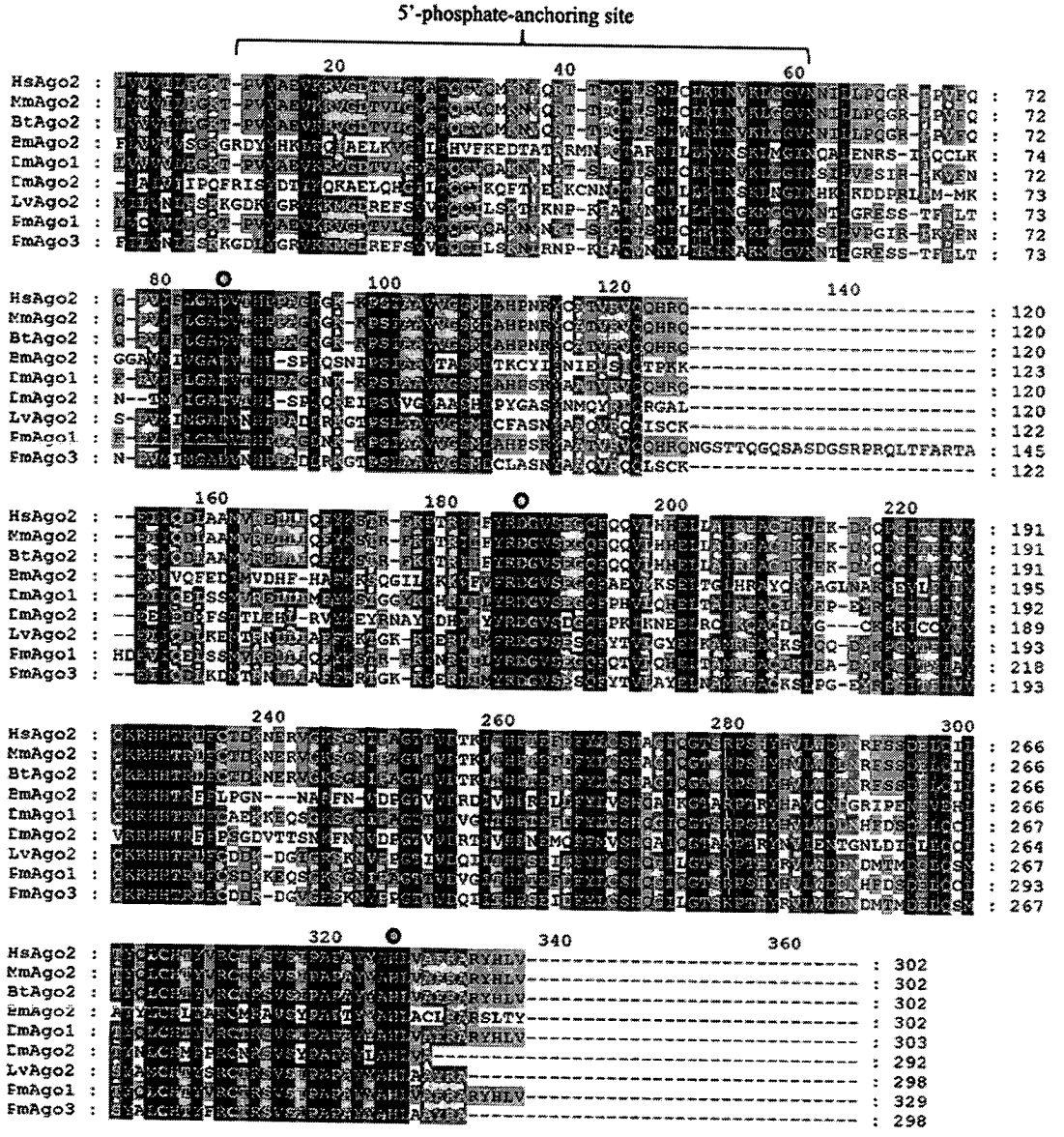

Fig. 2. Multiple sequence alignment of the PIWI domains from PmAgo3 and representative Ago proteins by ClustalW. Identical amino acids are highlighted in black, while similar amino acids are highlighted in gray. Abbreviations are listed in Table 2. The position of catalytic residues DDH motif is indicated with solid circle (●).

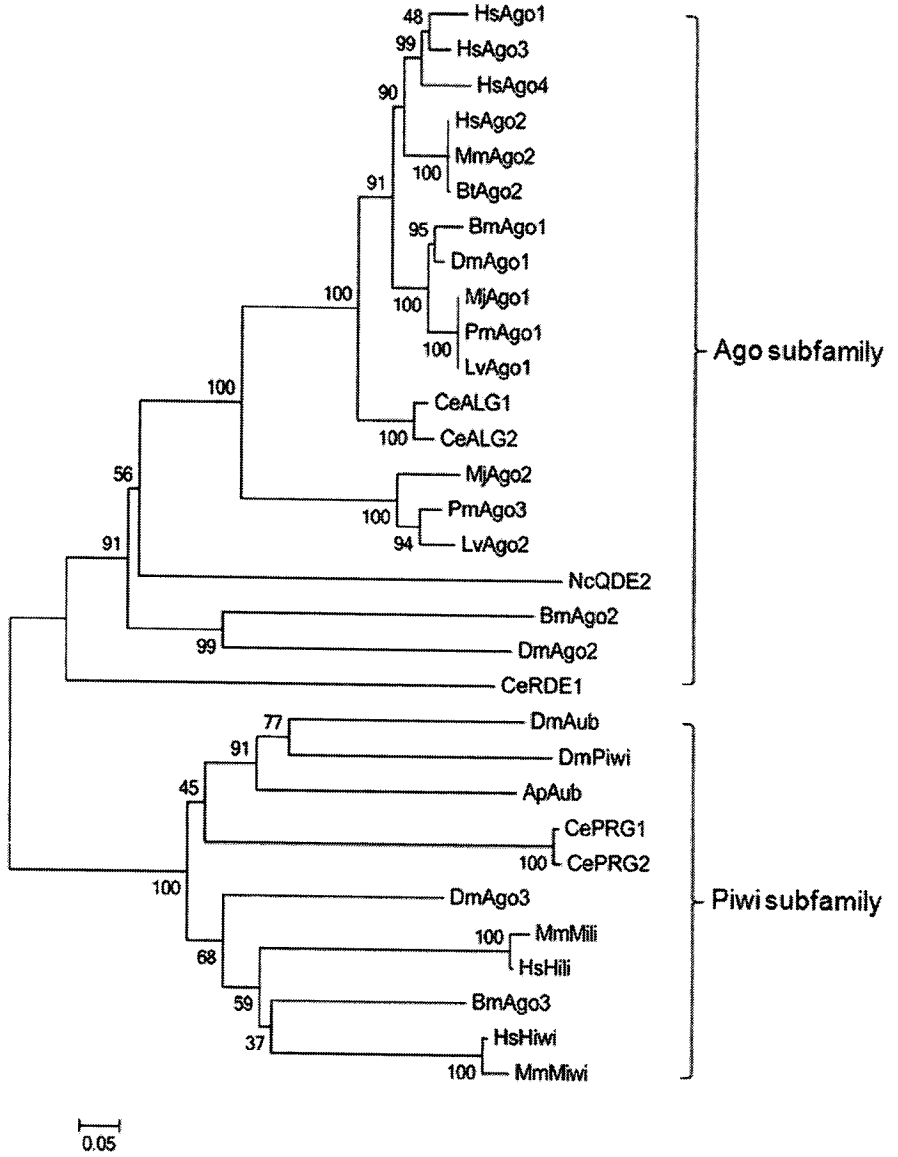

Fig. 3. Phylogenetic relationship of Argonaute proteins. Multiple sequence alignment of PIWI domains was performed by ClustalW. The Neighbor-joining tree was constructed by MEGA 5.05 program. Abbreviations are listed in Table 2. Bootstrap values from 1000 replicates are indicated at the nodes.

analysis of *YHV* and *β-actin* demonstrated that expression of YHV can be detected in all samples at 72 h-post YHV challenge (Fig. S1). These data showed that *PmAgo3* expression was stimulated by dsRNA, but not by YHV challenge.

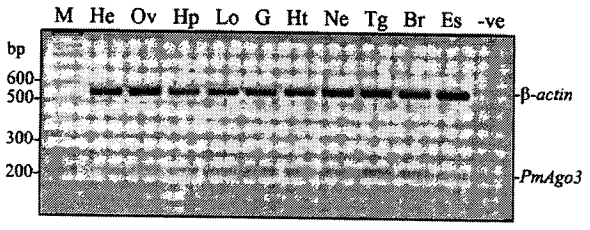

Fig. 4. Tissue distribution of *PmAgo3* expression. A representative gel represents RT-PCR products of *PmAgo3* and *β-actin*. M, 100-bp DNA ladder; He, hemolymph; Ov, ovary; Hp, hepatopancreas; Lo, lymphoid organ; G, gill; Ht, heart; Ne, nerve cord; Tg, thoracic ganglia; Br, brain; Es, eyestalks; –ve, negative control.

3.4. Knockdown effect of PmAgo3 expression on YHV replication

To study the functional significance of PmAgo3 on YHV replication, shrimps were injected with dsAgo3 48 h prior to YHV challenge. Expression of *PmAgo3* can be completely suppressed after 48 h dsAgo3 injection (Fig. 6) whereas its expression was unchanged in the group that injected with NaCl. Similar to the previous result, expression of *PmAgo3* was slightly increased in dsGFP-injected group. In addition, expression of PmAgo1 was unchanged in dsAgo3-injected group suggesting the sequence specific inhibition of *PmAgo3* expression by dsAgo3 (Fig. S2). To determine the knockdown effect of *PmAgo3* on YHV replication, expression of YHV mRNA was determined from the hemolymph collected from *PmAgo3*-knockdown shrimp individually at 24, 30, 36 and 48 h-post YHV challenge. Interestingly, the expression of YHV mRNA could not be observed after 24, 30, 36 and 48 h-post YHV challenge in *PmAgo3*-knockdown shrimps. On the other hand, the expression of YHV mRNA can be detected at 48 h-post YHV challenge in shrimp

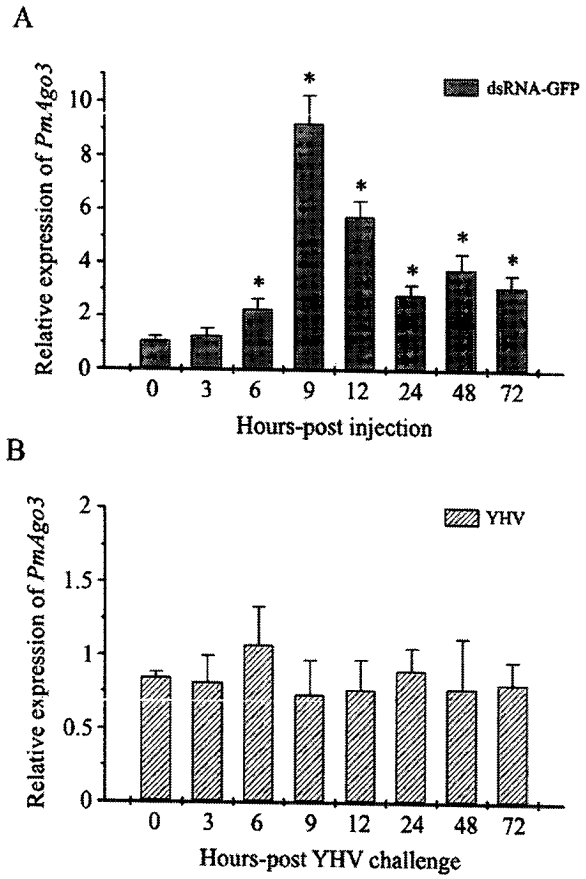

Fig. 5. Expression of *PmAgo3* in response to dsRNA-GFP (A) and YHV challenge (B). Hemolymph was collected from shrimps at various time points following dsRNA administration or YHV challenge. Relative expression of *PmAgo3* normalized by EF-1a was determined by qRT-PCR. Relative expression was calculated based on comparative Ct method ($2^{-\Delta\Delta Ct}$) by using zero time point as a calibrator group. Bars represent means ± SEM (n = 6–8). The asterisks (*) represent the significant difference ($p < 0.05$) of the relative expression of *PmAgo3* comparing to the zero time point.

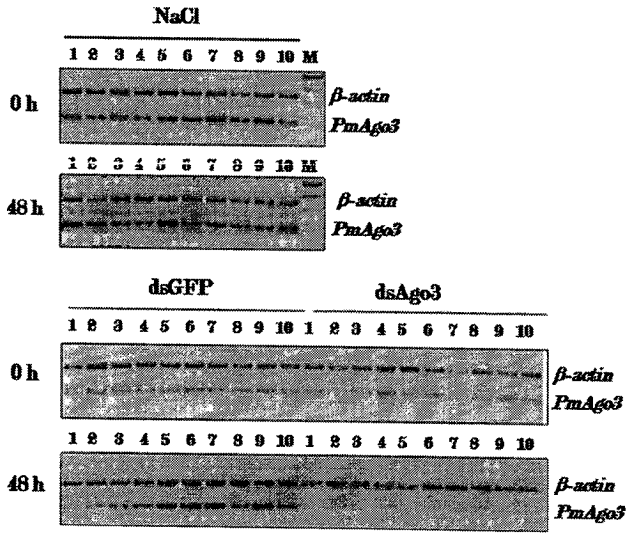

Fig. 6. Suppression of *PmAgo3* expression by dsRNA. Multiplex RT-PCR products of *PmAgo3* and *β-actin* amplified from hemolymph collected before (0 h) and 48 h after injection with 150 mM NaCl, 2.5 μg g^{-1} shrimp of dsRNA-GFP (dsGFP) or dsRNA-*PmAgo3* (dsAgo3). The same number at 0 and 48 h for each treatment group represents the same shrimp.

prior to injection with NaCl or dsGFP (Fig. 7). The knockdown effect of *PmAgo3* still persisted at 48 h YHV challenge in *PmAgo3*-knockdown shrimps (or 4 days after dsAgo3 injection) (Fig. S3). These data implied that *PmAgo3* knockdown could inhibit YHV replication.

4. Discussion

In this study, we have cloned and characterized a novel Argonaute gene from *P. monodon*, *PmAgo3*. As expected, the deduced amino acid of *PmAgo3* exhibited the two signature domains of the proteins in the Argonaute family, including PAZ and PIWI domains. *PmAgo3* was classified into Ago subfamily and clustered in the same group with LvAgo2 and MjAgo2 on the bootstrapped NJ tree, while shrimp Ago1 was closely related to the miRNA class Ago proteins such as DmAgo1, BmAgo1, CeALG1 and CeALG2 [26–28]. Based on the personal communication, PmAgo2 is specifically expressed in the ovary and testis whereas PmAgo3 is ubiquitously expressed in all examined tissues. The full-length open reading frame of PmAgo2 and PmAgo3 shared approximately 40% amino acid sequence identity while the PIWI domain of both proteins shared 56% amino acid sequence identity. Expression of PmAgo2 protein (His-Ago2; 92 kDa) is different from PmAgo3 (His-Ago3; 95 kDa) as shown in Phetrungnapha et al., 2013 [29]. These results suggested that PmAgo3 is unique and distinct from PmAgo2.

Induction of Argonaute expression by dsRNA is required for efficient RNAi pathway. Choudhary et al. demonstrated that high levels of QDE-2 (Argonaute-like protein) expression induced by dsRNA were required for efficient RNAi in *Neurospora crassa*. In addition, induction of DCL-2 (Dicer-like protein) by dsRNA led to an accumulation of QDE-2, suggesting the regulatory mechanism that allowed the optimal function of the RNAi pathway [30]. In this study, we asked whether *PmAgo3* responds to dsRNA or not. Monitoring of *PmAgo3* expression in hemolymph by qRT-PCR demonstrated a strong up-regulation of its expression following dsRNA administration, suggesting its involvement in dsRNA-mediated gene silencing. Up-regulation of Ago and other

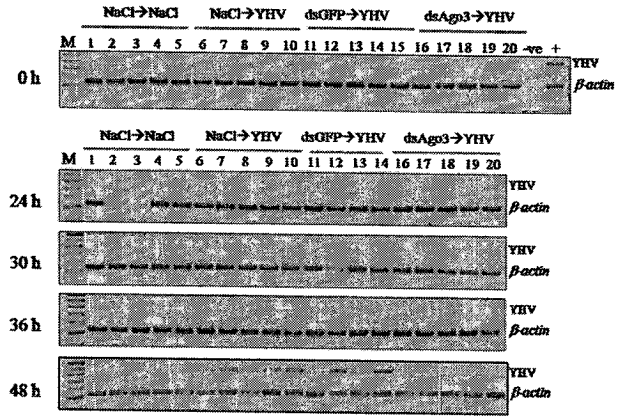

Fig. 7. Knockdown effect of *PmAgo3* expression on YHV replication. Multiplex RT-PCR products of *YHV* and *β-actin* amplified from hemolymph collected before (0 h) and 24, 30, 36, and 48 h after YHV challenge in shrimps prior injection of 150 mM NaCl (NaCl → YHV, lanes 6–10), 2.5 μg g^{-1} shrimp of dsGFP (dsGFP → YHV, lanes 11–15) or 2.5 μg g^{-1} shrimp of dsAgo3 (dsAgo3 → YHV, lanes 16–20). Shrimps injected with NaCl alone (NaCl → NaCl, lanes 1–5) were used as a control group. Lane +ve represents the positive control of RT-PCR using cDNA of YHV infected hemocytes as a template. Lane −ve represents the negative control of RT-PCR using sterile water instead of cDNA as a template. The same number at various time points for each treatment group represents the same shrimp. Shrimp #15 die after YHV challenge.

RNAi-related genes upon dsRNA administration was observed in *L. vannamei* [15,31] and *M. japonicas* (Phetrungnapha et al., unpublished data). In addition, similar pattern of Ago gene regulation was also observed in the tobacco hornworm, *Manduca sexta* Ago2 [32].

Likewise, viruses can trigger RNAi components, resulting in an antiviral response. For example, infection of the cucumber mosaic virus enhanced the accumulation of Ago1 protein in *A. thaliana* [33]. In the rare minnow, *Gobiocypris rarus*, expression of *GrAgo2* was up-regulated after infection with grass carp reovirus [34]. In this study, an alteration of *PmAgo3* expression was not observed following YHV challenge. In contrast, several studies demonstrated that RNAi components in penaeid shrimp responded to viral infection. Unajak et al. demonstrated that the expression of *PmAgo1* in lymphoid organ was increased during the early period of YHV infection [13]. In *L. vannamei*, *LvDicer-1* and *LvDrosha* were up-regulated following taura syndrome virus (TSV) and WSSV challenge, respectively [35,36]. In *Fenneropenaeus chinensis*, Fc-TRBP was up-regulated during WSSV infection [37].

RNAi is a potent antiviral defense mechanism in invertebrate [38]. The dsRNA replicative intermediates and plus-stranded viral RNAs with secondary structure are processed by Dicer, generating viral-derived siRNAs (viRNAs) which are subsequently loaded into Ago proteins and mediated the degradation of viral RNA, thereby conferring antiviral immunity [38–40]. The susceptibility of the host to viruses was increased upon suppression of RNAi machineries. For example, knockdown of Dicer or Ago increased the susceptibility of S2 cells to viral infection [41–43]. In *P. monodon*, knockdown of *PmDicer-1* expression increased the viral load of gill-associated virus, suggesting the importance of RNAi in an antiviral immunity in shrimp [44]. Therefore, to investigate the functional significance of *PmAgo3* in an antiviral immunity, *PmAgo3* was specifically knocked-down by using dsRNA and the level of YHV transcript was subsequently determined. Surprisingly, knockdown of *PmAgo3* inhibited the replication of YHV in shrimp, as the transcript of YHV could not be detected at 48 h when compared with the control groups (NaCl → YHV and dsGFP → YHV), suggesting the role of *PmAgo3* in YHV replication in shrimp. Recent studies in plants and *C. elegans* demonstrated that viRNAs not only contributed to the antiviral immunity but might involve in a viral counter-defense. Viruses utilized viRNAs to modulate cellular gene expression by mediating a potent silencing of host genes in a sequence-specific manner, thereby facilitating viral replication and production of disease symptom [45–47]. For instance, the Y-satellite of cucumber mosaic virus produced viRNAs to silence the chlorophyll biosynthetic gene, CHLI, leading to induction of viral disease production in *Nicotiana tabacum* [46]. In *M. japonicus*, the existence of the viRNAs of WSSV (WSSV-viRNAs) has been demonstrated by Huang et al. [17]. Moreover, the requirement of MjAgo2 (shared 83% amino acid sequence identity with PmAgo3) for the efficient function of WSSV-viRNAs has been also demonstrated [17]. Given the fact that YHV is a positive single-stranded RNA virus, it is plausible that YHV generates viRNAs (YHV-viRNAs) to modulate shrimp gene expression and facilitate its replication. Therefore, loss of *PmAgo3* might interfere the function of YHV-viRNAs, resulting in the inhibition of YHV replication. Identification of YHV-viRNAs should clarify this scenario better.

In conclusion, this study demonstrated that *PmAgo3* responded to dsRNA but not to YHV infection. The requirement of *PmAgo3* in YHV replication was demonstrated. Our study expands an understanding of the RNAi-based mechanisms in penaeid shrimp. Future researches are required to provide insights into the functions of Ago proteins and a regulatory mechanism in the RNAi pathway of these economically important aquatic animals.

Acknowledgments

The authors would like to thank Dr. Witoon Tirasophon for plasmid pET-3a-stGFP, and Ms. Chaweewan Chimwai for technical assistance. This work is supported by grants from the Thailand Research Fund (RSA5480002 to C.O., DPG5680001 to S.P.), the Mahidol University Research Grant, and the Office of the Higher Education Commission and Mahidol University under the National Research University Initiatives. Student fellowship granted to A.P. by the Royal Golden Jubilee Ph.D. Program.

Appendix A. Supplementary data

Supplementary data related to this article can be found at http://dx.doi.org/10.1016/j.fsi.2013.06.025.

References

[1] Hutvagner G, Simard MJ. Argonaute proteins: key players in RNA silencing. Nat Rev Mol Cell Biol 2008;9:22–32.
[2] Schirle NT, MacRae IJ. The crystal structure of human Argonaute2. Science 2012;336:1037–40.
[3] Song JJ, Smith SK, Hannon GJ, Joshua-Tor L. Crystal structure of Argonaute and its implications for RISC slicer activity. Science 2004;305:1434–7.
[4] Kwak PB, Tomari Y. The N domain of Argonaute drives duplex unwinding during RISC assembly. Nat Struct Mol Biol 2012;19:145–51.
[5] Lingel A, Simon B, Izaurralde E, Sattler M. Structure and nucleic-acid binding of the *Drosophila* Argonaute 2 PAZ domain. Nature 2003;426:465–9.
[6] Ma JB, Ye K, Patel DJ. Structural basis for overhang-specific small interfering RNA recognition by the PAZ domain. Nature 2004;429:318–22.
[7] Boland A, Tritschler F, Heimstadt S, Izaurralde E, Weichenrieder O. Crystal structure and ligand binding of the MID domain of a eukaryotic Argonaute protein. EMBO Rep 2010;11:522–7.
[8] Frank F, Sonenberg N, Nagar B. Structural basis for 5′-nucleotide base-specific recognition of guide RNA by human AGO2. Nature 2010;465:818–22.
[9] Wang Y, Sheng G, Juranek S, Tuschl T, Patel DJ. Structure of the guide-strand-containing argonaute silencing complex. Nature 2008;456:209–13.
[10] Carthew RW, Sontheimer EJ. Origins and mechanisms of miRNAs and siRNAs. Cell 2009;136:642–55.
[11] Yigit E, Batista PJ, Bei Y, Pang KM, Chen CC, Tolia NH, et al. Analysis of the *C. elegans* Argonaute family reveals that distinct Argonautes act sequentially during RNAi. Cell 2006;127:747–57.
[12] Dechklar M, Udomkit A, Panyim S. Characterization of Argonaute cDNA from *Penaeus monodon* and implication of its role in RNA interference. Biochem Biophys Res Commun 2008;367:768–74.
[13] Unajak S, Boonsaeng V, Jitrapakdee S. Isolation and characterization of cDNA encoding Argonaute, a component of RNA silencing in shrimp (*Penaeus monodon*). Comp Biochem Physiol B Biochem Mol Biol 2006;145:179–87.
[14] Chen YH, Jia XT, Zhao L, Li CZ, Zhang S, Chen YG, et al. Identification and functional characterization of Dicer2 and five single VWC domain proteins of *Litopenaeus vannamei*. Dev Comp Immunol 2011;35:661–71.
[15] Labreuche Y, Veloso A, de la Vega E, Gross PS, Chapman RW, Browdy CL, et al. Non-specific activation of antiviral immunity and induction of RNA interference may engage the same pathway in the Pacific white leg shrimp *Litopenaeus vannamei*. Dev Comp Immunol 2010;34:1209–18.
[16] Huang T, Zhang X. Contribution of the argonaute-1 isoforms to invertebrate antiviral defense. PLoS One 2012;7:e50581.
[17] Huang T, Zhang X. Host defense against DNA virus infection in shrimp is mediated by the siRNA pathway. Eur J Immunol 2013;43:137–46.
[18] Robalino J, Bartlett T, Shepard E, Prior S, Jaramillo G, Scura E, et al. Double-stranded RNA induces sequence-specific antiviral silencing in addition to nonspecific immunity in a marine shrimp: convergence of RNA interference and innate immunity in the invertebrate antiviral response? J Virol 2005;79:13561–71.
[19] Robalino J, Bartlett TC, Chapman RW, Gross PS, Browdy CL, Warr GW. Double-stranded RNA and antiviral immunity in marine shrimp: inducible host mechanisms and evidence for the evolution of viral counter-responses. Dev Comp Immunol 2007;31:539–47.
[20] Robalino J, Browdy CL, Prior S, Metz A, Parnell P, Gross P, et al. Induction of antiviral immunity by double-stranded RNA in a marine invertebrate. J Virol 2004;78:10442–8.
[21] Assavalapsakul W, Smith DR, Panyim S. Propagation of infectious yellow head virus particles prior to cytopathic effect in primary lymphoid cell cultures of *Penaeus monodon*. Dis Aquat Org 2003;55:253–8.
[22] Saitou N, Nei M. The neighbor-joining method: a new method for reconstructing phylogenetic trees. Mol Biol Evol 1987;4:406–25.
[23] Ongvarrasopone C, Roshorm Y, Panyim S. A simple and cost effective method to generate dsRNA for RNAi studies in invertebrates. ScienceAsia 2007;33:35–9.

[24] Ongvarrasopone C, Chanasakulniyom M, Sritunyalucksana K, Panyim S. Suppression of PmRab7 by dsRNA inhibits WSSV or YHV infection in shrimp. Mar Biotechnol (NY) 2008;10:374–81.
[25] Pfaffl MW. A new mathematical model for relative quantification in real-time RT-PCR. Nucleic Acids Res 2001;29:e45.
[26] Grishok A, Pasquinelli AE, Conte D, Li N, Parrish S, Ha I, et al. Genes and mechanisms related to RNA interference regulate expression of the small temporal RNAs that control *C. elegans* developmental timing. Cell 2001;106: 23–34.
[27] Miyoshi K, Tsukumo H, Nagami T, Siomi H, Siomi MC. Slicer function of *Drosophila* Argonautes and its involvement in RISC formation. Genes Dev 2005;19:2837–48.
[28] Wang G-H, Jiang L, Zhu L, Cheng T-C, Niu W-H, Yan Y-F, et al. Characterization of Argonaute family members in the silkworm, *Bombyx mori*. Insect Sci 2013;20:78–91.
[29] Phetrungnapha A, Panyim S, Ongvarrasopone C. *Penaeus monodon* Tudor staphylococcal nuclease preferentially interacts with N-terminal domain of Argonaute-1. Fish Shellfish Immunol 2013;34:875–84.
[30] Choudhary S, Lee HC, Maiti M, He Q, Cheng P, Liu Q, et al. A double-stranded-RNA response program important for RNA interference efficiency. Mol Cell Biol 2007;27:3995–4005.
[31] Chen YH, Zhao L, Jia XT, Li XY, Li CZ, Yan H, et al. Isolation and characterization of cDNAs encoding Ars2 and Pasha homologues, two components of the RNA interference pathway in *Litopenaeus vannamei*. Fish Shellfish Immunol 2012;32:373–80.
[32] Garbutt JS, Reynolds SE. Induction of RNA interference genes by double-stranded RNA; implications for susceptibility to RNA interference. Insect Biochem Mol Biol 2012;42:621–8.
[33] Zhang X, Yuan YR, Pei Y, Lin SS, Tuschl T, Patel DJ, et al. Cucumber mosaic virus-encoded 2b suppressor inhibits Arabidopsis Argonaute1 cleavage activity to counter plant defense. Genes Dev 2006;20:3255–68.
[34] Su J, Zhu Z, Wang Y, Jang S. Isolation and characterization of Argonaute 2: a key gene of the RNA interference pathway in the rare minnow, *Gobiocypris rarus*. Fish Shellfish Immunol 2009;26:164–70.
[35] Huang T, Xu D, Zhang X. Characterization of shrimp Drosha in virus infection. Fish Shellfish Immunol 2012;33:575–81.
[36] Yao X, Wang L, Song L, Zhang H, Dong C, Zhang Y, et al. A Dicer-1 gene from white shrimp *Litopenaeus vannamei*: expression pattern in the processes of immune response and larval development. Fish Shellfish Immunol 2010;29: 565–70.
[37] Wang S, Liu N, Chen AJ, Zhao XF, Wang JX. TRBP homolog interacts with eukaryotic initiation factor 6 (eIF6) in *Fenneropenaeus chinensis*. J Immunol 2009;182:5250–8.
[38] Sabin LR, Hanna SL, Cherry S. Innate antiviral immunity in *Drosophila*. Curr Opin Immunol 2010;22:4–9.
[39] Kemp C, Imler JL. Antiviral immunity in *Drosophila*. Curr Opin Immunol 2009;21:3–9.
[40] Aliyari R, Wu Q, Li HW, Wang XH, Li F, Green LD, et al. Mechanism of induction and suppression of antiviral immunity directed by virus-derived small RNAs in *Drosophila*. Cell Host Microbe 2008;4:387–97.
[41] Wang X-H, Aliyari R, Li W-X, Li H-W, Kim K, Carthew R, et al. RNA interference directs innate immunity against viruses in adult *Drosophila*. Science 2006;312: 452–4.
[42] van Rij RP, Saleh M-C, Berry B, Foo C, Houk A, Antoniewski C, et al. The RNA silencing endonuclease Argonaute 2 mediates specific antiviral immunity in *Drosophila melanogaster*. Genes Dev 2006;20:2985–95.
[43] Galiana-Arnoux D, Dostert C, Schneemann A, Hoffmann JA, Imler J-L. Essential function *in vivo* for Dicer-2 in host defense against RNA viruses in *Drosophila*. Nat Immunol 2006;7:590–7.
[44] Su J, Oanh DT, Lyons RE, Leeton L, van Hulten MC, Tan SH, et al. A key gene of the RNA interference pathway in the black tiger shrimp, *Penaeus monodon*: identification and functional characterisation of Dicer-1. Fish Shellfish Immunol 2008;24:223–33.
[45] Guo X, Li WX, Lu R. Silencing of host genes directed by virus-derived short interfering RNAs in *Caenorhabditis elegans*. J Virol 2012;86:11645–53.
[46] Smith NA, Eamens AL, Wang MB. Viral small interfering RNAs target host genes to mediate disease symptoms in plants. PLoS Pathog 2011;7: e1002022.
[47] Shimura H, Pantaleo V, Ishihara T, Myojo N, Inaba J, Sueda K, et al. A viral satellite RNA induces yellow symptoms on tobacco by targeting a gene involved in chlorophyll biosynthesis using the RNA silencing machinery. PLoS Pathog 2011;7:e1002021.

Program Book

THE 36th CONGRESS on SCIENCE and TECHNOLOGY of THAILAND (STT 36)

การประชุมวิชาการวิทยาศาสตร์และเทคโนโลยีแห่งประเทศไทย ครั้งที่ 36 (วทท 36)

Building Better Society through Science and Technology

สร้างสังคมที่ดีด้วยวิทยาศาสตร์และเทคโนโลยี

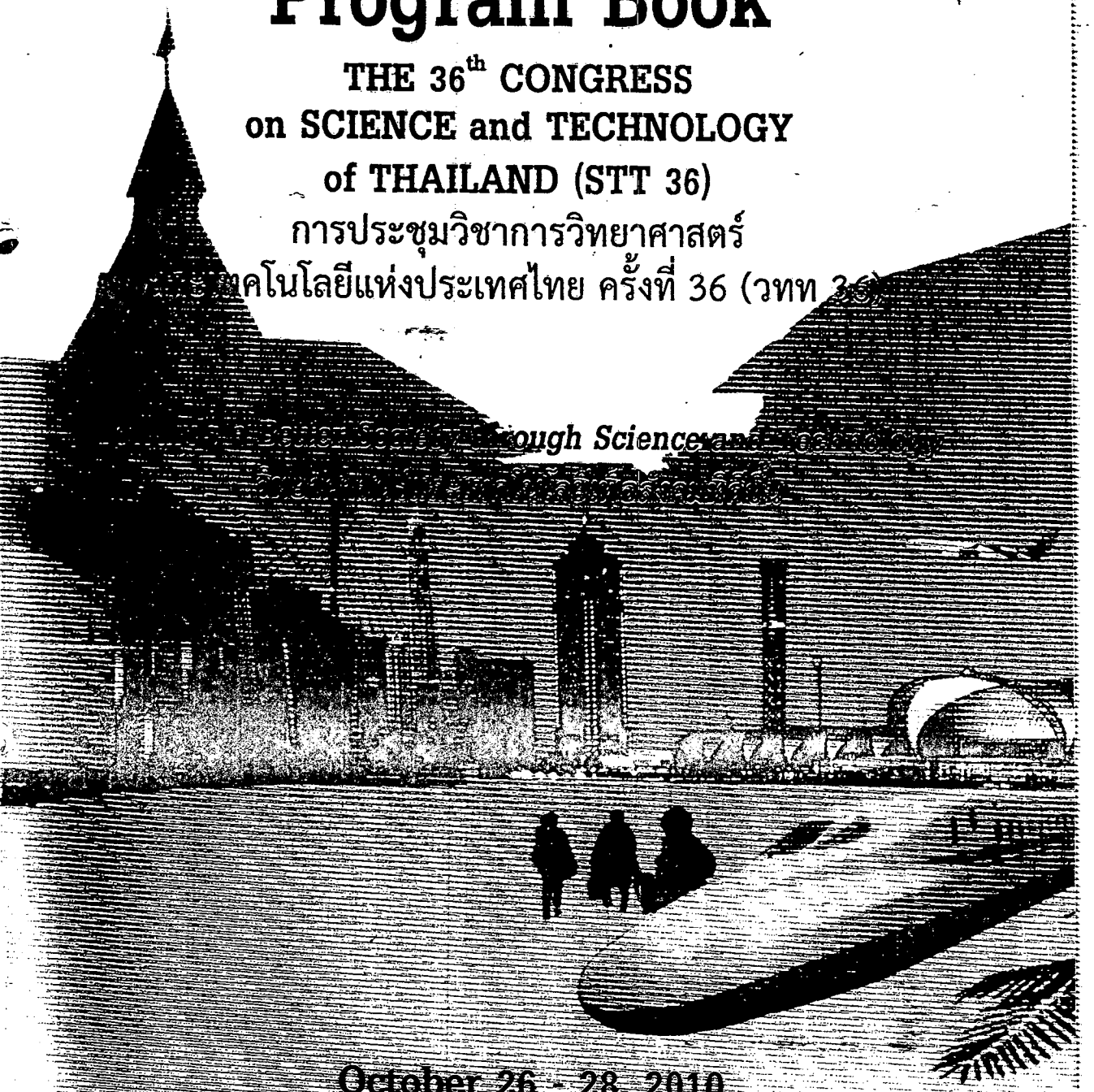

October 26 - 28, 2010

Venue: Bangkok International Trade & Exhibition Centre (BITEC), Bangkok, Thailand.

26 - 28 ตุลาคม 2553 ณ ศูนย์นิทรรศการและการประชุมไบเทค กรุงเทพฯ

www.stt36.scisoc.or.th

Kanlya Prapan[1,2], Panida Kongsawadworakul[3], Unchera Viboonjun[3], Hervé Chrestin[4] and Jarunya Narangajavana[1,*]
[1] Department of Biotechnology, Faculty of Science, Mahidol University, Bangkok, Thailand
[2] Rubber Research Institute of Thailand (RRIT), Thailand
[3] Department of Plant Science, Faculty of Science, Mahidol University, Bangkok, Thailand
[4] Institut de Recherche pour le Développement (IRD), Montpellier, France
*e-mail: scjnr@mahidol.ac.th

Abstract: Rubber tree, *Hevea brasiliensis* Muell. Arg., is one of the most important economic crops in Thailand as it is a major source for natural rubber. In order to improve the rubber clones via conventional breeding, at least 25-30 years are required. Therefore, a development of molecular markers would significantly accelerate the genetic improvement of this plant. The approach mainly relied on data mining of the IRD and CIRAD pipelines, allowing SSR search and primer design. The bioinformatics results from the various *H. brasiliensis* bark and latex SSH libraries, consisting of 10,321 ESTs from the cDNAs deposited in the MU-IRD *Hevea* ESTs database (ESTDB), revealed 431 SSR-containing ESTs (EST-SSRs). Di- and trinucleotide repeats were the most abundant with 46.6 and 44.3%, respectively. A total of 298 primer pairs could be designed from the 291 non-redundant EST-derived SSRs which classified into 8 groups of gene function. The newly developed DNA markers could be used for genetic mapping, genetic diversity study and marker assisted selection in rubber tree breeding program.

B4_B0079: Bioethanol production from banana peel by co-culture of *Saccharomyces cerevisiae* and *Candida tropicalis*

Nattiya Chanthawongsa*, Jirasak Kongkiattikajorn
[1] Division of Biochemical Technology, School of Bioresources and Technology, King Mongkut's University of Technology Thonburi, Bangkok 10150, Thailand
*e-mail: nutter_par@hotmail.com

Abstract: Banana peel, the solid waste obtained from food processing were used to produce bioethanol by the process called simultaneous saccharification and fermentation (SSF). Ethanol was produced from banana peel which were pretreated with diluted sulfuric acid by SSF with mono-culture of *Saccharomyces cerevisiae* KM 5221 or *Candida tropicalis* TISTR 5045 and co-culture of *S. cerevisiae* KM 5221 and *C. tropicalis* TISTR 5045. The results indicated that each strain of mono-culture was able to produce ethanol with high yield. *S. cerevisiae* KM 5221 could fermented banana peel pretreated with diluted sulfuric acid and steam at 121°C under pressure of 15 lb/inch^2 for 20 min to produce ethanol yield higher than that of *C. tropicalis* TISTR 5045 under the same condition. The fermentation by co-culture of *S. cerevisiae* KM 5221 and *C. tropicalis* TISTR 5045 could produce ethanol higher than that of by mono-culture.

B4_B0090: Production of pullulan, poly(β-L-malic acid), and heavy oil by fungus *Aureobasidium pullulans* isolated from Thailand

Chalisa Tuwichein[1], Porntip Krisraksa[1], Sasithorn Eardklay[1], Timothy D. Leathers[2], Christopher D. Skory[2], Napapan Pongpoungphet[3], Pennapa Manitchotpisit[1,*]
[1] Biomedical Sciences Program, Faculty of Science, Rangsit University, Patumthani 12000, Thailand
[2] Renewable Products Technology Research Unit, National Center for Agricultural Utilization Research, ARS, USDA, Peoria, IL 61604, USA
[3] Department of Chemistry, Faculty of Science, Rangsit University, Patumthani 12000, Thailand
*e-mail: pennapa@rsu.ac.th, pennapam@hotmail.com

Abstract: Fungus *Aureobasidium pullulans* is the main source of a polysaccharide, pullulan, in industrial production. Moreover, it can produce many bioproducts, e.g. xylanase, poly(β-L-malic acid) (PMA), and heavy oil. In this study, we isolated 15 *A. pullulans* isolates from various sources and habitats in Thailand and classified using morphological characteristic and sequencing analysis of 2 loci, i.e. ITS (internal transcribed spacer) and BT (beta tubulin). Comparison to database in GenBank, these isolates could be divided into 5 clades indicating the diversity of this fungus in tropical zone. Furthermore, representatives of each clade were selected to study pullulan, PMA, and heavy oil production compared to reference strains. The results showed that *A. pullulans* from each strain can produce both different yields and characters. This study would be useful for strain selection and development of production from this fungus in the future.

B4_B0098: Suppression of Tudor Staphylococcal Nuclease gene of *Penaeus monodon* through dsRNA targeting SN-like domain

Amnat Phetrungnapha[1,*], Sakol Panyim[1,2], Chalermporn Ongvarrasopone[1]

[1] Institute of Molecular Biosciences, Mahidol University, Phutthamonthon 4th Road, Nakhon Pathom, 73170, Thailand
[2] Department of Biochemistry, Faculty of Science, Mahidol University, Rama VI Road, Phayathai, Bangkok 10400, Thailand
*e-mail: amnatpht@gmail.com

Abstract: Tudor staphylococcal nuclease (TSN or p100) is a multifunctional protein which involves in a variety of cellular processes about RNA including transcription, RNA splicing, RNA editing and RNA interference (RNAi). In this study, we aim to investigate the role of TSN in RNAi pathway of *Penaeus monodon* or black tiger shrimp using double stranded (dsRNA) - mediated gene silencing approach. Two dsRNAs targeting the *P. monodon* TSN gene (PmTSN) were produced by *in vitro* transcription and *in vivo* bacterial expression. DsRNAs were introduced into shrimp body via intramuscular injection. The results showed that injection of dsRNA targeting SN3-like domain could effectively suppress the expression of PmTSN whereas the expression of PmTSN was not affected by dsRNA targeting tudor-SN5 domain. SN3-dsRNA will be used to study the role of PmTSN in RNAi pathway in the future.

B4

B4_B0099: Development of a novel gene expression system in *Pichia pastoris*

Sawarot Maibunkaew[1], Sutipa Tanapongpipat[2], Witoon Tirasophon[1,*]
[1] Institute of Molecular Biosciences, Mahidol University, Nakhon Pathom 73170, Thailand
[2] National Center for Genetic Engineering and Biotechnology, Pathumthani 12120, Thailand
*e-mail: mbwtr@mahidol.ac.th

Abstract: *Pichia pastoris* is an attractive microbial host for heterologous gene expression. *P. pastoris* was identified as generally regarded as safe (GRAS) microorganism which possesses a tightly controlled inducible but strong promoter (AOX1). These features make it an ideal host for recombinant protein expression. This study aims to engineer an alternative plasmid vector for efficient recombinant protein expression in *P. pastoris*. This novel plasmid was assembled from three major parts: an origin of replication in *E. coli*, a selectable marker that is functional in both *E. coli* and *P. pastoris* and a cassette for heterologous gene expression in *P. pastoris*. Functional analysis of this novel vector by expressing human granulocyte colony stimulating factor (GCFS) in *P. pastoris* KM71 showed that it has at least comparable efficiency to the commercial pPICZα plasmid.

B4_B0103: Pretreatment of lignocellulosic wastes for ethanol production

Kittamas Sirichai, Nantana Srisuk*, Savitree Limtong
Department of Microbiology, Faculty of Science, Kasetsart University, Bangkok 10900, Thailand
*e-mail: fscints@ku.ac.th

Abstract: Pretreatment of lignocellulosic waste was carried out using rice straw, cassava pulp and cassava peels. Acid, alkaline and were heat either individual or in combination to establish a feasible pretreatment method prior to enzymatic hydrolysis of individual substrates for further used in bioethanol production. Pretreatment of rice straw using 2% NaOH at 85°C for 1 hour prior to enzymatic hydrolysis yielded glucose and xylose as 430.0 ± 0.5 and 162.0 ± 0.2 mg per g dried substrate, respectively. The cassava pulp pretreatment by 1N HCl prior to enzymatic hydrolysis revealed the amount of glucose and xylose as 410.3± 0.5 and 31.2 ± 0.1 mg per g dried substrate, respectively. Similar acid pretreatment scheme was also found to be feasible for cassava peel as a result of 414.1 ± 0.5 mg glucose and 24.3 ± 0.1 mg xylose obtained per gram of dried substrate.

B4_B0106: BAX gene silencing with miRNA in H_2O_2-induced buffalo fibroblast cells (BFC)

Parisatcha Sangsuwan[1], Pirut Thong-Ngam[1], Yindee Kitiyanant[2,*]
[1] Institute of Molecular Biosciences, Mahidol University, , Nakhon Pathom 73170, Thailand
[2] Department of Anatomy, Faculty of Science, Mahidol University, Rama VI Rd.,Phayathai, Bangkok,10400, Thailand
*e-mail: scykt@mahidol.ac.th

Abstact: RNA interference (RNAi) technology is one of key methods used to control the expression of genes. This study, we designed short nucleotides which has complementary with BAX gene. Then insert these short nucleotides into suitable vector and transfected into buffalo fibroblast (BFC) cells. Apoptosis was induced by treatment with H_2O_2 . The results showed 80% viability in miBAX-BFC and 20% min miCont-BFC. RT-PCR revealed BAX gene expression decrease compared with miCont-BFC, but Bcl-2 gene expression was not different. BAX protein was reduced in miBAX-BFC and normal control cell, but Bcl-2

Proceedings of The 39th Congress on Science and Technology of Thailand

การประชุมวิชาการวิทยาศาสตร์ และเทคโนโลยีแห่งประเทศไทย

วทท STT39

ครั้งที่ 39

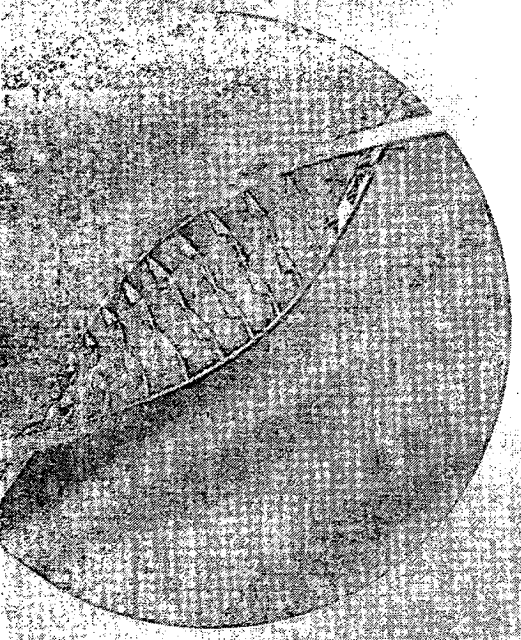

Innovative Science *for a Better Life*

นวัตกรรมวิทยาศาสตร์เพื่อชีวิตที่ดีขึ้น

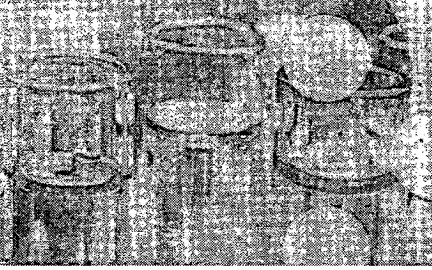

FSCI คณะวิทยาศาสตร์

KMUTT มจธ.

การประชุมวิชาการ
วิทยาศาสตร์และเทคโนโลยีแห่งประเทศไทย ครั้งที่ 39

ABSTRACTS

39th Congress on Science and Technology of Thailand (STT 39)

Innovative Science for a Better Life

October 21 - 23, 2013
Venue: Bangkok International Trade & Exhibition Centre (BITEC), Bangkok, Thailand

Organized by:
The Science Society of Thailand under the Patronage of His Majesty the King
in Association with Faculty of Science, King Mongkut's University of Technology Thonburi

Expression of *Penaeus monodon* Tudor staphylococcal nuclease protein for polyclonal antibody production

Primrata Patpol, Sakol Panyim, Chalermporn Ongvarrasopone

Institute of Molecular Bioscience, Mahidol University, Nakhon Pathom 73170, Thailand

Abstract

Penaeus monodon Tudor staphylococcal nuclease (PmTSN) is one of the RNA-induced silencing complex (RISC) components which plays roles in many biological processes including RNA interference (RNAi). In order to study the functions of PmTSN, antibody against PmTSN was generated to use in many assays such as *in vitro* pull-down, western blot analysis and immunofluorescent detection. In this study, the large scale expression of the fusion protein, GST-TSN (Tudor-SN5 domains) was optimized by varying time of induction. The *E.coli* cells strain Rosetta (DE3) harboring plasmid pGEX-5X-1 containing the Tudor-SN5 domains was induced by 1 mM IPTG at 37 ºC for 4 hours. The fusion protein was expressed as a 50 kDa protein as an inclusion body. Then the fusion protein was purified and subjected for polyclonal antibody production in rabbit. To test for the sensitivity and specificity of the anti-PmTSN antibody, dot blot and western blot analysis were performed. The anti-PmTSN antibody can detect the purified PmTSN protein at 0.025 µg at 5,000 dilutions. In the future, this antibody will be used to study the localization and expression levels of the PmTSN protein in shrimp tissues in order to understand the functions of PmTSN.

Introduction

Penaeus monodon Tudor staphylococcal nuclease (PmTSN) is identified as one of the RISC components which interacted with PmAgo1. It contains tandem repeats of the SN domains followed by a Tudor and SN5 domain. It encodes a protein of 889 amino acids with a predicted molecular weight of 99.7 kDa. In addition, TSN also plays roles in many biological processes such as a transcriptional coactivator, RNA splicing and RNA editing. In order to study the role or the interaction of the RISC component, PmTSN, polyclonal antibody against PmTSN could be generated. Therefore, the purpose of this study is to produce the PmTSN fusion protein for polyclonal antibody production and evaluate its sensitivity and specificity. This antibody will be used to study the localization of PmTSN protein in hemocyte cells in order to investigate whether PmTSN plays a key role during virus infection.

Methods

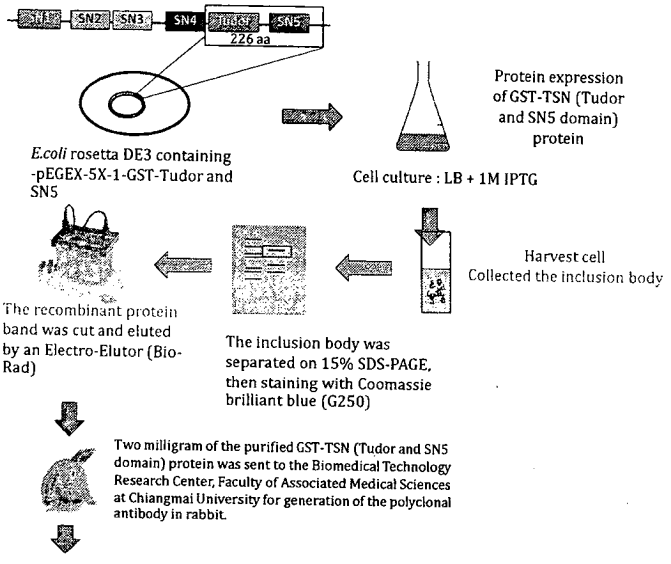

Results and Discussion

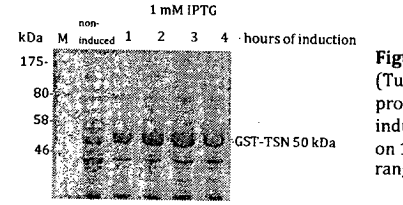

Figure 1. Expression of GST-TSN (Tudor and SN5 domain) fusion protein. The non-induced and induced proteins were analyzed on 15% SDS-PAGE. M is Broad range protein marker.

GST-PmTSN (Tudor and SN5 domain) protein, approximately 50 kDa was expressed at high levels as an inclusion body in the condition of 1 mM IPTG induction at 37 ºC for 4 hours.

Results and Discussion

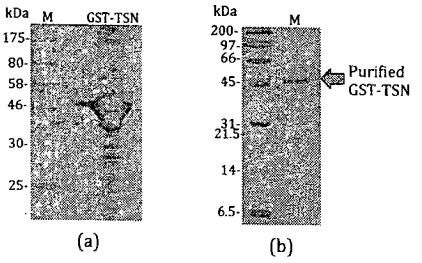

Figure 2. Large scale expression of the GST-TSN fusion protein
(a) The GST-TSN fusion protein was expressed in *E.coli* cells strain Resetta DE3 under 1 mM IPTG induction at 37 ºC for 4 hours.
(b) The purified GST-TSN fusion protein was analyzed on 15% SDS PAGE.
M is Broad range protein marker.

The GST-TSN fusion protein was purified by an Electro-Elutor (Bio-Rad) and the concentration is approximately about 1.00 mg/ml.

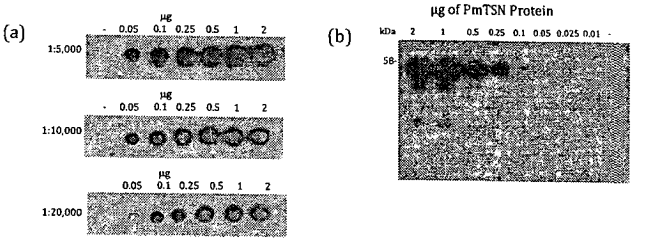

Figure 3. Investigation of the sensitivity and specificity of the anti-rabbit PmTSN antibody.
(a) Dot blot analysis of the anti-rabbit PmTSN antibody at 1:5,000, 1:10,000 and 1:20,000 dilutions.
(b) Western blot analysis using anti-rabbit PmTSN antibody.

The anti-rabbit PmTSN antibody can react with the purified GST-TSN fusion protein at least 0.025 µg at 1:5,000 dilutions on dot blot assay (Figure 3a). By using the western blot analysis, an anti-rabbit PmTSN antibody can detect the 50 kDa purified GST-TSN fusion protein at 0.1 µg at 1:5,000 dilutions (Figure 3b).

Conclusion

The anti-PmTSN antibody will be used to detect the PmTSN protein from various tissues of black tiger shrimp by western blot analysis and will be applied to study the localization PmTSN protein in hemocyte cell by an immunofluorescence technique in the future.

References

1. Phetrungnapha A, Panyim S, Ongvarrasopone C. Fish Shellfish Immunol 2013;34:875-84
2. Phetrungnapha A, Panyim S, Ongvarrasopone C. Fish Shellfish Immunol 2011;31:373-80.
3. Tong X, Drapkin R, Yalamanchili R, Mosialos G, Kieff E. Mol Cell Biol. 1995;15:4735-44.
4. Yang J, Valineva T, Hong J, Bu T, Yao Z, Jensen ON, et al. Nucleic Acids Res.2007;35 :4485-94.

Acknowledgement

We would like to thank Dr Amnat Phetrungnapha for plasmid, pGEX-5X-1-TSN (Tudor-SN5 domains).This work is supported by grant from The Thailand Research Fund (RSA5480002 to CO).

nuclear proteins showed a shift band of the DNA-protein complex on both DNA fragments that could be competed by specific competitor. The protein that binds to these DNA fragments will be further characterized. (full paper available on CD)

F_F0035: ANTIPROLIFERATION AND APOPTOSIS INDUCED BY NEEM FLOWER EXTRACT IN SELECTED HUMAN CANCER CELL LINES

Pirut Tong-ngam,[1] Sittiruk Roytrakul,[2] Piengchai Kupradinun,[3] Suthathip Kittisenachai,[2] Hathaitip Sritanaudomchai[4,*]
[1]Institute of Molecular Biosciences, Mahidol University, Nakhon Pathom 73170, Thailand
[2]National Center for Genetic Engineering and Biotechnology, Pathumthani 12120, Thailand
[3]Research Division, National Cancer Institute, Bangkok 10400, Thailand
[4]Faculty of Dentistry, Mahidol University, Bangkok 10400, Thailand
*e-mail: hathaitip.sri@mahidol.ac.th

Abstract: Neem flowers (*Azadirachta indica* A. Juss) is a common vegetable consumed in Thailand which they have antioxidant, anti-inflammatory and anticlastogenic activities. Here, we investigated the antiproliferative and pro-apoptotic effects of the methanolic extract of neem flowers (MENF) on oral cancer cell line HSC4, breast cancer cell line MCF7 and colon cancer cell line SW480. We found that MENF at concentrations of 50-500 µg/ml inhibits cell viability of all selected cancer cell lines in dose-dependent manner after 24 h culture. The MENF showed the lowest IC50 value (400 µg/ml) on MCF7 cells but was also more active on HSC4 cells (IC50 value of 215 µg/ml) and on SW480 cells (IC50 value of 250 µg/ml). Furthermore, we designed to examine the apoptosis inducing capacity of MENF using the apoptosis-associated genes caspase 3, caspase 7, caspase 8 and caspase 9 as markers. A significant decrease in HSC4 cells viability was accompanied by upregulation of caspase 3, caspase 7, and caspase 9 transcripts. The MENF treatment on MCF7 cell line resulted with increased expression of caspase 3, caspase 8, and caspase 9 whereas the MENF treatment on SW480 cells showed upregulated of caspase 3, caspase 7, and caspase 8 transcripts. Together, these results indicate that the chemopreventive effects of MENF may be mediated by growth suppression and induces apoptotic cell death of human cancer cells. Further investigations of the mechanism of action of MENF are warranted in evaluating the potential usefulness of this herbal remedy in the management of cancer patients. (abstract only)

F_F0036: EXPRESSION OF *Penaeus monodon* TUDOR STAPHYLOCOCCAL NUCLEASE PROTEIN FOR POLYCLONAL ANTIBODY PRODUCTION

Primrata Patpol, Sakol Panyim, Chalermporn Ongvarrasopone*
Institute of Molecular Bioscience, Mahidol University, Nakhon Pathom 73170, Thailand
*e-mail: chalermporn.ong@mahidol.ac.th

Abstract: *Penaeus monodon* Tudor staphylococcal nuclease (PmTSN) is one of the RNA-induced silencing complex (RISC) components which plays roles in many biological processes including RNA interference (RNAi). In order to study the functions of PmTSN, antibody against PmTSN was generated to use in many assays such as *in vitro* pull-down, western blot analysis and immunofluorescent detection. In this study, the large scale expression of the fusion protein, GST-TSN (Tudor-SN5 domains) was optimized by varying time of induction. The *E.coli* cells strain Rosetta (DE3) harboring plasmid pGEX-5X-1 containing the Tudor-SN5 domains was induced by 1 mM IPTG at 37 °C for 4 hours. The fusion protein was expressed as a 50 kDa protein in an inclusion body. Then the fusion protein was purified and subjected for polyclonal antibody production in rabbit. To test for the sensitivity and specificity of the anti-PmTSN antibody, dot blot and western blot analysis were performed. The anti-PmTSN antibody can detect the purified PmTSN protein at 0.025 µg at 5,000 dilutions. In the future, this antibody will be used to study the localization and expression levels of the PmTSN protein in shrimp tissues in order to understand the functions of PmTSN. (full paper available on CD)

F_F0036: EXPRESSION OF *Penaeus monodon* TUDOR STAPHYLOCOCCAL NUCLEASE PROTEIN FOR POLYCLONAL ANTIBODY PRODUCTION

Primrata Patpol, Sakol Panyim, Chalermporn Ongvarrasopone*
Institute of Molecular Bioscience, Mahidol University, Nakhon Pathom 73170, Thailand
*e-mail: chalermporn.ong@mahidol.ac.th

Abstract: *Penaeus monodon* Tudor staphylococcal nuclease (PmTSN) is one of the RNA-induced silencing complex (RISC) components which plays roles in many biological processes including RNA interference (RNAi). In order to study the functions of PmTSN, antibody against PmTSN was generated to use in many assays such as *in vitro* pull-down, western blot analysis and immunofluorescent detection. In this study, the large scale expression of the fusion protein, GST-TSN (Tudor-SN5 domains) was optimized by varying time of induction. The *E.coli* cells strain Rosetta (DE3) harboring plasmid pGEX-5X-1 containing the Tudor-SN5 domains was induced by 1 mM IPTG at 37 °C for 4 hours. The fusion protein was expressed as a 50 kDa protein in an inclusion body. Then the fusion protein was purified and subjected for polyclonal antibody production in rabbit. To test for the sensitivity and specificity of the anti-PmTSN antibody, dot blot and western blot analysis were performed. The anti-PmTSN antibody can detect the purified PmTSN protein at 0.025 μg at 5,000 dilutions. In the future, this antibody will be used to study the localization and expression levels of the PmTSN protein in shrimp tissues in order to understand the functions of PmTSN.

Introduction: RNA interference (RNAi) plays an important role as an antiviral defense in several organisms including black tiger shrimp. Understanding of the RNAi mechanism especially the RNAi machineries is very important to elucidate shrimp antiviral response and improve shrimp resistance to viruses. RNAi technology using double stranded RNA (dsRNA) is a promising tool to prevent or cure viral infection in shrimp and to identify gene function. Therefore, there is much interest to study the RNAi pathway. An identification of RISC component is essential for understanding the RNAi mechanism. Interestingly, *Penaeus monodon* Tudor staphylococcal nuclease (PmTSN) is identified as a one of the RISC components which interacted with PmAgo1.[1] It contains tandem repeats of the SN domains followed by a Tudor and SN5 domain. It encodes a protein of 889 amino acids with a predicted molecular weight of 99.7 kDa.[2] In addition, TSN also plays roles in many biological processes such as a transcriptional coactivator,[3] RNA splicing and RNA editing.[4] In order to study the role or the interaction of the RISC component, PmTSN, polyclonal antibody against PmTSN could be generated. Therefore, the purpose of this study is to produce the PmTSN fusion protein for polyclonal antibody production and evaluate its sensitivity and specificity. This antibody will be used to study the localization of PmTSN protein in hemocyte cells in order to investigate whether PmTSN plays a key role during virus infection.

Methodology: The recombinant plasmid, pGEX-5X-1 containing TSN (Tudor and SN5 domain) was transformed into *E .coli* cells strain Rosetta (DE3) and cultured in Luria-Bertani (LB) broth to an exponential phase. An expression of the recombinant protein was induced with 1 mM isopropylthio-β-galactoside (IPTG) and the expression conditions were optimized by varying time of induction at 1, 2, 3 and 4 hours at 37 °C. The fusion protein was expressed under 1 mM IPTG induction at 37 °C for 4 hours. After disrupted the cells, the inclusion body of the recombinant protein was harvested. The inclusion body was washed with 0.1, 0.5 and 1.0% Triton X-100 in 50 mM Tris-HCl, 1 mM EDTA, pH 8.0, respectively. Then, the inclusion body was resuspended with the sample buffer and separated on 15% SDS-PAGE. After staining with Coomassie brilliant blue (G250), the recombinant protein band was cut and eluted by an Electro-Elutor (Bio-Rad) (Protein Elution Buffer; 25 mM Tris-HCl, 192 mM Glycine and 0.04% SDS). The purified protein was collected and stored at 4 °C. An

estimation of the protein concentration was performed by comparison with the Board range protein marker. Two milligram of the purified GST-TSN (Tudor and SN5 domain) protein was sent to the Biomedical Technology Research Center, Faculty of Associated Medical Sciences at Chiangmai University for generation of the polyclonal antibody in rabbit. The dilutions of GST-TSN (Tudor and SN5 domain) protein from 2 to 0.0001 microgram were used to test the sensitivity of PmTSN antibody by dot blot assay and western blot analysis.

Results, Discussion and Conclusion: GST-PmTSN (Tudor and SN5 domain) protein, approximately 50 kDa was expressed at high levels as an inclusion body in the condition of 1 mM IPTG induction at 37 °C for 4 hours (Figure 1). After an expression of the fusion protein following the optimum condition, the protein concentration was determined by comparison with the Board range protein marker (BioRad SDS-PAGE Molecular Weight Standards, Broad Range 161-0317). The concentration of the purified GST-TSN (Tudor and SN5 domain) protein is 1.00 mg/ml (Figure 2).

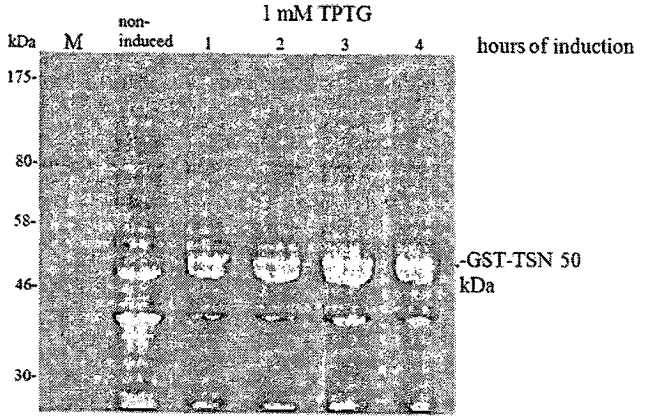

Figure 1. Expression of GST-TSN (Tudor and SN5 domain) fusion protein. The protein was expressed under 1 mM IPTG at 37 °C for 1, 2, 3 and 4 hours. The non-induced and induced at 1, 2, 3 and 4 hours were analyzed on 15% SDS-PAGE. M is Broad range protein marker.

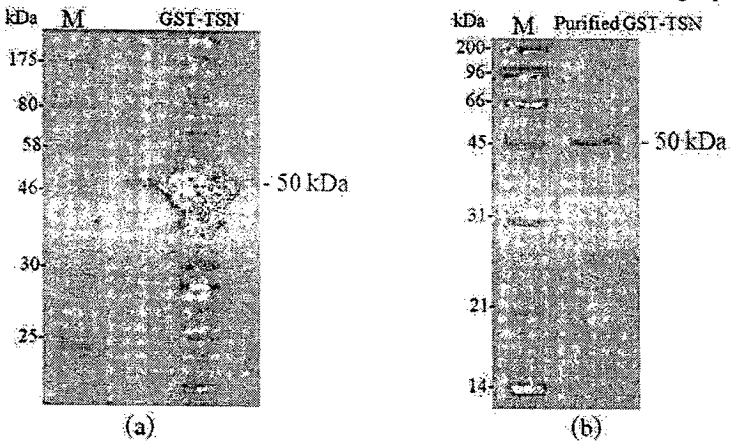

Figure 2. Large scale expression of the GST-TSN fusion protein (a) The GST-TSN fusion protein was expressed in *E.coli* cells strain Resetta DE3 under 1 mM IPTG induction at 37 °C for 4 hours. (b) The purified GST-TSN fusion protein was analyzed on 15% SDS PAGE. M is Broad range protein marker.

To evaluate the sensitivity of anti-rabbit PmTSN antibody, the dot blot assay was performed. The anti-rabbit PmTSN antibody can react with the purified GST-TSN fusion protein at least 0.025 μg at 1:5,000 dilutions on dot blot assay. By using the western blot analysis, an anti-rabbit PmTSN antibody can detect the 50 kDa purified GST-TSN fusion protein at 0.1 μg at 1:5,000 dilutions (Figure 3). The anti-PmTSN antibody will be used to detect the PmTSN protein from various tissues of black tiger shrimp by western blot analysis

and will be applied to study the localization PmTSN protein in hemocyte cell by an immunofluorescence technique in the future.

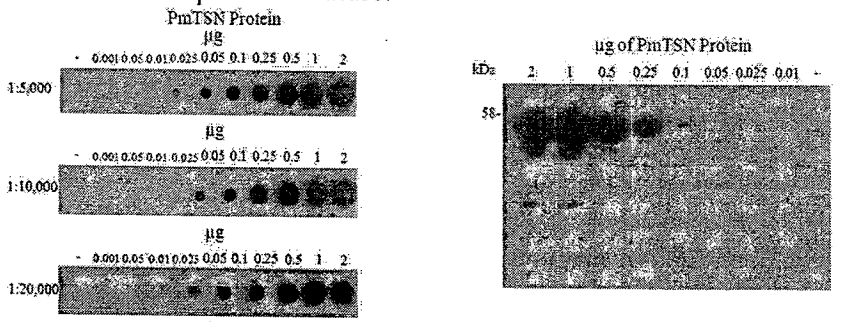

Figure 3. Investigation of the sensitivity and specificity of the anti-rabbit PmTSN antibody. (a) Dot blot analysis of the anti-rabbit PmTSN antibody at 1:5,000, 1:10,000 and 1:20,000 dilutions. The antibody can detect the purified GST-TSN protein at least 0.025 µg at 1:5,000 dilution, and at least 0.05 µg at 1:10,000 and 1:20,000 dilutions, respectively. (b) Western blot analysis using anti-rabbit PmTSN antibody. The antibody can detect the purified GST-TSN protein at least 0.025 µg at 1:5,000 dilution.

References:

1. Phetrungnapha A, Panyim S, Ongvarrasopone C. Fish Shellfish Immunol 2013;34:875-84.
2. Phetrungnapha A, Panyim S, Ongvarrasopone C. Fish Shellfish Immunol 2011;31:373-80.
3. Tong X, Drapkin R, Yalamanchili R, Mosialos G, Kieff E. Mol Cell Biol 1995;15:4735-44.
4. Yang J, Valineva T, Hong J, Bu T, Yao Z, Jensen ON, et al. Nucleic Acids Res 2007;35:4485-94.

Acknowledgements: We would like to thank Dr. Amnat Phetrungnapha for plasmid, pGEX-5X-1-TSN (Tudor-SN5 domains).

Keywords: RNA interference (RNAi), tudor staphylococcal nuclease (TSN), polyclonal antibody, *Penaeus monodon*.

RGJ - Ph.D. Congress XIII

การประชุมวิชาการ
โครงการปริญญาเอกกาญจนาภิเษก ครั้งที่ 13

6-8 เมษายน 2555

โรงแรมจอมเทียน ปาล์ม บีช รีสอร์ท เมืองพัทยา จังหวัดชลบุรี

สำนักงานกองทุนสนับสนุนการวิจัย

The Thailand Research Fund

S3-P7

Penaeus monodon Tudor Staphylococcal Nuclease and Its Function in RNAi Pathway

Amnat Phetrungnapha,[a] Sakol Panyim[a,b] and Chalermporn Ongvarrasopone[a]

[a]*Institute of Molecular Biosciences, Mahidol University, Phutthamonthon 4th Rd, Nakhon Pathom, 73170, Thailand.*
[b]*Department of Biochemistry, Faculty of Science, Mahidol University, Rama VI Road, Phayathai, Bangkok 10400, Thailand.*

Introduction and Objective

Gene silencing *in vivo* by double-stranded RNA (dsRNA) has greatly facilitated our understanding of gene function and has been considered as a new promising therapeutic modality to combat viral infection in shrimp. However, the information of RNAi-based mechanism in shrimp is remained largely elusive. Tudor staphylococcal nuclease (TSN or p100) is a multifunctional protein which found to be the component of RNA-induced silencing complex in *Drosophila melanogaster*. To gain more insights in RNAi-based mechanism and antiviral response in shrimp, we aim to identify TSN gene from the black tiger shrimp, *Penaeus monodon* and investigate the involvement of this protein in RNAi pathway.

Methods

RACE-PCR and inverse PCR were used to clone the full-length cDNA encoding *P. monodon* tudor staphylococcal nuclease (PmTSN). Gene silencing approach was used to investigate the involvement of PmTSN in RNAi. Quantitative real-time PCR and cumulative mortality assay were used to validate the efficiency of RNAi in normal comparing to *PmTSN*-knockdown shrimps.

Results

The full-length cDNA of PmTSN is 2897 bp, with an open reading frame encoding a putative protein of 889 amino acids. Silencing of *PmTSN* by dsRNA resulted in partial impairment of dsRNA-mediated gene silencing in shrimp, as the reduction of the silencing effect of dsRNA targeting endogenous gene was observed. Moreover, the reduction of the efficiency of dsRNA targeting YHV was observed in shrimp that *PmTSN* was silenced.

Conclusion

The full-length cDNA encoding PmTSN was cloned. To our knowledge, this is the first report of TSN in crustacean. Our results imply that PmTSN is involved in dsRNA-mediated gene silencing and thus we identified the novel RNAi-related protein in shrimp. However, the mode of action of PmTSN in the shrimp RNAi pathway is still unknown. Therefore, identification of the PmTSN-interacting proteins will provide more insights in RNAi-based mechanism in shrimp.

Keywords: black tiger shrimp, tudor staphylococcal nuclease, RNAi, double-stranded RNA

Selected References:

1. Caudy, A. A.; Ketting, R. F.; Hammond, S. M.; Denli, A. M.; Tops, B. B. et al. A micrococcal nuclease homologue in RNAi effector complexes. *Nature*, **2003**, 411-414.
2. Labreuche, Y.; Veloso, A.; de la Vega, E.; Gross, P. S.; Chapman, R. W.; Browdy, C. L.; Warr, G. W. Non-specific activation of antiviral immunity and induction of RNA interference may engage the same pathway in the Pacific white leg shrimp *Litopenaeus vannamei*. *Dev. Comp. Immunol.*, **2010**, 1209-1218.

Amnat Phetrungnapha (อำนาจ เพชรรุ่งนภา) **RGJ 10**
Naresuan University, Thailand, Microbiology, B.Sc. 2007
Research field: Shrimp molecular biology

Penaeus monodon Tudor Staphylococcal Nuclease and Its Function in RNAi pathway

Amnat Phetrungnapha[1], Sakol Panyim[1,2] and Chalermporn Ongvarrasopone[1,3]

[1]Institute of Molecular Biosciences, Mahidol University, Phutthamonthon 4 Road, Nakhon Pathom, 73170, Thailand.
[2]Department of Biochemistry, Faculty of Science, Mahidol University, Rama VI Road, Phayathai, Bangkok, 10400, Thailand.
[3]Aquatic Animal Research Center, Mahidol University, Phutthamonthon 4 Road, Nakhon Pathom, 73170, Thailand.

Introduction

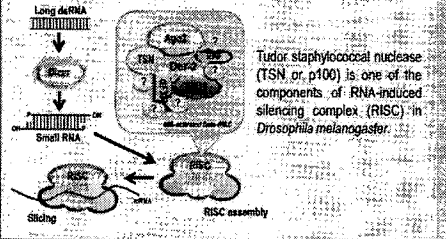

Tudor staphylococcal nuclease (TSN or p100) is one of the components of RNA-induced silencing complex (RISC) in *Drosophila melanogaster*.

Objective

To gain more insights in RNAi-based mechanism in shrimp, this study aims to investigate the role of *P. monodon* TSN (PmTSN) in RNAi pathway.

Cloning of the full-length cDNA of PmTSN

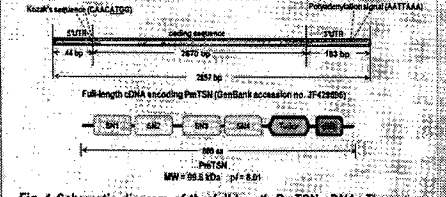

Fig. 1 Schematic diagram of the full-length PmTSN cDNA. The entire ORF can be translated into a 100-kDa protein, consisting six functional domains. SN, Staphylococcal nuclease-like domain; Tudor, Tudor domain.

Preparation of double-stranded RNA (dsRNA)

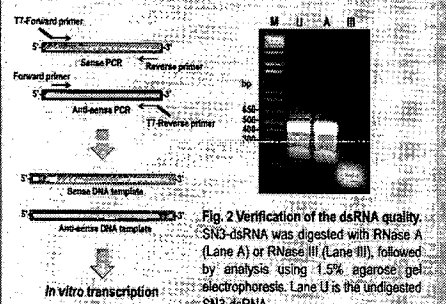

Fig. 2 Verification of the dsRNA quality. SN3-dsRNA was digested with RNase A (Lane A) or RNase III (Lane III), followed by analysis using 1.5% agarose gel electrophoresis. Lane U is the undigested SN3-dsRNA.

In vivo gene knockdown

For *in vivo* PmTSN knockdown, shrimps (5 g) were injected with 25 µg of SN3-dsRNA or GFP-dsRNA. Hemolymph was collected before and after 1, 3, 5 and 7 days post dsRNA injection. Multiplex RT-PCR was employed for monitoring the PmTSN mRNA level.

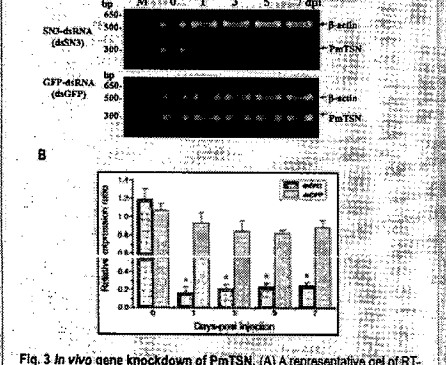

Fig. 3 *In vivo* gene knockdown of PmTSN. (A) A representative gel of RT-PCR products showing PmTSN expression at 0, 1, 3, 5 and 7 days post dsRNA injection. β-actin was used as an internal control. (B) Relative expression of PmTSN normalized with β-actin. Bars represent mean ± SEM (n = 6). The asterisks represent the significant difference ($p < 0.05$) between before and after dsRNA injection.

Functional study of PmTSN in RNAi pathway

To investigate the involvement of PmTSN in dsRNA-mediated gene silencing, the efficiency of Rab7-dsRNA in silencing of PmRab7 gene was compared in normal and PmTSN-knockdown shrimps. The schematic diagram of the dsRNA injection is shown below.

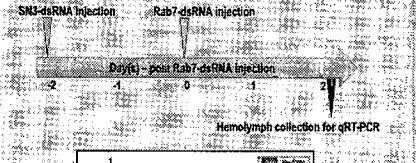

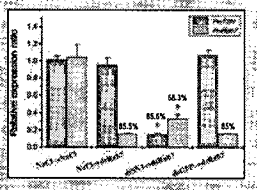

Fig. 4 Efficiency of RNAi in PmTSN-knockdown shrimp. Quantitative real-time PCR was performed with specific primers for PmTSN and PmRab7. EF-1α was used as an internal control for normalization. The relative expression of PmTSN and PmRab7 was calculated by comparative Ct method ($2^{-\Delta\Delta Ct}$). Bars represent means ± SEM (n = 6). The asterisks (*) represent the significant difference ($p < 0.05$) of the relative PmTSN and PmRab7 expression among dsSN3→dsRab7 group and other groups.

Cumulative mortality assay

Cumulative mortality assay was performed to observe the efficiency of YHV-protease dsRNA in inhibition of YHV replication in normal, comparing to PmTSN-knockdown shrimps. Schematic diagram of the dsRNA injection and YHV challenge is shown below.

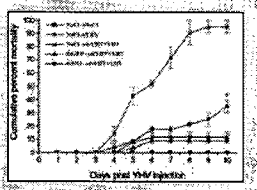

Fig. 5 Increase in cumulative mortality upon YHV challenge in PmTSN-knockdown shrimp. Cumulative percent mortality in each treatment group (9 – 15 shrimps/group) is presented as means ± SEM. Two independent experiments were performed. An asterisk (*) represents the significant difference ($p < 0.05$) among PmTSN-knockdown shrimp (dsSN3→dsYHV + YHV) and other groups.

Expression and purification of GST-TSN

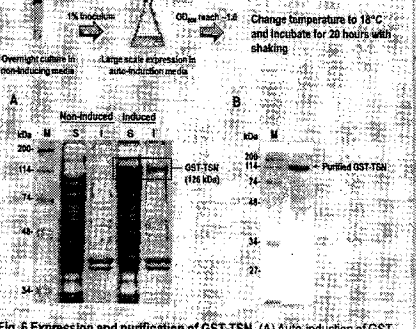

Fig. 6 Expression and purification of GST-TSN. (A) Auto-induction of GST-TSN expression. *E. coli* Rosetta (DE3) containing pGEX-5X-1-TSN expression vector was grown in auto-induction media at 18°C, and subsequently lysed by sonication. The soluble fraction (S) and insoluble fraction (I) were analysed on 10% SDS-PAGE. (B) Purification of GST-TSN. The recombinant GST-TSN was purified by using affinity chromatography, followed by anion-exchange chromatography. M, Pre-stained SDS-PAGE standards.

Expression of His-tagged Argonaute

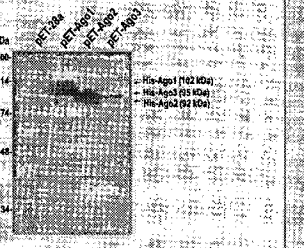

Fig. 7 Verification of the recombinant His-tagged Argonaute (His-Ago) expression. *E. coli* Rosetta (DE3) harboring pET-Ago expression vectors were induced with 0.5 mM IPTG at 18°C for 6 hours (His-Ago1) or 20 hours (His-Ago2 and His-Ago3). Cells were lysed by sonication, followed by centrifugation. The expression of His-Ago in soluble fraction was detected by using western blot with anti-His antibody.

In vitro pull-down assay

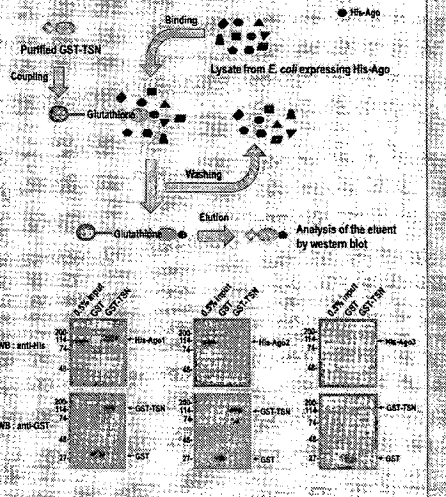

Fig. 8 Analysis of the interaction between PmTSN and PmAgo using *in vitro* pull-down assay. Purified GST-TSN was coupled with glutathione-agarose resin and then mixed with lysate from *E. coli* expressing His-Ago1, His-Ago2 or His-Ago3. Western blot analysis with anti-His or anti-GST antibody was used to detect the presence of His-Ago or GST-TSN, respectively.

Conclusions

The full-length cDNA of PmTSN was cloned and the function of PmTSN in RNAi pathway was characterized. Silencing of PmTSN expression resulted in the reduction of the Rab7-dsRNA efficiency in PmRab7 silencing. In addition, the efficiency of dsRNA against YHV was decreased in PmTSN-knockdown shrimps, indicating the involvement of PmTSN in dsRNA-mediated gene silencing. *In vitro* pull-down assay revealed the interaction between PmTSN and PmAgo1, suggesting the role of PmTSN in PmAgo1-RISC. This study provides more insights in the RNAi-based mechanism in shrimp.

References

1. Phetrungnapha A, Panyim S, Ongvarrasopone C. A Tudor staphylococcal nuclease from *Penaeus monodon*: cDNA cloning and its involvement in RNA interference. Fish Shellfish Immunol. 2011;31:373-80.
2. Studier FW. Protein production by auto-induction in high density shaking cultures. Protein Expr Purif. 2005;41:207-34.
3. Caudy AA, Ketting RF, Hammond SM, Denli AM, Bathoorn AM, Tops BB, et al. A micrococcal nuclease homologue in RNAi effector complexes. Nature. 2003;425:411-4.

Acknowledgement

This work is supported by grants from the Thailand Research Fund (TRF), Commission on Higher Education (CHE) and Mahidol University research grant under the National Research University Initiatives. A student fellowship granted to A.P. by the Royal Golden Jubilee Ph.D. Program.